

Editorial

Advances in Metal Casting Technology: A Review of State of the Art, Challenges and Trends—Part II: Technologies New and Revived

Dirk Lehmus 

Fraunhofer Institute for Manufacturing Technology and Advanced Materials IFAM, Wiener Straße 12, 28359 Bremen, Germany; dirk.lehmus@ifam.fraunhofer.de; Tel.: +49-421-2246-7215

1. Introduction

The present text is the second part of an editorial written for a Special Issue entitled *Advances in Metal Casting Technology*. The first part, which was published in November 2022, contains an overview of the global metal casting industry and highlights specific aspects that have led to changes in markets and products, such as e-mobility, the associated advent of Gigacasting technology, or the increasing pressure on the casting industry to justify and minimize the environmental impact of its processes [1]. This second part assumes a different perspective by examining the technological developments within the industry that can either be seen as general trends or as responses to the preceding challenges; in other words, this text discusses technologies both new and revived. In doing so, it cannot possibly be complete, but it may provide readers with points of attack for further study. The final chapter is dedicated to the contributions to the Special Issue, contextualizing them with respect to the fields of technology that were previously discussed in detail. As in Part I, based on the author's primary field of activity, there may be a bias toward the high-pressure die casting (HPDC) of aluminum alloys, which I hope the reader will accept.

2. Technologies New and Revived

It is a platitude that science and technology do not necessarily evolve along straight paths. Instead, cycles may occur which can sometimes, but not always, be explained by technology-centered models, such as the famed Gartner hype cycle [2–4], or more generally by economy-level observations, such as Kondratiev waves and all their relatives [5]. In other cases, new ideas, new market needs, or the expiration of limiting patents may support the reemergence of technologies. The casting industry has experienced its share of such effects, and in as far as they concern changing markets and boundary conditions, these have already been discussed in the preceding Part I of this text. The delimitation between both these parts is illustrated in Figure 1, which has also been included in a similar form in Part I [1].

2.1. Semi-Solid Processing

Semi-solid metal processing is not a new topic [6,7], but it certainly is one that has met with renewed interest in recent years. This is underlined from an industrial perspective by Jorstadt et al., assuming an industrial perspective [8], but also is demonstrated by academic activity in the field. A rough measure in this respect is the number of publications, as derived from sources such as Google Scholar or Scopus, on semi-solid casting, of which Figure 2 provides an overview. The respective diagrams show that the number of publications reached a peak in the mid-2000s according to Scopus data, while Google Scholar suggests a constant rise, except for the special case of thixocasting, which peaked in the 2000s and 2010s before declining toward a low in 2022. The data for rheocasting match this pattern, though in the most recent years since 2018, Scopus data, too, indicate a rise



Citation: Lehmus, D. Advances in Metal Casting Technology: A Review of State of the Art, Challenges and Trends—Part II: Technologies New and Revived. *Metals* **2024**, *14*, 334. <https://doi.org/10.3390/met14030334>

Received: 25 February 2024

Accepted: 8 March 2024

Published: 14 March 2024



Copyright: © 2024 by the author. Licensee MDPI, Basel, Switzerland. This article is an open access article distributed under the terms and conditions of the Creative Commons Attribution (CC BY) license (<https://creativecommons.org/licenses/by/4.0/>).

that is not apparent in the data for semi-solid casting in general. Meanwhile, thixocasting exhibits a decline in both data sets. However, while thixo processes will not be discussed in detail here, they are certainly not obsolete; on the contrary, they are an established production process in certain areas, such as the processing of magnesium alloys [9–11], as a recent overview of activities in China reveals [12]. The focus here, however, is primarily on thixomolding rather than thixocasting—the former process transfers the principles of plastic injection molding to the processing of metals, using materials in granulated form, as well as extruders for partial melting and plastification [13]. In 2019, more than 170 machines of this type were installed in China, with the vast majority of them in a locking force range of 650 tons and above. The main markets are components for electronic systems such as housings for laptops, etc., where wall thicknesses down to a minimum of 0.35–0.4 mm are reportedly achieved [12].

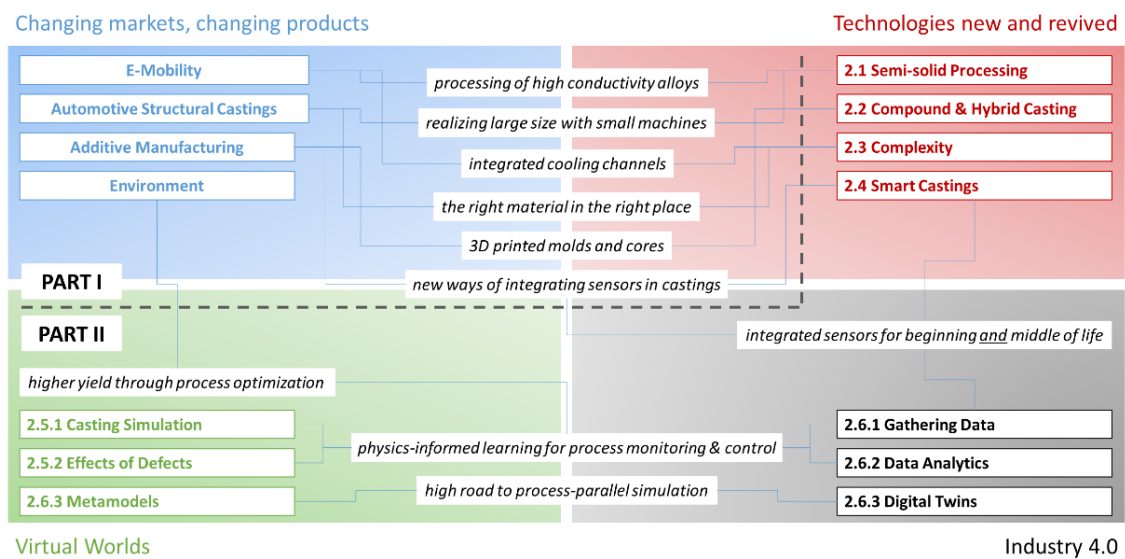


Figure 1. An overview of topics covered in the present text. The graphic shows the areas of interest discussed in the previously published first part of this editorial (PART I in the diagram, see [1]) as well as those focused on in this second part. While Part I concentrated on boundary conditions, Part II is technology oriented.

In contrast to thixocasting and molding, rheocasting methods approach the required semi-solid state of the melt from the liquid rather than from the solid state. In practice, this eliminates the need for specially prepared and, thus, costly precursor materials [14]. Instead, in most cases, the melt is conditioned directly at the machine on a “per shot” basis. Thus, a distinctive feature of rheocasting, setting it apart from thixocasting, is the “slurry on demand” principle. This means that in contrast to thixocasting, not only the use of conventionally produced casting alloys but also the remelting of defective parts, runners, etc. and the direct re-use of the material in the same process are possible. Needless to say, this has a significant impact on both the economic and ecological viability of the process. Furthermore, in terms of boundary conditions such as tool design (gate cross sections, etc.) and process parameters, rheocasting is effectively closer to conventional HPDC than to classical thixocasting. In both cases, even though semi-solid processes proceed with slower filling velocity [15], the fact that less heat must be extracted from the already partly solidified melt results in cycle times that are comparable to conventional HPDC processes. Further, the general advantages of rheocasting over HPDC include the following:

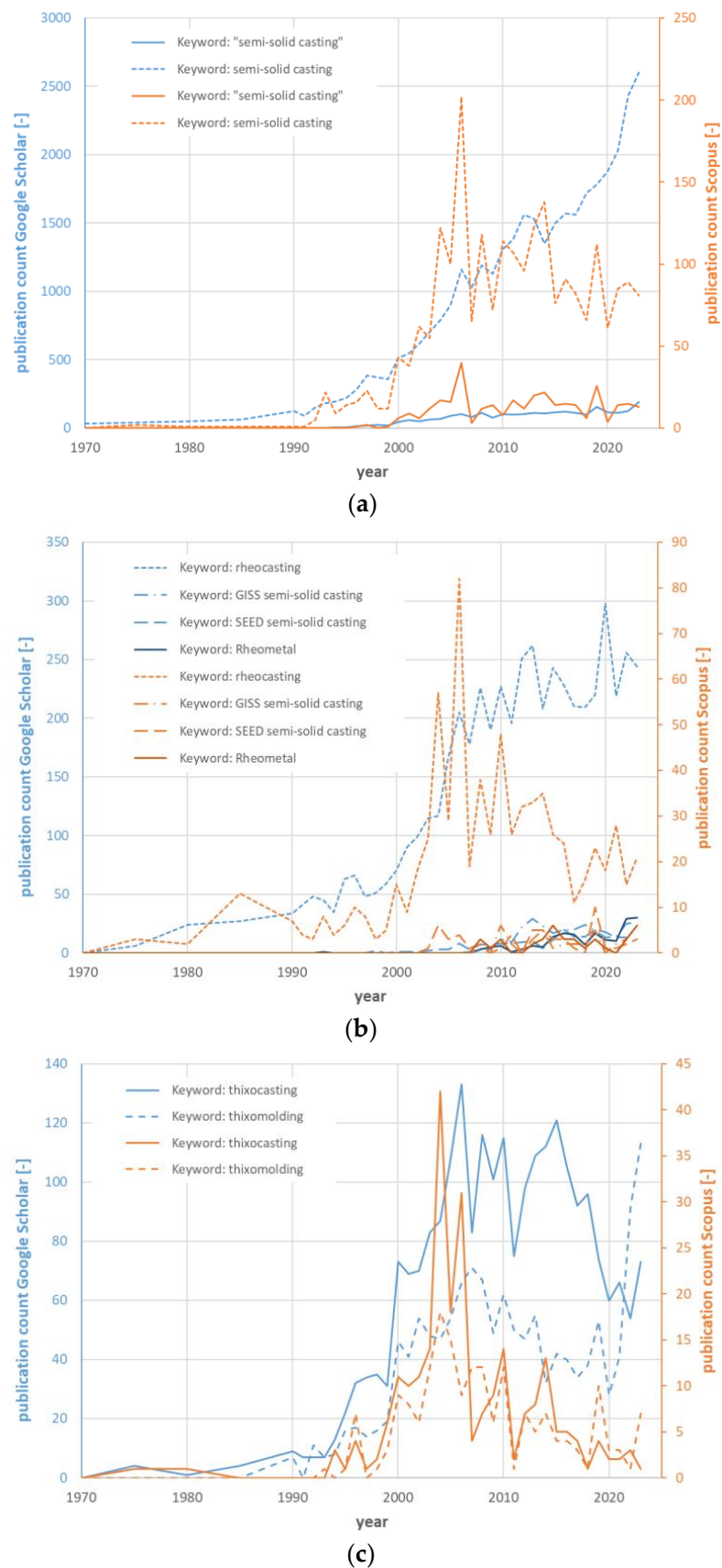


Figure 2. Publication numbers sourced from Google Scholar and Scopus on semi-solid casting technologies: (a) semi-solid casting in general, (b) rheocasting and (c) thixocasting process family examples. Note that keywords had to be adapted slightly for scanning different databases.

- Lower solidification shrinkage due to fraction solid:
 - Reduction in residual stresses and distortion
 - Improvements in dimensional accuracy, allowing tighter tolerancing and/or the abandoning of mechanical or other secondary alignment processes
 - Reduction in shrinkage-induced porosity
- Laminar flow during mold filling:
 - Reduction in gas entrapment
 - Reduction in entrainment and oxide film defect levels
 - Access to T6 treatment in conjunction with intensification pressure decrease
- Improved feeding efficiency due to globulitic solidification:
 - Lower intensification pressure requirements
 - Reduction in porosity levels
 - Reduction in entrapped gas pressure
 - Access to T6 treatment in conjunction with reduced gas entrapment
 - Access to cost-efficient lost core techniques not suitable for HPDC
 - Reduction in locking force needs, facilitating large projected area castings from limited scale machines
- Lower thermal energy levels of the melt and heat transfer coefficient (HTC) values:
 - Increased lifetime of molds due to reductions in thermomechanical loads and the attenuation of thermal shock

In the past, several different rheocasting methods have been proposed, with Midson and Jackson reporting up to 18 different variants already evaluated by the mid-2000s [16,17]. Recent overviews have been provided, e.g., by Bakhtiyarov and Siginer as well as Jarfors, focusing on aluminum alloys [18,19]. On a wider scale, Kapranos also reviewed thixocasting and -molding [15]. Li et al., in their overview, name a total of 16 additional rheocasting process variants developed by Chinese researchers alone [20]. In essence, all these approaches must tackle the problems around (a) providing initial nuclei for crystallization, (b) avoiding dendritic growth in favor of the globulitic growth of these nuclei—typically by means of the agitation of the melt—and (c) controlling the amount of solid vs. liquid fraction. With respect to rheocasting, from today's perspective, the following are among the most important processes, in alphabetical order:

- **Gas-Induced Semi-Solid (GISS):** A porous graphite mixer is lowered into the melt just prior to casting. Through it, inert gas is fed into the melt, causing cooling and agitation and potentially providing seeds for crystallization [21].
- **New Rheocasting (NRC):** A separate metal volume in a cylindrical container is first cooled from the outside using air to reach the desired temperature, then heated to maintain the temperature until it is transferred into the shot chamber [22–24].
- **Rapid Slurry Formation (RSF, also known as RheoMetal™):** A separate piece of metal, the so-called enthalpy equilibration material (EEM), is cast and fixed to a stirring rod. While stirring, the EEM dissolves into the melt, providing cooling and seeds as the stirring itself accounts for breaking of dendrites [25,26].
- **Swirled Enthalpy Equilibration Device (SEED):** A single-shot volume of metal is filled into a container and swirled to achieve thermal equilibrium with the latter. Initial conditions such as the temperature, heat capacity and volume of the container and melt define the equilibrium reached and, thus, the final temperature and fraction solid. The claim is that no temperature control is needed; furthermore, fraction solid can be increased by the drainage of liquid phase from the container [27]. The drawback is that the latter procedure will influence the alloy composition.
- **Semi-Solid Rheocasting (SSR™):** As in the GISS process, a graphite cylinder is lowered into the single shot melt volume, but in this case, no gas is introduced. Instead, the cylinder is used for stirring and cooling, thus initiating crystallization primarily via temperature control as in NRC, but with cooling from the inside rather

than the outside. Prior to casting, the melt is left to rest for a defined amount of time to control the level of further solidification. The process was developed by the Italian HPDC equipment manufacturer, IDRA, the Gigacasting pioneers [28].

For HPDC foundries, introducing rheocasting is facilitated by the fact that investment costs are limited to slurry preparation and handling equipment, while the HPDC machines themselves can serve both processes. Comptech, a provider of RSF/RheoMetal™ processing equipment, describes the process as follows on their website: “It is not a new casting process, it is a melt preparation HPDC process” [29]. Jarfors provides an analysis of the market penetration of the major rheocasting processes, GISS, RSF/RheoMetal™ and SEED, in terms of their use in manufacturing commercial products [19]. Typical applications in which rheocasting excels include complex, thin-walled structures combining such geometrical features with requirements for high thermal or electrical conductivity—radio filters for 4G and 5G antennae systems fall in this category, as do radiator housings, heat sinks or cooling units for electronics, including, e.g., automotive power electronics housings. As Li et al. point out, the advantage of rheocasting in these applications may become manifest in the combination of geometrical capabilities and low defect levels, as base material conductivity does not differ substantially from HPDC alloys and products [30]. Figure 3 depicts an example of a radio filter cast according to the RSF/RheoMetal™ process. The low wall thickness is a hallmark of this process, which operates at 30–40% fraction solid, with shear thinning effective specifically between 30–35%. Such conditions result in favorable Reynolds numbers, and the time period available for filling the die is extended by a factor of six. Furthermore, flow lengths reach a maximum at shear rates of 100 mm/s, supported by reduced heat transfer from melt to die. In an experimental die, flow lengths of up to 2.2 m at 3 mm thickness were successfully demonstrated [31].

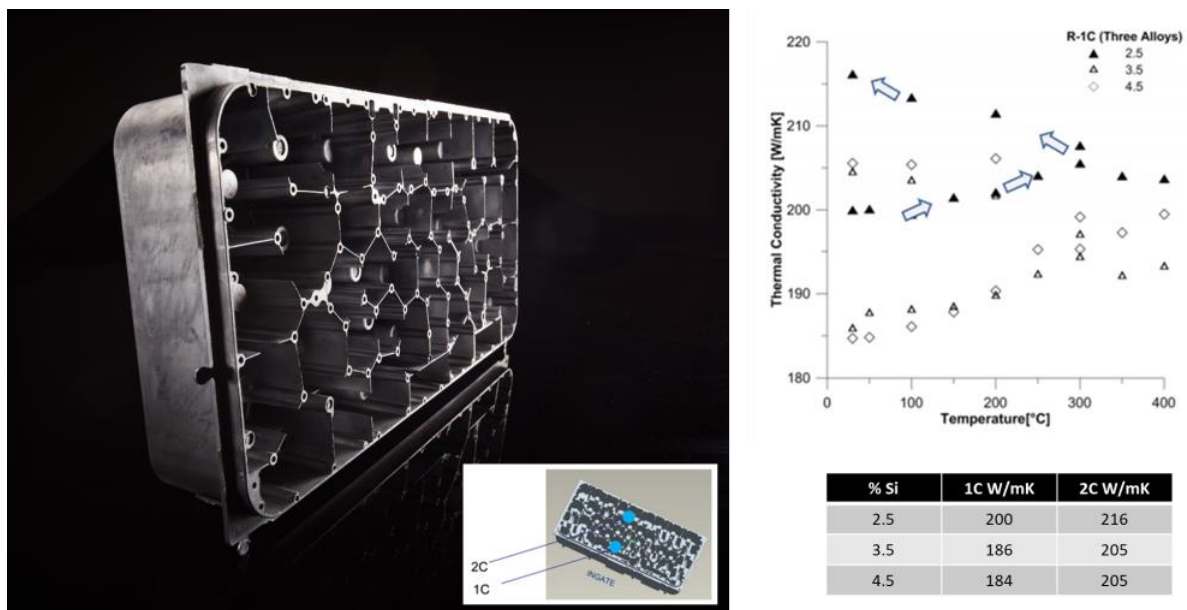


Figure 3. Radio filter produced by means of the RSF/RheoMetal™ process. A unique feature of this product is the weight reduction of 1.6 kg facilitated by wall thicknesses as low as 0.4 mm at 40 mm height (aspect ratio 100). High conductivity low Si alloys were used, and thermal transport properties further increased by up to 20% depending on the alloy composition by means of heat treatments, as depicted in the top right diagram by means of arrows denoting the course of the latter (images provided by Comptech AB, Skillingaryd, Sweden).

Apart from castability and conductivity, the effects of reduced shrinkage and laminar flow during mold filling on porosity and other defects provide advantages in terms of as-cast properties while also facilitating heat treatment. The latter opens up additional

potential for adjusting and enhancing mechanical properties. Figure 4 below provides an overview of the ultimate tensile strength (UTS), yield strength (YS) and elongation at failure (EaF) of rheocast in contrast to high and low pressure as well as gravity die cast aluminum alloys. Apparent from this diagram is the advantage in ductility that rheocast alloys exhibit at comparable strength, represented by the size of the circles. Relative to low pressure and gravity die casting, rheocasting achieves such properties at a significantly reduced cycle time.

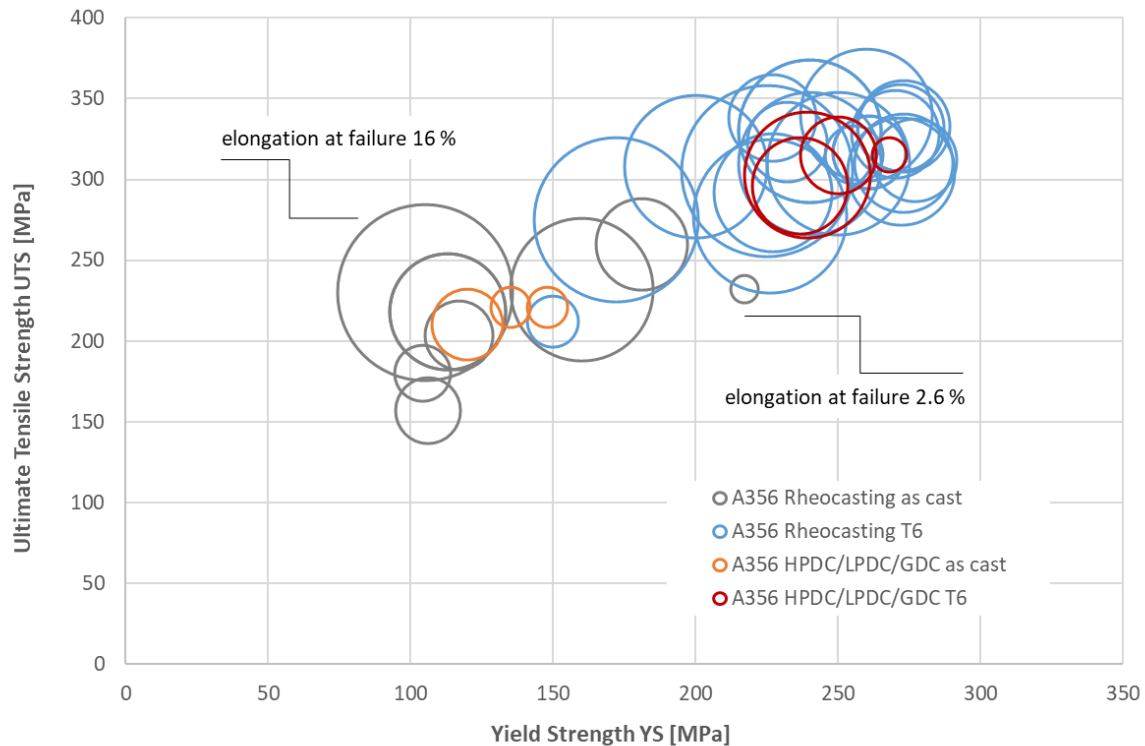


Figure 4. Overview of rheocast and high-pressure die-cast aluminum and magnesium alloys in as-cast and T6 states in terms of yield strength, ultimate tensile strength and elongation at failure. The latter is represented by the size of the spheres. Data are sourced from [20,32–43].

A major aspect of semi-solid processes is their apparent applicability to alloys typically not considered for casting. Atkinson summarized efforts in this direction in 2012, highlighting the use of the process class, among others, for wrought aluminum alloys and creep-resistant magnesium alloys, but also higher-melting-temperature materials such as copper, cast iron, stellites or steels [44]. While the applications of such uncommon alloys remain limited, there is doubtlessly an interest in the processing of wrought aluminum alloys, the motivation being the exceptional strength of many of these alloys in the wrought and age-hardened state. Table 1 summarizes some such studies, providing additional information on the material properties achieved. More detailed reviews on the topic were published by Curle in 2010 [45] and Li et al. in 2020 [46].

Table 1. Overview of published research on semi-solid casting of wrought aluminum alloys. Alloys, semi-solid casting process, achieved mechanical properties and references are given.

Alloy/State	Process	UTS ¹ [MPa]	YS ² [MPa]	EaF ³ [%]	Ref.
1420/ <i>as-cast</i>	RCP	227	141	2.6	[47]
1420/T6	RCP	405	242	6.4	[47]
1420/ <i>as-cast</i>	RCP	305	248	1.6	[48]
1420/T6 ⁴	RCP	457–462	366–391	1.7–3	[48]
2024/T6	CSIR-RCS	385	351	5.1	[45]
6004/T6	CSIR	189	148	13.1	[38]
6004/T6	CSIR	237	207	12.0	[38]
6061/ <i>as-cast</i> ⁵	SEED	310–350	250–300	10–20	[49]
6061/T6	SEED	340	301	14.4	[50]
6082/T6	CSIR-RCS	365	341	3.6	[45]
6082/T6	CSIR	305	278	5.4	[38]
6082/T6	CSIR	344	323	4.2	[38]
7075/T6	SEED	513	467	3.2	[45]
7075/T6 ⁶	SEED	513	467	3.2	[51]
7075/T6 ⁶	SEED	516	458	4.5	[51]
7075/T6 ⁶	SEED	516	453	5.3	[51]
7075/ <i>as-cast</i>	FCR-Rheo	337	249	5.2	[52]
7075/T6	FCR-Rheo	543	506	4.1	[52]
7075/ <i>as-cast</i>	ACSR-Rheo	351	254	3.9	[53]
7075/T6	ACSR-Rheo	547	494	3.2	[53]
7075/T6 (4 h/450 °C)	GISS	483.67	-	2.67	[54]
7075/T6 (4 h/ 400 °C + 4 h/450 °C)	GISS	408.65	-	5	[54]
7075/T6 (8 h/ 400 °C + 4 h/450 °C)	GISS	448.90	-	6	[54]
7075/T6 (12 h/ 400 °C + 4 h/450 °C)	GISS	426.55	-	4	[54]

¹ Ultimate tensile strength. ² Yield strength. ³ Elongation at failure. ⁴ Ageing temperature and time varied (140–180 °C, 10–35 h). The source claims that almost 500 MPa UTS and 437 MPa YS were reached as maxima, but solution heat treatment as well as artificial ageing temperature are not given for the respective sample. ⁵ T6 discussed as option in the source, but data appear to apply to *as-cast* state. ⁶ Three different compositions were compared representing different levels of grain refinement (increasing from top to bottom), all conforming to the EN AW-7075 specification.

Special cases among such wrought alloys are those that are not primarily selected for structural properties but rather for functional properties like thermal or electrical conductivity. Here, a link to e-mobility applications, as discussed in Part I of this work, is apparent, e.g., in rotor casting [1]. Classical rotor aluminum Al99.7 is almost pure and characterized by limited castability; nevertheless, it is employed in HPDC to produce electrical engine components [55]. Alternatives include low alloyed materials such as AlMn1.6, as, e.g., offered by Rheinfelden, which do pose similar castability problems but add strength, increasing yield strength from Al99.7's 20–40 MPa to 90–120 MPa [56]. Increasing interest in such materials is also exemplified by recent patent applications, e.g., from Tesla [57,58]. The aspect of strength is introduced here due to the fact that there is a tendency in the automotive industry to increase electrical traction motor speed to allow for more compact designs, a trend which will raise the centrifugal forces acting on the rotors [59,60]. Beyond this, requirements regarding conductivity resemble those for radio filters and other electronic components as described above (see Figure 3). The link to rheocasting is established by its proven capability to handle materials with inferior castability. Candidate, low alloyed material systems like some of those summarized in Table 1 could profit from this.

2.2. Compound and Hybrid Casting

The use of the term hybrid when referring to hybrid materials and structures is not self-explanatory, as its detailed discussion by Ley et al. clearly shows. A general notion may be derived from the translation of a hybrid object as being “of mixed ancestry”. where, however, ancestry may refer to material or process, or both, and where the delimitation in terms of materials may be broader or narrower [61]. In the following, compound casting is understood to imply the joining, by casting, of materials originating from the same material class, i.e., metals. Hybrid casting, in contrast, implies a bond created during casting between materials of different classes, i.e., metals and polymers or metals and ceramics. As the topic is casting, it is assumed that it is always the metal which is in liquid or at least semi-solid state when the formation of the link between both materials is initiated. Furthermore, processes which are aimed at providing semi-finished materials rather than finished products, such as continuous casting or strip casting, are considered here only in as far as they provide insight into interface formation.

Having said this, what is the motivation behind devoting a section of this text to compound and hybrid casting technologies? In the preceding Part I of this Editorial, Gigacasting [62,63] was presented as one approach toward the realization of large structural castings for automotive applications [1]. There are, however, alternatives to this technique which may succeed in eliminating some of the drawbacks of the former approach. Compound and hybrid casting both imply integrating separate components with a casting, using the primary forming process for joining, too—this can be used to limit flow lengths in large structural castings, or to optimize material usage by following the dictum of employing “the (technically and economically) right material in the right place”, which is essentially, in its technical sense, a lightweight design paradigm. Furthermore, replacing part of the casting’s volume with sheet metal or extruded components effectively reduces the projected area and, thus, the locking forces required to produce the respective part. As a consequence, in HPDC, smaller machines can be used to produce parts with dimensions that were otherwise only achievable through Gigacasting. Compound casting can, thus, open up a parallel road to Gigacasting that is also suitable for brownfield scenarios, making it advantageous for established OEMs as opposed to newcomers such as Tesla or emerging Chinese enterprises like HiPhi, NIO or Wecan, which are often building up production facilities from scratch, leaving them a wider choice of options from an economic perspective, with Gigacasting quite naturally among them [64–67]. It is, thus, no coincidence that in view of such competitors, several established European manufacturers are actively investigating both Gigacasting and alternative paths. For example, when this text was written, Volkswagen was still evaluating the greenfield option of setting up an entirely new plant including Gigacasting facilities in Wolfsburg versus brownfield strategies based on design solutions allowing for the production of large castings using available HPDC machines in the locking force range below 5000 tons. In addition, Volvo recently acquired two Bühler Carat 840 HPDC machines exceeding 8000 tons locking force for their Torslanda plant [68–72].

This, then, is the starting situation which defines the perspective guiding the following observations, and a recent publication by Blala et al. shows that the technique is actively being discussed for automotive applications [73]. However, beyond the automotive structural and Gigacasting challenge, there are other applications that warrant compound or hybrid casting approaches, some of them requiring heat or current transfer across an inter-material interface rather than mechanical strength. Examples from e-mobility were discussed in Part I of this Editorial, including aluminum cooling channels for e-motor housings or copper conductor bars for hybrid e-motor rotors, both produced via HPDC [1]. Irrespective of the application background, a main concern in both compound and hybrid casting remains the establishment of a stable and reproducible bond between castings and inserts. In principle, there are three paths toward achieving this aim (see Figure 5): material joints; form fit on micro-, meso- or macroscopic scale; and force fit. Needless to say, combinations of these approaches are also possible. For the transfer of forces, all three solutions can be tuned

to satisfy a wide range of technological requirements. In contrast, if the aim is thermal or electrical conduction across the interface, a material joint is typically required.

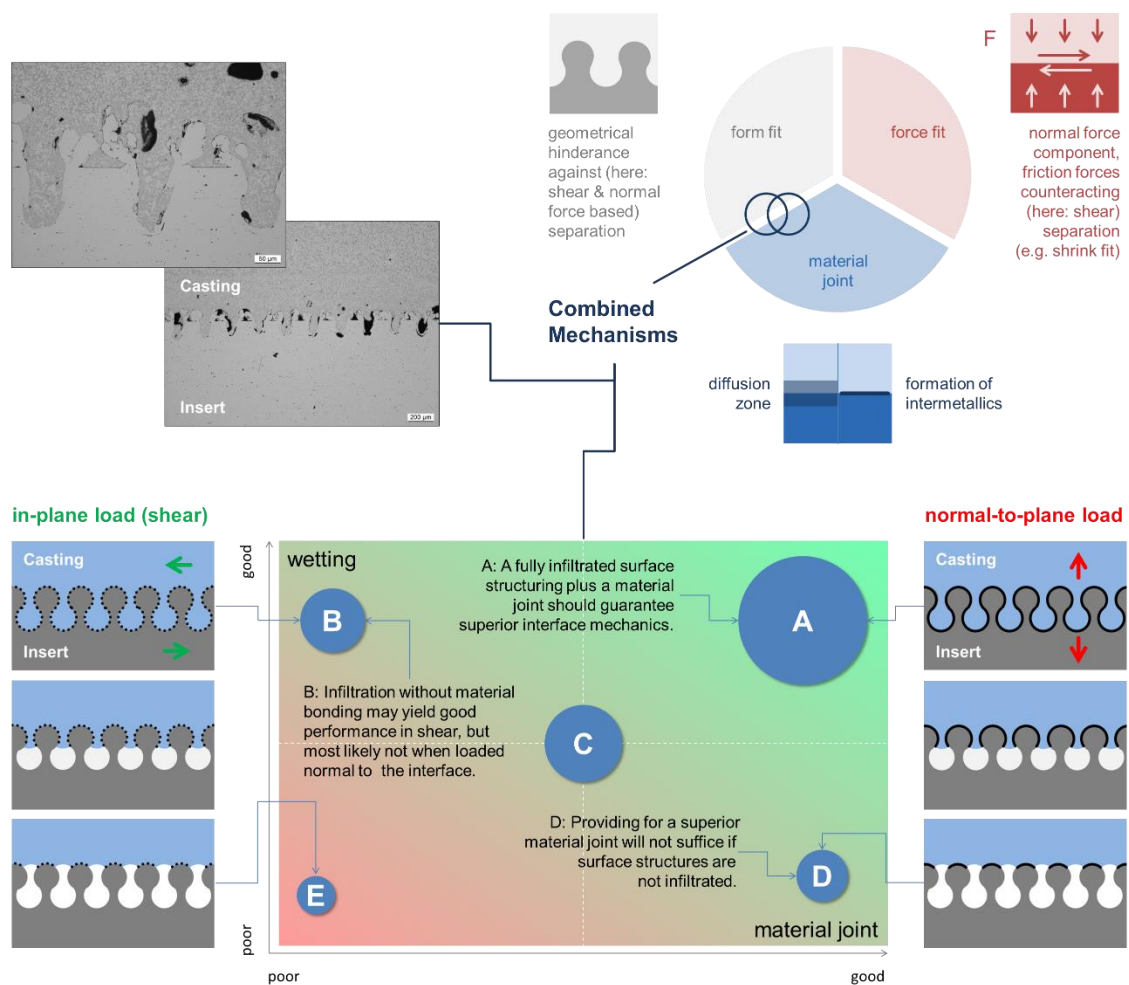


Figure 5. An overview of principles controlling strength in compound casting. The image in the top left corner shows metallographic sections of infiltrated surface structures created via laser pulses to facilitate a micro-scale form fit. E in the image marks the worst case, poor wetting and bonding, while C denotes the middle position. More interesting are the extreme cases described in the image.

Material joints imply close contact and some physical or chemical interaction between the materials in question. Among metals, the formation of intermetallics as well as solid solutions and diffusion zones extending into either or both partners are possible. **Form fit** is based on some geometrical hinderance like, e.g., interlocking, which acts against the separation of the partners. It can occur on different length scales, ranging from macro- to meso- to the microscopic range. **Force fit** relies on normal forces acting on the contact surface between the two components. In conjunction with friction coefficients, cohesion under shear loads is achieved. To realize this effect, solidification and cooling must be controlled. Typically, when casting around an insert, solidification will start from this cooler foreign body, causing the melt to shrink away from rather than onto it.

There are several motivations for realizing compound casting, some of which have already been mentioned:

- **Lightweight design I:** Combining different materials based on their structural materials properties without a need for fasteners, etc.

- **Lightweight design II:** As an alternative to the current practice in the automotive industry of producing large structural castings, in which local wall thickness is not necessarily defined by loads, but by processing requirements.
- **Design freedom I:** Realizing preferably local structural reinforcements to reduce weight and/or required design space.
- **Design freedom II:** Facilitating local complexity by the integration of, e.g., additively manufactured structures to reduce mold complexity or realize geometries that are otherwise not feasible, e.g., for complex, optimized water jacket solutions [74].
- **Smart products:** Integrating functional devices like sensors, actuators or RFID systems (see Section 2.4 for an overview).
- **Production efficiency:** Dispensing with joining and assembly operations.
- **Transfer of heat:** Providing large-area thermal contact superior, e.g., to adhesive bonding.
- **Conduction of electricity:** Providing electrical connections, like, e.g., in hybrid rotor castings with Al short-circuit rings and Cu conductor bars.

Naturally, parts produced by compound casting processes inherit properties both from their constituents and processing history. The market penetration of this technology is not substantial, despite its theoretical potential. In research, the Al–steel system is clearly dominating the scene [75–77]. The application background is structural, in this case. For similar reasons, Al–Al [78–85], Mg–Al [86,87] and even Mg–steel [88] have been studied, with the foremost likely taking second place in terms of the number of publications. In contrast, Cu–Al [89,90] and in some cases also Al–Al [91] are scrutinized with respect to thermal or electrical conductivity. Several other dissimilar metal systems, such as Al–Ti or Ni–Cu, have yet to be evaluated in detail, though individual publications exist [92]. Liu et al. [91] attempted the compound casting of aluminum alloy A356 onto SiCp/AA8009 composite. Further extensive studies on Al–Al compound casting focusing, e.g., on optimum surface pretreatment include those by Schwankl et al. or Rübner et al. at Friedrich-Alexander Universität Erlangen. These studies examined sand blasting combined with electroless zinc coating and ultimately suggested the zincate treatment as the method of choice for the HPDC process [80,81,83]. Researchers at Oak Ridge National Laboratory and Rice University successfully demonstrated the centrifugal casting of aluminum alloy A356 into a complex lattice structure produced by the laser powder-bed fusion of austenitic stainless steel AISI 316L [93]. Bührig-Polaczek and associated researchers have studied Al–steel combinations produced by HPDC as a means of stiffening steel sheet metal structures, providing the necessary transfer of forces primarily via macroscopic force fit solutions according to the so-called Variostruct approach [94]. Similar macroscopic solutions have been applied by Schittenhelm et al. for reinforcing steel inserts embedded in aluminum HPDC components [77], the geometry of which was optimized using the so-called multi-phase topology optimization (MPTO) technique [95,96]. The drawback of such form fit approaches is the local introduction of structural weaknesses, a side effect which motivates studies addressing either material joints or micro-scale form fit, or combinations of both.

Since the 1950s, several studies addressed interface formation and characteristics between unmodified solid steel and liquid Al, hinting at Fe_2Al_5 (η phase) as the dominant phase, often taking a tongue-like shape extending into the steel part [97]. In between the η phase and the Al matrix, thin layers of $\text{Fe}_4\text{Al}_{13}$ or FeAl_3 (θ phase) are observed. Both intermetallics are exceedingly brittle and undermine the properties of steel–Al hybrid parts, which is why many studies center on suppressing their emergence. Constraining the interlayer thickness to roughly below 10 μm is considered sufficient to suppress negative side effects [98,99]. Beyond this, certain alloying additions to Al, in particular, Si, can help minimize the amount of these undesirable intermetallic phases [100]. This has been demonstrated by Bobzin et al., showing that in the combination of (Al-coated) DC04 steel with a Si-rich AlSi9Mn melt, the interface is dominated by less critical β -AlFeSi phases [101]. Further approaches based on surface modification include zinc coatings [102]. Similarly, both zinc and nickel coatings reportedly work well for the compound casting of copper

inserts with aluminum [89,90]. Bobzin et al. investigated the combinations of coatings with surface structuring, using a cold spray process to create approx. 100 μm thick Cu layers on steel substrates into which notches were introduced via cold rolling [103]. Senge et al. created additional undercuts by means of a secondary rolling process. The shear strength of such joints reached 45 MPa perpendicular to the notches [104], but directionality and difficulties in processing (a) shaped parts and (b) local variations in surface structuring remain as unresolved issues hampering widespread commercial introduction. Laser micro-structuring [105] offers unique possibilities both for achieving micro- or nanoscale form fit and for influencing wetting behavior, as well as material joint formation through compositional adjustment—the effects of which, thanks to the tool-free process, can also be varied locally over the part surface. These potentials have yet to be evaluated in detail in a compound casting context: In laser texturing, high-energy laser pulses are used to locally melt and vaporize the metal surfaces in a patterned manner for generating a three-dimensional (3D) surface structure. The geometry, dimensions and orientation of the surface structure can be controlled by adjusting the process parameters. Laser texturing can profoundly influence the solid/liquid wetting behavior, as demonstrated by Bizi-Bandoki et al. [106] and Cunha et al. [107], though not in view of compound casting. In an unsuccessful patent application, Lao Bin and Bührig-Polaczek describe metallic compounds consisting of a metal sheet and a die cast part in which, for optimum joint formation, metal sheets are structured in a regular fashion prior to the casting process, e.g., via laser treatment [108]. A critical aspect to consider is the possibility of the incomplete infiltration of surface structures caused by insufficient venting or wetting, or the combination of both, leading to air entrapment in the critical interface area. If flexible structuring processes are employed, the knowledge of local melt flow directions and patterns can be exploited to adapt the structural features accordingly. Typically, laser structuring is performed via ultra-short, pulsed laser (femto- or picosecond pulsed lasers) [109,110]. The respective systems have high investment costs at relatively low productivity. Furthermore, the treatment of complex geometries is hampered by complex beam guidance based on conventional optics and mirrors. In contrast, nanosecond pulsed lasers, especially in the near IR region, are commercially available in a broad power range and can be equipped with glass fiber systems for beam guidance. Nevertheless, a broad introduction in compound casting is still pending. For HPDC, the suitability of the process has been demonstrated by Nolte et al. in an Al–Al compound casting context, with lap shear strength values of up to 138 MPa recorded for optimized structures [111,112]. Further experiments based on LPDC have shown, though, that successful infiltration in HPDC is linked to intensification pressure and/or melt velocity—without both, as in LPDC, small-scale structures successfully tested in HPDC tend not to be infiltrated and may, thus, promote separation rather than the joining of materials [113].

Al–Al compound casting is pursued both in view of structural as well as thermal and electrical applications. The main obstacle in this latter case is not necessarily the formation of intermetallics but rather the formation of an oxide layer covering the Al inserts, which proves exceedingly hard to remove and, if removed, forms anew almost instantaneously. A reasonably successful approach to overcome this difficulty is electroless zinc deposition preceded by extensive surface pretreatments including degreasing, acid pickling, etc. This so-called zincate treatment has been described and evaluated in terms of its mechanical properties by Schwankl et al., reaching lap shear strengths of 40 ± 0.7 MPa for an AlMg₃, 54.4 ± 2.0 MPa for an AlMg_{4.5}Mn_{0.7} and 61.8 ± 7.4 MPa for an AlCu₄MgSi insert, all in combination with an AlSi₁₀Mg casting alloy [83]. While falling short of what is achievable via the aforementioned laser surface treatment, these values still exceed the typical properties of structural adhesive joints, which generally reach approximately 20–30 MPa in lap shear tests [114]. In addition, they are subject to considerable scatter. However, the advantage of the zincate treatment as an immersion process is its applicability to complex structures which may not be accessible by laser, as well as its superior productivity. A recent alternative relies on a cold spray process to break the oxide layer by means of the

kinetic energy of the powder particles. This technology has been successfully demonstrated for use in the copper, brass and zinc alloy coating of EN AW-5754, EN AW-6061 and EN AW-7075 inserts and the HPDC of AlSi10MnMg. An evaluation of strength is still ongoing. However, latest results suggest that specifically CuZn14, CuZn37 and ZnMg2.7 as coating materials on EN AW-6061 substrates can ascertain property levels exceeding structural adhesives in lap shear testing, while heat treatments at temperatures slightly above the liquidus temperature of the interface can further improve its mechanical characteristics. Some issues remain to be solved, though, such as the formation of porosity in the transient liquid-phase region at the interface between insert and cast materials [115]. In the case of copper coating, interface formation is likely to show similarities to observations on Al–Cu compound casting as discussed below, though it may still prove possible to fully eliminate certain phases via diffusion processes in the course of heat treatment.

For the Al–Cu system, a major difference is that here, the focus is entirely on thermal and/or electrical conductivity, which is why material joints are of even greater importance. As in the case of Al–steel, difficulties are caused by the large variety of intermetallics in the Al–Cu system, many of which are characterized by lower thermal conductivity than either of the partners to be joined. Pintore et al. investigated interface formation between pure Al and pure Cu using a sophisticated setup which first allowed the casting and solidification of copper, followed by the casting of aluminum onto the copper substrate at temperatures of the latter of 500 and 900 °C. Interface layer thickness was found to depend heavily on the thermal conditions present during its formation. For the higher substrate temperature, starting from the substrate, a phase sequence of Al₄Cu₉ (<0.7 μm), Al₃Cu₄ (12.3–13.7 μm), AlCu (4.7–10.2 μm) and Al₂Cu (340–1100 μm) followed by the Al–Al₂Cu eutectic (1600–2200 μm) and a transition zone between eutectic and pure Al (2000–3100 μm) was identified. For the lower substrate temperature, no Al₄Cu₉ phase was detected, and the individual layer thickness was reduced to 9.3–12.1 μm for Al₃Cu₄, 2.7–5.5 μm for AlCu, 20–200 μm for Al₂Cu, 900–1300 μm for the eutectic and 450–3200 μm for the transition phase [116]. Further experiments at substrate temperatures of 300, 400, 500 and 700 °C were performed by the same authors with no bond obtained at 300° and significant interface defects at 400 °C. Above that, previous experiments were confirmed in terms of the layer thickness increasing with temperature [117]. Liu et al. performed similar experiments, varying interface cooling conditions through the adaptation of the liquid aluminum to copper insert volume ratio. At cooling rates between 0.8 and 1.83 K/s in sand casting, they found hypereutectic microstructures dominating the remelting zone during fast cooling and hypoeutectic ones prevailing during slow cooling. Interface mechanics, however, are dominated by intermetallics situated in between these phases and the copper substrate; their effects are least detrimental at lowest thickness [118]. Higher cooling rates have been realized by Liu et al. via a squeeze casting process and varied via melt temperature levels of 680, 700, 720 and 740 °C. Cu samples were mechanically polished, degreased, acid pickled, deoxidized and activated prior to Zn coating by thermal spraying to inhibit renewed oxide formation. Interface compositional analysis showed Al₄Cu₉, Al₂Cu and eutectic layers at the lower three temperatures, plus an additional Al solid solution layer at 740 °C. The thickness grew from approximately 70 μm altogether at 680 °C to 90 μm at 700 °C, 140 μm at 720 °C and 200 μm at 740 °C. In contrast, increasing the applied pressure reduced the thickness from 105 μm at 30 MPa to 95 and 80 μm at 70 and 110 MPa, respectively. In the first experimental series, pressure was maintained at 70 MPa, while in the second, temperature remained unchanged at 700 °C [89].

None of the intermetallic phases are considered beneficial in terms of thermal and electrical conductivity. Pintore et al. measured the specific electrical resistance of Al–Cu interface layers, confirming the expected rise in resistance with increasing interface thickness [116]. Liu et al. confirmed these findings for higher cooling rates, measuring an increase in resistance by almost 70% for a melt temperature of 740 °C compared to 680 °C, with corresponding interface thicknesses of 200 vs. 70 μm. Applied pressure showed no influence on resistance [89]. Thus, a reduction in the thickness of this layer is usually the

target to improve electrical and, thus, thermal conductivity. Alternative approaches support the formation of alternative phases, e.g., via coating. Klose et al. performed extensive studies on Zn and brass-type Zn alloy coatings of copper inserts for HPDC, achieving material joints and a satisfactory overall thermal conductivity of compound cast samples matching that of the casting alloy despite the interface's thermal contact resistance. Coating materials, too, were characterized in terms of their individual thermal conductivity. Here, ZnAl₃₁Cu₄ showed highest levels at approx. 120 W/mK at room temperature, rising to roughly 135 W/mK at 200 °C. Interface thickness was once more shown to depend strongly on the thermal history of the sample: the lower the thermal load, the thinner the interface area. This effect was demonstrated through the investigation of specimens subjected to water quenching and air cooling after casting [119].

An exemplary overview of recent publications on compound casting, also outlining the relevant application scenario and/or the objective of the specific study, is provided in Table 2 below.

Table 2. Exemplary overview of recent publications on compound casting. Note that most studies attempt to achieve a material joint.

Material Pair ¹	Casting Process	Type of Bond Supported by	Comments (Alloys, Application, etc.)	Ref.
Al–Al	HPDC	material joint <i>electroless Zn</i>	AlSi9Cu3(Fe)/AlMg3; piezoelectric transducer integration via sheet metal substrate	[120]
Al–Al	HPDC	material joint <i>zincate treatment</i>	AlSi10Mg/AlZn5.5MgCu and AlCu4MgSi; evaluation of lap shear strength	[83]
Al–Al	HPDC	material joint <i>zincate treatment</i>	AlSi10Mg/AlZn5.5MgCu and AlCu4MgSi; effect of heat treatment on composite strength	[121]
Al–Al	HPDC, LPDC	material joint <i>cold spray coating</i>	AlSi10MnMg (HPDC)/EN AW-5754, -6061 and -7075; cold spray coatings based on Cu, CuZn and ZnMg systems	[115,122]
Al–Al	LFC	material joint <i>Zn interlayer</i>	A356/pure Al; structural components (?); liquid–liquid process	[123]
Al–Al	SC	material joint <i>Zn coating</i>	A356/AA 6101; structural components	[86]
Al–Cu	GDC	material joint <i>degreasing, acid pickling, oxide removal, surface activation</i>	pure Al/pure Cu; thermal management, e.g., heat sinks for electronics; dependence of interface resistance on thickness of intermetallics; details on interface phases	[117]
Al–Cu	SC	material joint <i>Zn therm. spray</i>	pure Al/pure Cu; thermal management; thermal spray following degreasing, acid pickling, oxide removal, surface activation	[89]
Al–Cu	HPDC	material joint <i>Zn coating, flux</i>	AlSi9Cu3(Fe)/pure Cu; thermal management, e.g., heat sinks for electronics	[119]
Al–Mg	LFC	material joint -	A319/AM50; structural components; interface characterization, hardness measurement	[124]
Al–steel	HPDC	material joint <i>Zn, Al-Si coating</i>	AlSi9MgMn/DC04, CPW 800, MBW 1500 steel; interface characteristics, shear strength > 18 MPa for Zn-coated CPW 800	[76]
Al–steel	HPDC	macro form fit -	AlSi10MnMg/S355MC (1.0976); structural reinforcement (strut dome)	[77]
Al–steel	LPDC	material joint <i>galv./flux coating, heat treatment</i>	AlSi7Mg/St37; influence of surface and T6 heat treatment on interface formation	[125]
Al–Ti	Gravity Casting	material joint <i>heat treatment</i>	pure Al/pure Ti; influences on interface studied; shear strength of 60 MPa achieved	[92]
Al–Ti	GDC	material joint <i>heat treatment</i>	pure Al/pure Ti (99.8 wt.% each); interface formation involving trapped air explained	[126]

Table 2. Cont.

Material Pair ¹	Casting Process	Type of Bond Supported by	Comments (Alloys, Application, etc.)	Ref.
Cu–steel	GSC	material joint <i>degreasing, heat treatment</i>	pure Cu/S45C steel; mechanically reinforced conductors; microstructure evaluation, shear strength ≤ 8.33 MPa	[127]
Mg–Al	GDC	material joint	AZ91/AlSi17; structural components, AlSi17 for enhanced wear resistance	[128]
Mg–Al	GSC	material joint <i>Zn interlayer</i>	pure Mg/A356; structural components; shear strength 14.12–33.14 MPa across DoE	[129]
Mg–Mg	dipping in melt	material joint <i>alkaline cleaning, degreasing</i>	AZ31/We43; structural applications; interface characteristics; shear strength up to 108 MPa measured	[130]
Mg–steel	GDC	material joint <i>galvanizing</i>	AZ91D/45 steel; structural applications; average push out strength 11.81 MPa	[88]

¹ Liquid phase named first.

Figure 6 depicts examples of compound and hybrid casting produced either via LPDC or HPDC. Besides different materials combinations, the images illustrate the concepts of joining by casting (a, b), the realization of thermally optimized components (c) and lightweight design solutions (d).

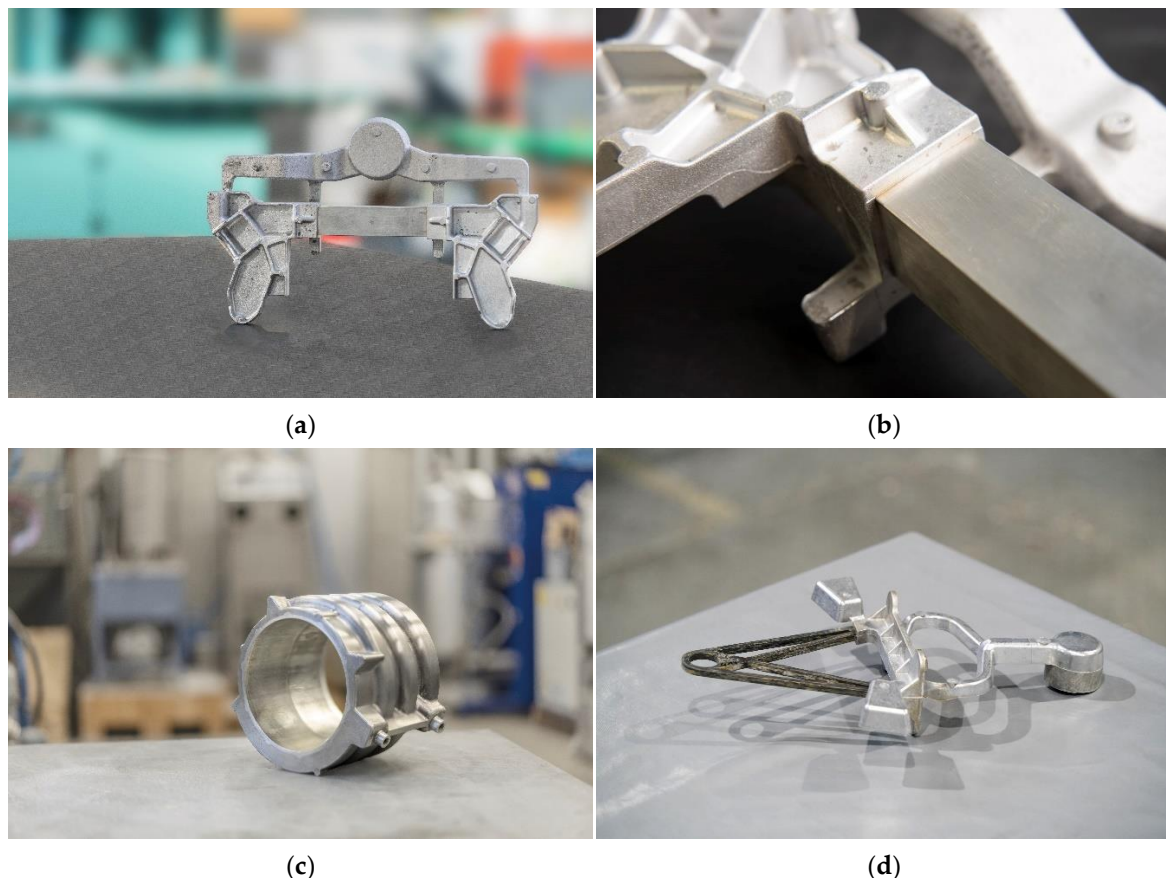


Figure 6. Sample images of parts produced by compound (a–c) and hybrid casting (d); (a,b) AlSi7Mg0.3 LPDC subsize front axle carrier frame demonstrator with integrated EN AW-6060 extrusion, general (a) and detail view (b); (c) AlSi9Cu3 HPDC e-motor housing demonstrator with integrated aluminum tubes as cooling channels, cast by ae group AG, Gerstungen, Germany; (d) aerospace secondary structure hybrid bracket combining a CFRP and an aluminum HPDC component [131] (all images by Fraunhofer IFAM).

The literature on combining metals and polymers via metal casting through a hybrid casting approach is scarce in comparison to that on compound casting and shall be treated accordingly here [131–135]. The main problem arises from the fact that the thermal stability of polymers is typically far below the typical metal-casting temperatures, which means that the respective polymer may be subject to thermal degradation or even decomposition. Schmid et al. have addressed this issue by means of placing a protective layer based on the high-temperature thermoplastic polyether ether ketone (PEEK) between a carbon fiber reinforced polymer (CFRP), also having a thermoplastic PEEK matrix, and the liquid metal. PEEK has a melting temperature of 343 °C and can effectively shield the CFRP, preventing its decomposition under HPDC conditions, as thermal energy input is limited in this process due to the typical, very fast cooling rates. In addition, the PEEK interlayer provides electrical decoupling between CFRP and aluminum under service conditions and thus alleviates the risk of galvanic corrosion. Samples were cast using an Al alloy. In lap shear tests performed on such compounds, strength levels of 13–16 MPa were obtained following a T5 heat treatment and artificial ageing [132]. These findings were employed in manufacturing the demonstrator component shown in Figure 6d [131]. Further optimization of processing conditions allowed for an increase in the shear strength values to 22 MPa, which matches those known from typical structural adhesive joints [136].

A major prerequisite for designing and specifically dimensioning compound and hybrid casting components is the availability of methods for predicting interface strength and simulating interface performance under service conditions. Major contributions in this respect have been made by Bitsche, who investigated combinations of Al and steel and discussed the influence of solidification conditions, the emergence of residual stress fields based on deviations in thermal history, and the thermomechanical properties of cast materials and inserts [137]. In a more recent study, Struss et al. extended these investigations by suggesting and validating a cohesive zone model capable of describing the interface characteristics of cast hybrid joints, while simultaneously outlining the experimental procedures required for the parameterization of this model [135]. Further to the modelling of casted compound or hybrid joints, evaluating the quality of such components is an object of study. Non-destructive testing (NDT) solutions are required in order to monitor quality in series production. Initial approaches in this respect have been proposed and evaluated by Leinenbach et al. using coupon-type samples of both compound and hybrid casting types for the validation of X-ray computed tomography (CT) [138]. A potential drawback of CT methods is that delamination-like defects between the insert and casting may be difficult to discern in CT due to their limited extension perpendicular to the fault plane. This is of even greater relevance in view of potential future components of larger size, as CT resolution typically goes down as the volume covered increases. A solution to this problem may be local CT scans focusing specifically on critical areas within the casting. Methods of this kind have been developed for large components, generally based on dedicated robotic rather than conventional CT systems [139–141]. Alternatives may be NDT techniques which are specifically suited to detect material discontinuities, such as ultrasonic testing or thermal methods. In order to optimize the use of either of these options, further research efforts must identify the most critical areas based on process simulation. To date, the prediction of local interface properties based, e.g., on casting or combined casting and FEM simulation approaches is—specifically for material joints—a problem that is not yet solved in its entirety. An interesting step toward solving this issue was recently published by Glück Nardi et al., which involved simulating the interface evolution of a liquid Al–solid Cu system. Their model incorporates heat transfer across the interface as well as diffusion, solution and intermetallic phase formation. Its validity has been proven against experimental findings gathered from a continuous casting process [142]. Further progress in this respect would also support the design and dimensioning of compound and hybrid casting components, specifically with respect to the layout of interface geometries, sizes and locations in conjunction with the casting system and the processing conditions.

2.3. Achieving Complexity

2.3.1. Complexity: What It Is and How to Get There

Castings can be of complex shapes by nature; however, there are certain technologies which specifically support increasingly intricate shapes; some of these shall be discussed below. But to start, what is complexity? Beyond the general notion of complexity as including internal cavities, high surface-to-volume ratios and the like, a taxonomy of this characteristic is needed. In fact, such a taxonomy has been suggested specifically in view of cast parts by Joshi and Ravi. In their study, they suggest a multi-parametric equation capable of quantifying the relative complexity of a given part based on CAD data. Their aim is to provide designers with a tool allowing them to better estimate costs—this illustrates that naturally, complexity has a price. The parameters they suggest include the number of cored features, the volume and surface area of the cast part, core volume, section thickness and draw distance. Values of these parameters are determined based on forty benchmark cases, i.e., casting designs, representing various levels of complexity, as perceived subjectively. The results are then fed into a regression analysis, from which weighting coefficients for each of the parameters are derived, allowing the determination of a single measure of complexity for any new design. As a result, the highest importance is given to the number of cores and core volume, partly due to the fact that complexity is linked to cost, and the evaluation also allows for an estimation of relative production cost based on the determination of the overall complexity factor for a given part geometry [143]. Their solution is in line with more general studies attempting to classify CAD models irrespective of the underlying manufacturing process [144,145]. At Youngstown State University, Almaghariz proceeded with a similar study to determine when AM techniques are recommendable for the production of sand molds from an economic perspective. A main point in this regard is that for AM, as opposed to conventional manufacturing techniques, the cost driver is not complexity but rather the volume of the bounding box of the printed part. Effectively, this means that AM becomes more competitive the more complex the part is, and the further development of AM productivity will shift the break-even point to lower and lower levels of complexity [146,147]. Martof et al. followed up on this phenomenon in 2018, arriving at similar conclusions [148]. Their measure of complexity is clearly inspired by the AM process itself, as it derives the information from layer-based criteria such as the number of contours or concave features, or contour length divided by the enclosed area per layer, as well as combinations of these. The results obtained for selected geometries are compared to data obtained following the approaches by Almaghariz et al. [146,147], who, in turn, built on Joshi and Ravi [143], for several product categories, within each of which complexity was increased stepwise. Contrasting both methods showed that they generally agree in terms of tendencies, with either reacting more sensitively depending on the part family under scrutiny. The advantage of Martof et al.'s suggestion in terms of predicting costs, however, is that it is entirely geometry based and does not require information about the manufacturing technique. Martof et al. close their study by comparing the costs of AM and the conventional model, mold and core production as function of complexity and production volume, highlighting the fact that the combination of both together determines whether AM processes are viable in a specific case [148].

Thus far, having successfully defined and measured complexity in a casting context, though with a clear focus on sand casting, the following question remains: how can complexity actually be achieved or increased? In practice, there are several approaches which may differ based on the casting process. Here, the question is specifically focused on the type of molds and models employed in the casting process. While permanent molds may e.g., afford sliders to realize undercuts, as shown before, sand casting as well as investment casting can rely on the geometrical flexibility of AM processes in this and many other aspects. Table 3 provides an overview of techniques that aim to increase the complexity of castings, sorted by casting process. Since some of these have already been discussed, such as compound casting solutions, where complexity is introduced through

an insert, the main focus of the present section will be on cores in general, as well as AM of lost and permanent molds.

Table 3. Selected examples of approaches toward increasing complexity in different casting processes. Note that besides direct paths, indirect solutions like the improvement of flow paths or thermal management may also contribute to facilitating increased part complexity.

Casting Process	Cast Material ¹	Approach	Ref.
IC ²	diverse	Additive manufacturing (AM) of wax patterns	[149]
IC ²	diverse	AM of patterns via stereolithography (SLA)	[150]
IC ²	diverse	AM of patterns via fused deposition modeling (FDM) and multi-jet modeling (MJM)	[151]
LFC/EPC	diverse	AM of lost models and/or components thereof made from expanded polystyrene (EPS) via segmented object manufacturing (SOM), including combination with subtractive manufacturing	[152,153]
SC	diverse	Direct AM of molds via the binder jetting process	[154,155]
SC, GDC, LPDC	diverse	AM of sand cores via the binder jetting process	[154,155]
GDC, HPDC ³	Al, Mg, Zn	Reinforcement of salt cores using bauxite, sericite and glass fiber powder, tested in Zn die casting	[156]
HPDC ³	Al, Mg, Zn	LPDC of salt cores able to withstand HPDC conditions	[157]
HPDC ³	Al, Mg, Zn	Reinforcement of salt cores using glass fibers	[158]
HPDC ³	Al, Mg, Zn	Extrusion-based AM of salt cores	[159]
HPDC ³	Al	Evaluation of Al ₂ O ₃ + SiO ₂ + K ₂ O ceramic cores for HPDC production of an automotive crossbeam	[160]
HPDC ³	Al	HPDC process parameter adaptation to limit peak loads of cores, thus facilitating use of sand cores	[161]
HPDC ³	Al, Mg, Zn	Use of sand cores with water-soluble binder and sealant for limited complexity undercuts and hollow sections	[162]
HPDC ³	Al, Mg, Zn	Multi-plate die technology to optimize flow paths, thus facilitating increased part complexity	[163]
HPDC ³	Al, Mg	Switch from conventional HPDC to semi-solid processing for increased flow paths and lower achievable wall thickness	[164]
GDC, LPDC, HPDC ³	diverse	Implementation of improved heat conduction in dies through multi-material AM approaches	[165]
GDC, LPDC, HPDC ³	diverse	Implementation of conformal cooling via AM of a die insert for HPDC of a Zn alloy	[166,167]
diverse	diverse	Use of compound and hybrid casting technologies (see Section 2.2) to integrate complex geometry components in HPDC parts; use of identical or different materials and material classes for casting and insert possible	[74,134,168]

¹ Cast material refers to applicability of the approach rather than material used in the cited study. ² Note that indirect approaches like the use of AM to realize more complex molds for production of IC lost models are not listed separately here. ³ HPDC is meant to include related semi-solid casting processes, too, in this context.

2.3.2. New Core Technologies

Realizing complexity in terms of internal cavities is the domain either of the integration of hollow structures or inserts by means of compound casting (see Section 2.2), or of lost cores. Similarly, cores may be employed to realize undercuts. Technologies for core production as well as core materials are closely linked to cast materials and casting processes and too diverse to cover in full here; thus, a focus is set on lost cores for HPDC, as well as new developments in decoring represented by the concept of collapsible cores [169], while the additive manufacturing of cores is discussed further below in Section 2.3.3 (note that general links to studies in this field may also be found among the entries in Table 3 above).

Lost cores for HPDC are not readily available on the market. None of the conventionally manufactured sand or salt cores can withstand the combined thermal and mechanical boundary conditions associated with this process, which have been scrutinized in great detail by Kohlstädt using computational fluid dynamics (CFD) methods [170–172], as well

as by Fuchs et al. [173]. The latter considered a simple reference mold yielding a hollow section of rectangular shape, with the inner cavity of the casting realized by a pressed and sintered salt core mainly consisting of sodium chloride and having a bending strength of 6.5 MPa at relevant temperature levels of 175 °C. Their experimental program foresaw variation in in-gate velocities ranging from 15 to 35 m/s with the in-gate extending over almost the full length of the casting. The failure of cores was observed at all velocities exceeding 15 m/s. In addition, inhomogeneous filling of the cavity surrounding the core contributed to failure. Parallel simulation covering fluid–structure interactions confirmed that core strength levels were surpassed under these conditions. On the positive side, the chosen simulation approach—which can obviously be transferred to other types of cores, too—was successfully confirmed as being able to predict core failure. Hence, the study underlined the limited viability of pressed and sintered salt cores for HPDC, suggesting the improvement of bending strength levels and optimized in-gate design as mandatory prerequisites for applying lost cores under typical HPDC conditions [173].

Kohlstädt and Kohlstädt et al. provided detailed studies on the factors affecting core failure in HPDC. Their findings, based on experimentally validated computational continuum mechanics simulations using the OpenFOAM framework and toolbox, indicate that the initial impact of the melt is a critical phase during the casting process, which is not adequately covered in standard commercial casting simulation software. To capture this effect, Kohlstädt et al. relied on more complex models incorporating fluid–structure interactions, though not covering the plastic deformation of cores. The workaround suggested for addressing the latter issue is to evaluate core deformation at 95% filling rather than after its completion. Thus, their study can be applied to virtually evaluate core viability for a given core material and casting system. The downside, which they frankly acknowledge, is the fact that in the triangle constituting the accuracy, stability and efficiency of the simulation approach, it is impossible to achieve an optimum for all of these aspects at the same time [170–172].

The apparent scarcity of suitable cores for HPDC has motivated several research activities. General evaluations of various core-making technologies for HPDC with a focus on salt-based solutions have recently been published by both Jelínek and Adámková, as well as Kallien [174,175]. A primary approach is increasing the strength of these materials in comparison to conventional, pressed salt cores. To this end, HPDC equipment manufacturer Bühler investigated the HPDC of salt cores, proving the general feasibility of this technique but failing to achieve significant market penetration [176,177]. However, the insight that salt cores produced from the melt rather than based on pressing can sustain the harsh HPDC process conditions has since fueled further research. A broad overview of the HPDC production of salt cores, updating and extending the aforementioned earlier studies by Bühler, was recently provided by Becker in his PhD thesis [178]. Further work on salt cores originating from a molten state was, e.g., performed by Findeisen et al., directed toward the gravity and low-pressure die casting of salt and salt mixtures [157].

An alternative is the strengthening of conventionally produced salt cores using reinforcing materials and structures, essentially following a composite materials approach. Gong et al. combined casting and reinforcement when studying the influence of glass fiber reinforcement of KNO₃-type salts on microstructure and mechanical characteristics when varying fiber lengths from 12.5 to 74 µm and stepping up content levels from 10 to 30 wt.%. Grain refinement, fiber pull-out and crack deflection were identified as primary mechanisms leading to a maximum bending strength of 41.32 MPa. Compared to non-reinforced materials, bending strength and impact toughness were increased by 55.9 and 315.1%, respectively [158]. In an earlier publication, Gong et al. reported results regarding Na₂SO₄–NaCl materials containing bauxite powders. This study is of particular interest, as it relies on extrusion-based additive manufacturing for shape generation, suggesting a path to highly complex core geometries. Mechanical properties are further enhanced via a liquid phase sintering step at 630 °C, resulting in up to 24.43 MPa of bending strength [159]. A further extension of these investigations was recently published by Gong et al. in which

strength levels of 59.08 MPa are reported for codundum powder reinforced salt cores with an matrix composed of Na_2SO_4 and NaCl [179]. Similar studies by Tu et al. extended the scope of this research by focusing on bauxite, glass fiber and sericite powders as strengthening additions at varied content levels. Depending on the type of reinforcement, bending strengths in the range of 35.08 to 40.88 MPa were achieved at an optimum powder fraction of 20 wt.%. While the added particles reduced shrinkage and had a positive effect on the hygroscopic properties of the materials, a decrease in the water solubility rate by roughly 20% as consequence of adding 20 wt.% of filler content may be seen as a drawback of the approach [156].

Beyond salt cores, sand cores, too, remain in focus for use in HPDC. Their general feasibility also for larger parts with considerable flow lengths was demonstrated by Koya et al., who considered a hollow casting for application as a motorcycle rear swing arm. Their studies confirmed aspects of the previously cited work by Kohlstädt et al. [170–172], showing that the impulsive pressure waves that were theoretically predicted and later experimentally confirmed contribute significantly to the loads acting on the core, but they can be alleviated via the adaptation of flow paths and filling conditions, thus opening up a process window for the use of sand cores in large component HPDC [161]. Currently, several suppliers of molding materials, such as Hüttenes-Albertus or Foseco, are taking up this approach and are actively working on or have already presented sand cores suitable for HPDC. While these typically remain limited to geometries of lower complexity, they are still likely to find their niche in select applications [162,180,181].

Having said this, there may be ways of circumnavigating the strength issue altogether: The lowered mechanical and thermal loads exerted by rheocasting on molds and cores may facilitate the use of more conventional core-making techniques while still yielding results that are economically competitive with HPDC components. With this in mind, Michels et al. evaluated several core materials and production techniques in view of their suitability, if not for HPDC, then at least for rheocasting. Prior to the advent of commercial sand core solutions for HPDC, they managed to show that surface-conditioned sand, as well as salt and even zinc cores, reach the required quality levels in rheocasting [182]. In a sense, their data indirectly confirms the aforementioned dominant effect of fluid impact on core failure identified by Kohlstädt et al. [170–172]. Considering the current, renewed interest in rheocasting discussed in Section 2.1, as well as the growing need of the automotive industry for housings incorporating water jacket cooling solutions fueled by the e-mobility transition (see [1]), this observation could open up an additional market for a growing rheocasting industry.

As far as the required strength of cores is concerned, casting processes like gravity sand and die casting, as well as investment casting, are less demanding than HPDC. This opens up alternative paths toward the realization of lost cores that diverge from the current state of the art. An entirely new approach in this respect is so-called collapsible cores, which are not dissolved for removal but destroyed by means of hydrostatic pressure. As such, the concept is based on so-called syntactic foams, i.e., materials with significant levels of engineered porosity introduced via hollow filler particles such as metal hollow spheres, glass or ceramic microspheres and cenospheres [183,184]. Materials of this type are well established based on polymeric matrices, e.g., as buoyancy devices in submarine and deep-sea exploration techniques [185,186], but they have also been produced with metallic matrices [187]. When used as cores, inorganic matrix materials are selected to which glass microspheres are added. Processing conditions are chosen to guarantee a certain level of open and, thus, interconnected matrix porosity. Via this porosity, it is possible to exert sufficient pressure on the hollow filler particles to make them collapse. The core can then simply be washed out as slurry in a batch process utilizing cold isostatic pressing (CIP) to build up the required levels of pressure [169]. The fundamental principle of this approach is illustrated in Figure 7 below.

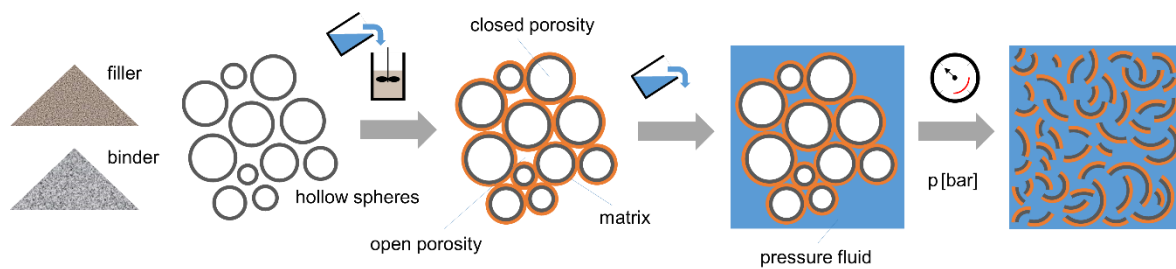


Figure 7. The fundamental principle behind the concept of collapsible cores. Hollow microspheres are embedded in an open-porous matrix. Decoring is achieved via cold isostatic pressing. Fluid entering the open porosity of the matrix in which the microspheres are embedded exerts pressure on the latter, making them collapse. The integrity of the core is lost, and its remainders can easily be washed out [169,188].

Detailed studies of this type of material have allowed for the identification of suitable hollow sphere and matrix types, indicating that the main challenge is maintaining the fine balance between providing sufficient strength for the casting process and limiting this property for the ease of decoring. This is best achieved at hollow particle volume fractions as high as 65%, combined with a filler consisting of magnesium oxide, monoammoniumphosphate and amorphous silicic acid, all mixed with silica sol in a ratio of 45:55 [188].

2.3.3. Printing of Cores, Molds and Patterns, Permanent and Lost

Additive manufacturing (AM) was discussed as a challenge the casting industry is confronted with in Part 1 of the present text (see Section 3.2.3 in [1]). However, it does also offer major benefits when employed not for the production of parts otherwise cast but of molds, patterns, cores and inserts, both lost and permanent. Thus, metal AM offers its generic benefits to casting if it is not seen as competing part production technology, as was the perspective in Part I of this Editorial [1], but rather in the context of permanent mold design and manufacturing. Links to the relevant AM processes are generally shorter than one might think, as related techniques such as build-up welding have been used for the repair and remanufacturing of molds for a considerable time. Of potentially even greater immediate benefit for the casting industry is, thus, the direct printing of sand molds and cores by means of binder jetting, a powder bed process in which the particles that form the powder are joined via a binding agent, printed layer by layer via an inkjet printhead into the powder bed [189].

Since the initial development of AM processes for metals, progress has been made in productivity, part size, accuracy and flexibility. The latter aspect nowadays even extends to producing multi-material structures. Still, the dominant process for metal AM remains the so-called laser beam melting (LBM) or laser powder bed fusion (LPBF) process, which relies on a powder bed built up layer by layer on a building platform and the fusion of powder particles via one or several lasers [190]. While powder bed technologies like this do not lend themselves easily to multi-material processing [191]—though some approaches have been realized and even commercialized, e.g., by companies like Aerosint via selective powder deposition [192,193]—methodologies that fall into the directed energy deposition category do [191,194]. These techniques transport the building material directly to the spot where the consolidation of the part occurs. A metal-based example of this kind is the LENS process, which is closely related to powder-based laser cladding processes [195]. In this case, the building material is transferred to the focal point of a laser as a powder by means of a carrier gas, where it is fused to the already existing structure. In short, the process allows for building up features on top of an existing, even non-planar, substrate, and it supports facile switching from one type of powder to another. With such characteristics, AM processes are optimally suited for complex die inserts. Their main benefit is the realization of complex, thermally optimized structures by means of facilitating the following:

- Conformal cooling, with cooling channels of complex geometry directly adjacent to the die surface, and/or
- Heat spreading, by combining materials providing strength with others supporting controlled transport of thermal energy.

Anand et al. recently dedicated an extensive review to this topic, which specifically stresses the benefits of conformal cooling for energy consumption, which is achieved directly by improving thermal management, as well as indirectly via superior process control. As a result, fewer scraps need to be remelted [167]. In both the conformal cooling and the heat spreading scenarios, laser-based AM processes profit from an extensive development history, which, over time, has covered most materials that are relevant for the manufacturing of permanent molds and dies. These include common tool steels, which can be processed by LPBF [196], binder jetting [197] and powder- and wire-based directed energy deposition (DED) processes [198,199], as well as highly conductive materials like copper [200–202] or even tungsten, which combines strength with attractive thermal properties [203]. If the highest productivity is sought, combinations of wire-based AM (WBAM) techniques with intermediate subtractive machining may also be considered. Machining is required due to the limited resolution of this process compared to the common powder-based techniques. Intricate internal cavities are, thus, difficult to produce, as they lack access for surface machining. However, multi-material structures have successfully been produced by means of such processes [204]. In cases where even higher productivity is required, wire arc additive Manufacturing (WAAM) may be considered as an alternative to laser-based technologies [205]. Achieving the required surface finish may require a hybrid manufacturing approach, combining additive with subtractive manufacturing both in the case of powder- and wire-based processes [167]. While all these technologies are available, their application in series production remains limited. Among the reasons are the cost of additively manufactured die inserts and also the technical concerns related to die life and to the danger of leakage. As a consequence, toolmakers still tend to acquire additively manufactured die inserts from external suppliers specializing in the respective processes and acting as contract manufacturers for a variety of industries, or for several foundries.

Much better established on an industrial scale is the printing of lost patterns, cores and molds. A recent review encompassing the full range of the topic was published by Shah et al. [206]. Specifically, the printing of sand cores and molds—often referred to as 3D sand printing (3DSP) - has already developed into a standard process. While there are solutions based on selective laser sintering (SLS) using binder-coated sand [207,208], binder jetting clearly dominates the field [155]. The massive advantage of this technique is that it combines the fundamental characteristics of the well-recognized sand-casting process with the productivity of a fast AM process. In essence, for sand casting, this unleashes all the geometrical freedom of the AM process but, for the final parts, saves the often-horrendous material costs associated with direct metal printing processes. As an added benefit, the possible part sizes surpass the typical limitations of common metal AM systems by far [1]. This new flexibility can be used to optimize the part itself but also to adapt the casting system, e.g., in terms of flow conditions yielding low-defect and, thus, high-performance parts. The latter approach was demonstrated by Sama et al. [209,210], who went even further by using AM processes for the integration of sensors in sand molds in order to facilitate the direct monitoring of melt flow, mold filling, core shift or ventilation during production [211–213]. Recent reviews on sand printing technology and use were provided by Upadhyay et al. and Sivarupan et al., who both stress the advantages of the process and highlight the evolution of the field [154,155], while Thiel et al. dedicated their slightly earlier study to the materials employed in this process [214]. An important aspect, which clearly illustrates the difference between sand printing and direct metal additive manufacturing processes, is the performance data documented in their studies: In sand printing, build rates reach more than 100 L per hour instead of cubic centimeters as in the case of powder-based metal AM, while the dimensions of the largest systems' build envelopes are measured in meters [155,215]. Major equipment providers like ExOne

or Voxeljet offer systems with maximum build volumes of up to 1.9 and 8 cubic meters, respectively. Figure 8 provides an idea of the sizes of such system, as well as an example of a complex core package printed using two types of binders.

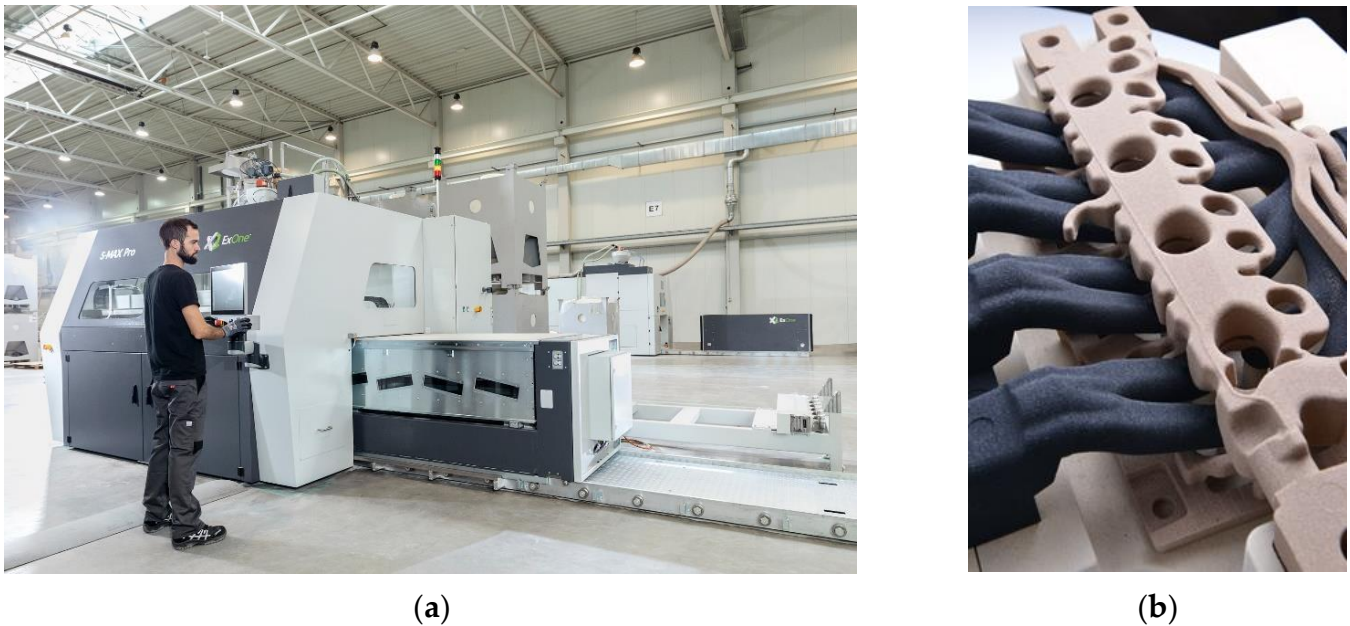


Figure 8. (a) S-Max Pro sand printer as offered by ExOne, offering a build box of $1800 \times 1000 \times 700$ mm (build volume 1260 L) and a build rate of up to 145 L/h, (b) examples of a printed core package for an internal combustion engine block consisting of furan-bonded components in black and hot hardened phenol-bonded components in beige (pictures kindly provided by ExOne (North Huntingdon, PA, USA); Copyright: ExOne).

However, despite such achievements, development needs remain with respect to new binder systems that are less hazardous and environmentally critical than, e.g., common furan resins [154,155]. Realizing such alternative binder systems would mirror developments in conventional sand casting, where aluminum foundries have, in many cases, already adopted inorganic binder systems [216] and new solutions are becoming available that are also suited for iron and steel [217,218]. The challenge has in fact been taken up already by the respective industries, with the result that printable inorganic binders are available commercially for the casting of light alloys [215,219], while others suitable for the casting of higher melting materials are either under development [220] or are currently being evaluated on a semi-commercial basis. The chemistry of such inorganic binders is typically based on alkali-silicates or waterglass. A disadvantage of this system is the need for additional curing at elevated temperatures, which is not required for the common organic systems, and a certain sensitivity to moisture, which calls for adequate packaging and storage measures.

Interestingly, in a recent study conducted in the USA, Lynch et al. find obstacles against broad introduction of 3DSP similar to those highlighted above for permanent die inserts when investigating the manufacturing ecosystem, with a special focus on small- and medium-sized foundries. They conclude that, among others, limited knowledge of the process on both the casting supplier and customer sides combined with considerable capital costs favor business models featuring specialized suppliers of cores and molds acting as hubs serving multiple foundries [221]. Beyond 3D sand printing, further AM techniques have gained importance in the production of lost cores. A very special example is the extrusion-based AM of Na_2SO_4 - NaCl salt cores, as proposed by Gong et al. Depending on the composition, which may include bauxite powders as reinforcing additive, their materials achieved room-temperature bending strength levels of up to 24.43 MPa, exceeding

the salt cores evaluated by Fuchs et al. in HPDC by one third [173] and, thus, possibly paving the way for the introduction of 3D-printed lost cores to this demanding process [159].

It is only a small step from the printing of lost cores or molds to the printing of lost models or patterns as used, e.g., in investment or lost foam casting. Investment casting has, thus, absorbed additive manufacturing technology basically in two different forms: the indirect method, which implies printing a master pattern used to create typically soft (e.g., silicone) molds for the actual patterns used in casting; and the direct method, producing the latter via AM [222,223]. The indirect approach will be disregarded here, as it is not necessarily a means to achieve increased complexity. For the direct approach, when using wax as printing material, a process very similar to conventional investment casting can be adopted. In contrast, producing patterns from either thermoplastic or thermoset polymers like epoxy, PLA or ABS calls for burning out rather than melting. An intermediate solution is the use of wax-like thermoplastic polymers typically processed as filaments using the FDM process. These combine the required strength with suitable melting characteristics for conventional removal techniques. Their advantages are, thus, rooted in the side effects of burning or thermally decomposing the patterns, among which are shell cracking, incomplete pattern removal or the accumulation of residual ash within the shell. Countermeasures against this deficiency of the process include limiting the amount of material used for the pattern. While the pattern's outer shell must necessarily be closed and of sufficient surface quality, internally, an intricate lattice rather than fully dense structures may provide the necessary strength by constituting a kind of 3D sandwich structure in which the skin takes the role of the face sheets. Needless to say, investment casting can also profit from rapid tooling approaches when it comes to the manufacturing of wax injection molding dies. In this respect, advantages match those already discussed above in a permanent mold casting context, as dies are typically made of metals—a fact which further distinguishes this method from the aforementioned indirect approach of producing a master pattern. Besides, as in sand casting, the direct production of molds—i.e., shells—using ceramic AM techniques is available and, according to Cheah et al., offers the largest lead time reductions in all additively supported processes [223]. The AM of ceramic materials in general has recently been summarized by Zocca et al. as well as Lakhdar et al.—in both cases, their use in investment casting is considered among the relevant application scenarios [224,225]. Table 4 below provides an overview of AM processes and materials for applications specific to investment casting, thus excluding the production of permanent dies for wax injection molding, and indicates the content of associated studies in the field.

Wang et al. recently summarized the various technologies used in rapid investment casting (RIC) and highlighted its benefits for the investment casting industry. As does 3DSP for sand casting, these techniques facilitate the production of highly complex, structurally optimized components. The drawback is, once more, productivity, such that the technique can mainly be employed for individual part to limited-scale series production, while conventional mold-based processes prevail for a larger series of components characterized by lower complexity limits [149]. However, according to Cheah et al., what seems to be a limitation in effect opens up a new opportunity for investment casting, which is not accessible to the conventional processing route due to its extended lead times (typically between 13 and 21 weeks according to this source, which can be reduced down to an optimum of 2.5 weeks by AM-based techniques) and the cost of tooling [223].

Table 4. Overview of AM processes used in rapid investment casting (RIC), as well as associated materials and specific application in the investment casting context.

Use Case	AM Process	Materials	Focus of Study	Ref.
Lost pattern production	FDM	diverse	Review of FDM application in RIC.	[226]
	FDM	ABS, PLA	Evaluation of surface quality.	[227]
	FDM/FFF	wax filament	Reduction of ash residues through using wax instead of PLA filament.	[228]
	FDM, multijet		Evaluation of surface quality.	[151]
	FDM, SLA, MJM, MJF	diverse, incl. ABS, PLA, PA 12, PVA	Experimental study on process applicability in view of lead time, cost and part quality aspects.	[229]
	SLA		Shell cracking during pattern removal.	
	SLA	photopolymer w. 20% wax	Review on SLA approaches, focus on dimensional accuracy.	[230]
	FDM, SLA	FDM—PVB, PLA; SLA—castable wax	AM process parameter influence on surface roughness of pattern, cast part.	[231]
	SLA	diverse	Review of SLA application in RIC.	[150]
	DLP	PMMA	Study on geometrical limitations.	[232]
Shell production	SLS	wax, polystyrene	Review on SLS application in rapid casting, covering sand and investment casting.	[208]
	SLS, binder jetting (BJ)	SLS—PrimeCast®; BJ—PMMA	Focus dimensional accuracy; need for wax impregnation of patterns.	[233]
	SLA	refractory fused silica	Kinetics and effects of cristobalite transition on shell mechanics, stability.	[234]
	SLS	ZrSiO ₄	Experimental production of investment casting shells and cores, part quality evaluation.	[235]
	DLP	Al ₂ O ₃ ·2SiO ₂	Material characterization and process evaluation in stainless steel investment casting.	[30]
	material extrusion	silica sol bauxite	Dimensional accuracy dependence on wall thickness, filling pattern.	[236]

2.4. Smart Castings

Endowing components of all kinds with some level of intelligence is an ongoing trend [237]. The purposes are manifold and include the monitoring and control of production or logistic processes [238], as well as the constant supervision of the components' state—the Structural Health Monitoring (SHM) case [239]—and the gathering of usage data [240] to optimize next generation product design [241] or facilitate predictive maintenance [242,243], to name but a few application scenarios. The motivation behind these can naturally be transferred to any kind of component, irrespective of the manufacturing process. However, while there are a wide range of publications about smart structures based on fiber-reinforced composites—partly based on their mechanical behavior, which may heighten the need for monitoring and is, thus, linked to the SHM topic in the aerospace sector [244–246]—there are far fewer studies focusing on smart castings. The reason is not necessarily a lack of interest in the field but rather the difficulties linked to the comparatively high process temperatures in metal casting, which afford specific protective measures. Lehmhus et al. recently suggested a classification of such approaches distinguishing between the four generalized principles illustrated in Figure 9 below [247].

Table 5 below offers an overview of the published literature, sorting studies by their main approach according to Figure 9, casting process, material and type of sensor. This listing is far from complete and should mainly provide a rough idea of the methods that are actually in use today. What is apparent from this collection is that in most cases, a combination of the enabling measures, namely simplify, distribute, harden and protect, is employed.

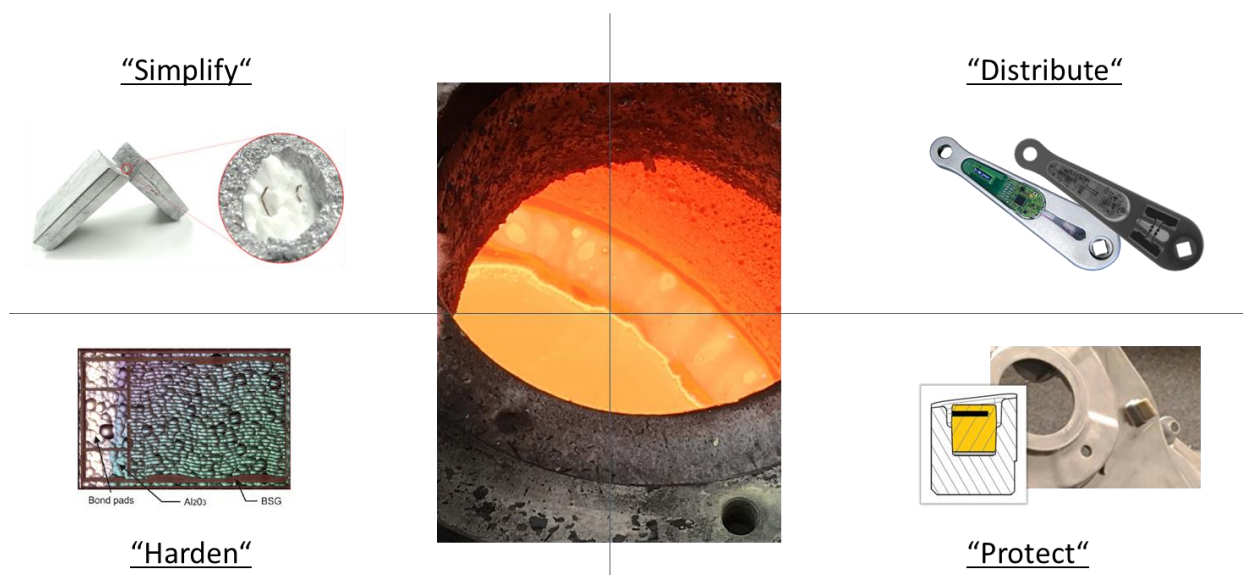


Figure 9. How to enable sensors and electronic systems to survive integration in metal castings—general principles: Top left, simplify—example of a rip wire sensor [247]; top right, distribute—integrate just those components that need to be integrated [248]; bottom left, harden—use materials that can withstand the process loads [249]; bottom right, protect—shield the integrated system against thermal and/or mechanical loads [250].

Of all the examples in Table 5, not surprisingly, most refer to the processing of aluminum alloys. This is partly due to the ease of processing associated with lower melt temperatures but also due to the emerging application scenarios in the area of automotive and unmanned aerial vehicles (UAV) for passenger transport. In both cases, the structural monitoring of safety-relevant components is the primary motivation—for the automotive industry, this aspect is gaining importance due to the advent of autonomous driving techniques, as well as new mobility concepts like car sharing. Both these trends imply that the car users are less aware of the state of the car they are occupying, as they are either not actively involved in driving or do not perceive themselves as being responsible for the car in the same way as they would if they owned it. As a consequence, the task of supervising condition and, thus, safety must be transferred to the vehicle—and for this purpose, it must be endowed with the necessary senses.

Beyond the direct impact of structural health monitoring and related techniques on safety, additive manufacturing has opened up a new perspective on sensor integration, which can be applied to metal casting primarily via the 3D printing of lost molds. Lehmus et al. have suggested a framework in which component-integrated sensors provide feedback on in-service loads to the manufacturer and, thus, allow product optimization. In an AM context, irrespectively of whether it relies on direct part manufacturing or the indirect, casting-related approach, such knowledge could be used to facilitate design improvements not only from product generation to product generation, but from individual part to individual part [241]. The principle is illustrated in Figure 10. Needless to say, knowledge about the state of a component and/or the loads it has seen can also help form decisions about its suitability for potential reuse once the overall system has reached the end of its service life.

Table 5. Selected examples of published research on functional system integration in metal casting.

Main Protective Approach	Casting Process	Material	Type of Functional Component Use Case/Objective of Study	Ref.
simplify, distribute, harden	SC	cast iron	mechanical vibration-based wire type sensor; <i>evaluation of sensing principle, sensor materials (SiO₂, Al₂O₃, Ti, W, 316L, FeCrAl)</i>	[251–253]
simplify, distribute, harden	SC	aluminum, cast iron	mechanical vibration-based wire type sensor; <i>load monitoring via shift in peak frequency of transmitted vibrations (proof of concept)</i>	[254]
simplify, distribute	GDC	aluminum	detection of overloading events via a rip wire type sensor with ceramic encapsulation; <i>integration process</i>	[247]
simplify, distribute	GDC	AlSi9Cu3	fiber-optic sensor (Regenerated Fiber Bragg Grating, RFBG); <i>monitoring of solidification shrinkage</i>	[255,256]
simplify, distribute	GDC	aluminum	fiber-optic sensor (Regenerated Fiber Bragg Grating, RFBG); <i>in-service monitoring of temperature, mechanical strain</i>	[257,258]
simplify, distribute	GDC	CuSn2	fiber-optic sensor (Regenerated Fiber Bragg Grating, RFBG); <i>temperature monitoring</i>	[259]
harden, distribute	LPDC	AlSi7Mg0.3	hybrid piezoresistive sensor system produced via screen printing and PVD; <i>structural health monitoring of safety-relevant castings, transfer to LPDC</i>	[260]
harden, distribute	LPDC	AlSi7Mg0.3	fully screen-printed piezoresistive sensor system; <i>structural health monitoring of safety-relevant castings, transfer to LPDC</i>	[261]
harden, distribute	HPDC	aluminum	piezoresistive DLC-type thin film pressure sensor; <i>load/structural health monitoring</i>	[262]
harden, distribute	HPDC	aluminum	screen printed piezoresistive thick film strain sensors; <i>load/structural health monitoring</i>	[263]
harden, distribute	HPDC	AlSi9Cu3	thermogenerator on borosilicate glass; <i>energy harvesting, feasibility study</i>	[264,265]
protect, distribute	HPDC	aluminum	piezoelectric transducers (LTCC/PZT); <i>strain and vibration sensing, vibration attenuation</i>	[266–268]
protect, distribute	HPDC	AlSi9Cu3(Fe)	piezoelectric transducers (LTCC/PZT); <i>structural health monitoring, demonstration of process chain</i>	[120]
protect	SC	aluminum	RFID tags; <i>part identification</i>	[269]
protect	HPDC	AlSi10MnMg	RFID tags; <i>part identification, demonstration of series production approaches</i>	[250,270]

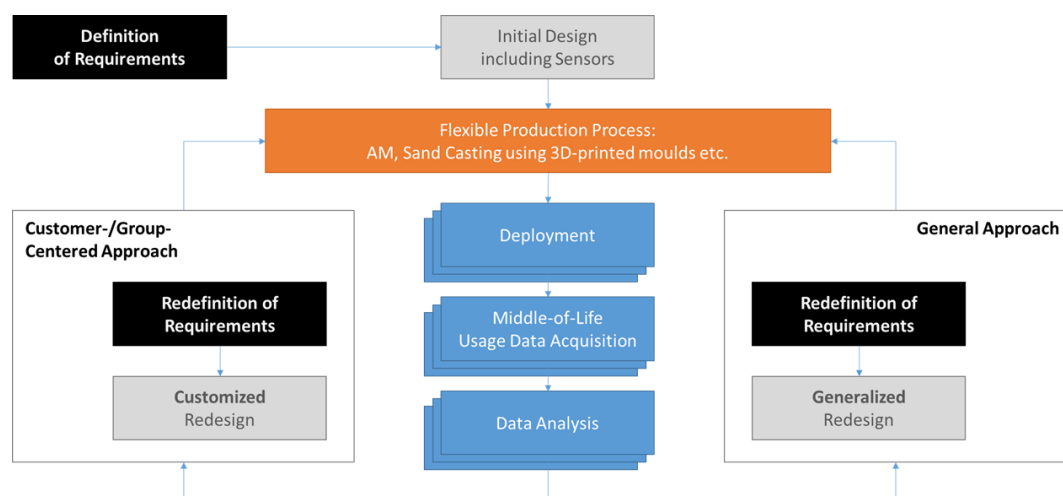


Figure 10. Schematic diagram describing a concept for constant product evolution relying on monitoring of in-service loads and conditions in combination with a highly flexible manufacturing process like indirect AM, i.e., the printing of sand molds.

Further investigations on the overarching topic of sensor integration in metal casting are available from Lehmkus et al., providing an overview of additional application scenarios as well as a more detailed description of selected technological approaches, including combined thick and thin film techniques for sensor deposition via screen printing [247,260].

2.5. Virtual Worlds: Modelling, Simulation and Optimization

2.5.1. Casting Simulation: State of the Art

From its humble beginnings, casting simulation has developed into a standard technique used by the majority of producers of castings as well as designers of molds over the last 30–40 years [271]. By now, several well-established commercial software packages exist, including, e.g., MAGMASOFT®, WinCast® expert, FLOW-3D® CAST and ProCAST, to name a few. Flender and Sturm offered a fascinating overview from the early years to the recent past in 2010, tracing major developments back to the 1950s and 1960s [272]. Even today, different numerical approaches are employed to cover the mold filling and solidification process, such as volume of fluid, finite element, finite difference or finite volume methods (VoF, FEM, FDM, FVM), as well as combinations of these. Less common are meshless methods like solid particle hydrodynamics (SPH), discrete element methods (DEM) or cellular automaton (CA) techniques, though the applicability of these to fluid dynamics problems is well known and their transferability to casting [273] and even HPDC are proven [274–276]. Recent extensive overviews of this subject area have been provided by Khan and Sheikh [277–279] as well as Danylchenko [280].

Currently, innovation in this area is typically not situated in the field of advanced numerical methods but rather dedicated to improvements in usability, the development of new output variables promising better predictions of local defects and/or material properties and increases in knowledge about the boundary conditions which affect the outcome of both simulations and actual casting. The latter aspect certainly remains a critical issue, as meaningful simulation requires a sound understanding of the models used in the physical problem. Here, the correct representation of heat transfer coefficients over time, including effects like the formation of gaps between the casting and the die, remains an area of research [281]. This is illustrated by the fact that two contributions to the present Special Issue are related to the topic [282,283].

A primary objective of almost any casting simulation is to identify and avoid sources of defects in castings. However, the difficulties associated with this task depend on the type of defect. While shrinkage-related defects, as well as gas porosity, can be forecasted reasonably well, oxide inclusions or oxide bi-films remain a challenge in this respect. Reasons for the difficulties observed are manifold and include both the higher complexity and the stochastic nature of formation mechanisms of the latter defects, as well as, on the physical side of the metal, a certain lack of associated non-destructive identification and localization methods which could otherwise support the efficient validation of predictive models. As a consequence of the difficulties in capturing defect formation via physics-based approaches, several researchers have reverted to AI and related model-free techniques to predict defect characteristics, some of which shall be covered in Section 2.6.2. A deficiency of many commercial casting simulation software packages is the fact that they do not model multiphase flow. This means that representations, e.g., of gas entrapment, may be questionable. Cao et al. recently demonstrated the capabilities of enhanced simulation techniques for the HPDC of zinc alloys [284]. An extensive review of simulation-based efforts at capturing casting defects is available from Jolly and Katgerman, covering both shape and direct chill (DC) casting. Though their review concentrates on aluminum casting, several of its conclusions are of general validity—this is particularly true for the major challenges the authors list in concluding their work, namely the “coupling of process physics”, access to “good process data for [model] validation [...]” as well as “thermophysical data and boundary conditions” and advanced “chemistry and process physics models to enable prediction of the defect formation” [273]. As a side note, it may be highlighted that Jolly published a similar review 20 years earlier, which already hinted

at many of the aforementioned deficiencies, indicating that the progress made is still not fully satisfactory. Other issues covered in this earlier work seem to have improved, though, including the adequate and accessible representation of results. However, as already stated above, speed was a matter of concern back then just as it is today in conjunction with digital twin concepts [285] (for digital twins, see Section 2.6.3).

Among other points, the statements by Jolly and Katgerman reflect the fact that software packages like those listed at the beginning of this section necessarily start from a macroscopic perspective and, thus, tend to express micro-scale phenomena like grain size or secondary dendrite arm spacing (SDAS), plus its effects on local material properties, in a simplifying manner, e.g., via phenomenological models, just as they describe certain defects in a cumulative manner by, e.g., providing an element-level estimate of average porosity. However, general material properties that are needed for this type of simulation, if not experimentally determined, can be calculated for arbitrary material compositions using computational thermodynamics approaches like CALPHAD [286,287]. Software packages and associated thermodynamic databases building on and supporting such techniques are readily available and typically allow the direct export of material datasets for casting process simulation, thus facilitating the virtual evaluation of varying and new alloy compositions. Examples include Thermo-Calc[®], JMatPro[®], MTDATA and Pandat. While originally addressing equilibrium states of the respective systems, several derivatives of the above approaches have been developed to cover non-equilibrium aspects like diffusion or precipitation phenomena. At the same time, the accuracy of predictions, e.g., of equilibrium states, is improved by increasingly augmenting or even replacing curve-fitting procedures applied to describe system compositions not directly reflected in experimental data with quantum mechanical calculations using density functional theory (DFT) or similar approaches [287]. Further solutions like MICRESS[®] are extending the capabilities of CALPHAD-based techniques toward the simulation of actual microstructures in 2D as well as 3D via combining them with a phase field approach [288]. Similar results have been obtained by Chen et al. and Gu et al. for somewhat larger volume elements at the cost of geometrical detail, relying on a cellular automaton solutions [289,290]. The backward coupling of these methods to process simulations providing the locally relevant boundary conditions of phase formation and microstructure evolution can, thus, be employed to capture the micro-scale characteristics of castings via links to macroscopic simulation [290]. Such capabilities have also been demonstrated by Jakumeit et al. in an HPDC context [291], while Wang et al. reviewed the broader field in view of Mg casting—their study is recommendable for those interested in immersing themselves deeper in the topic, as it also provides extensive background information about the phase field approach in general [292]. Such level of detail, however, comes with a price tag; though in principle, the size of the systems that can be covered is a function of the available memory size and the speed of calculation, the time required for calculating domains described in terms of mm remains prohibitively long.

In casting, as in product development in general, the outcome of the design phase determines the majority of costs, which is why the optimization of the mold design and process parameters is of considerable interest to the industry. The objectives of such efforts range from the control of defect occurrence to economics, the latter including a reduction of circulation material fractions, cycle time and reject rates, as well as, more recently, energy consumption. In response to this need, several software packages nowadays incorporate special optimization tools [293]. MAGMASOFT[®], for example, offers the automated generation and simulation of DoEs for user-defined parameter sets, plus diverse visualization tools for facilitating the evaluation of the outcome over several output parameters, the latter including user-defined criteria derived from standard output data via a broad selection of mathematical operations. Besides process parameters and boundary conditions, geometry variation is also possible and has been used successfully, e.g., in the layout of runner and gating systems [294–296]. Benefits of such techniques have been illustrated

quite graphically in conjunction with 3D-printed sand molds (see Section 2.3.3), making use of an almost unlimited design freedom for achieving optimum flow conditions [209,210].

While all of the aforementioned approaches are in general use today, they suffer from one severe drawback—the computational effort they require. The time constraint this implies effectively limits the number of parameter combinations as well as the level of detail that can be evaluated in practice—hence motivating the interest in metamodels and AI (discussed also in Section 2.6.3), which was already predicted more than 20 years ago by Jolly [285].

2.5.2. Effects of Defects in Castings, and How to Capture Them in Simulation

Accurately predicting the occurrence of casting defects is only part of the game. A challenge of similar magnitude and importance is the description of their effects on the performance of the final product, where the definition of performance depends on the use case and may include mechanical as well as functional aspects. Among the former, distinctions between quasi-static, dynamic and cyclic (fatigue) properties are necessary. Among the latter, thermal or electromagnetic properties may be mentioned, exemplified by the need to eliminate porosity in cast conductor bars of electric motors [297,298]. There are several studies which address the effects of certain types and expressions of defects in castings. It is impossible to cover these in detail here, though some will be mentioned below. For more detail, the reader is referred to reviews on the topic [299]; however, few are available which cover the full breadth of the topic. Instead, detailed studies concentrating on specific types of defects, materials or casting processes or a limited set of properties are numerous. The focus in the following will be on how the accumulated data can be used in early design phases, when no physical samples are available yet, and on efforts aimed at a deeper understanding of the influence of more complex defect populations on performance.

In principle, a connection between simulation-based methods of defect prediction and part performance evaluation is provided by many casting simulation software packages. Tools like MAGMASOFT® can transfer the simulation results of scalar, vector or tensor type to FE models for the simulation of the component's structural behavior. Others like WinCast® expert integrate such capabilities by being directly based on an FEM approach. These options also cover information about defects and can even include user-defined data (so-called user results). However, what is handed over to the FEM software is typically agglomerated, element-based data like porosity levels, whereas—in this specific case—information, e.g., on average pore size, size distribution or shape is missing [300,301]. These, however, have a significant influence on the actual effects of such defects. Blair et al. pointed out the need for the accurate prediction of location as well as property-determining features of casting defects already, back in 2005. While showing positive examples, e.g., in terms of microporosity effects on the fatigue limits of cast steel parts, they lament the fact that common casting simulation usually does not yield, e.g., pore size or size distribution data and call for more sophisticated models to provide higher levels of detail. In addition, though they present examples addressing these issues, they lament a lack of knowledge in forecasting both the extent and consequences of other types of defects, specifically cracks and tears, as well as inclusions predominantly caused by air entrainment, coining the term “unquantifiable factors” in this context [299].

In terms of porosity and other defects that can actually be detected via CT, a direct, though computationally demanding solution, to create the respective link is the accurate recreation of defects like pores in FEM simulations. This technique is supported by state-of-the-art software solutions for the analysis of CT data, which support the transformation of volumetric information into an FEM mesh, as recently demonstrated once more by Lauterbach and Nigge [302]. In practice, however, the computational effort associated with representing meso- or even micro-scale defects in an FEM mesh typically forbids the component-wide use of this approach. Instead, critical areas are identified where, e.g., excessive loads and defects coincide, and only these are modeled in full detail. Still,

when used as described, this technique requires the actual parts and their non-destructive analysis, based on which they can be classified individually as a quality part or as a reject. It is, thus, not directly suited for application in the design phase. In view of the latter, its main advantage is the increase in knowledge it promises regarding the effect of predominantly geometrical features of defects (size, shape, orientation relative to loads, etc.) on local material properties, while many studies concentrate on pore size and porosity alone [303]. The actual variability of such features found in HPDC was recently scrutinized by Nourian-Avval and Fatemi, who also studied and compared metallography, X-ray scans and CT as common means of capturing descriptive information, mainly on porosity in aluminum castings. Not surprisingly, their data suggests that the method of investigation will influence the outcome [304]. What remains is the problem of predicting such characteristics with a comparable level of accuracy. Meanwhile, to describe and better understand their effects, generating models of defect distributions artificially and testing them virtually is common practice. To simplify or even automate this process, different approaches are considered. Andrieux et al. base their solution on a generalization of the Ising Model, so-called Markov Random Fields (MRF). Models of porosity distributions are built from individual blocks which are either empty, thus representing a pore volume element, or not. Their spatial distribution is controlled by a material-related parameter, the attractiveness, β . Values of β are derived from CT scans performed on samples containing the type of defect under scrutiny. Their value may differ depending on the defect class. With this information at hand, several realistic expressions of defect distributions can be created for a pre-selected defect volume fraction. The respective models can then be transformed into FEM models constituting RVEs accessible to virtual testing [305]. A competing approach relies on generative adversarial networks or nets (GAN), which consist of two coupled neural networks engaged in a zero-sum game, the generator and the discriminator component [306]. A review on the theoretical background and use of such systems was recently published by Gui et al. [307]. In the suggested case, the discriminator would be trained using either physical or manually built samples (here, the MRF-based methodology could, in principle, come in once more) representing defect populations. The generator would provide alternative defect distributions, which could then be checked by the discriminator and either accepted or rejected. Over the course of this process, both the generator and the discriminator continue to learn and, thus, continuously improve their respective capabilities. This way, the models are not only produced automatically, but also with increasing efficiency. The method has, e.g., been used and described extensively by Raghavendra et al., though their focus is on the microstructure generation techniques, which explains why they omit the virtual testing of mechanical properties [308].

So, given the fact that the detailed prediction of defect characteristics on the part level is neither accessible in process nor in performance simulation, which paths can be adopted to address the issue of correctly dimensioning safety-critical castings? The common approach, i.e., the setting of safety factors based on worst case assumptions regarding defect features, will likely lead to a weight increase, which is contrary to the higher-level aims of energy and resource efficiency. In contrast, Andrieux et al. have suggested a stochastic modelling approach which promises at least a better justification of safety factors. Essentially, their technique is based on a combination of non-destructive evaluation, physical testing and the generation of simulation models describing defect distributions to facilitate additional, virtual testing—all this not so much in order to pinpoint explicit strength levels associated with certain structural features but instead to determine the range and statistical distribution of properties such as yield strength or elongation at failure, which are linked to the higher-level characteristics that casting simulation may actually offer, like porosity levels [305,309]. At present, the approach is, thus, very much focused on specific types of defects, namely gas and shrinkage porosity, and neglects additional factors like base material properties as, e.g., influenced by locally varying solidification conditions. Aspects of the latter kind have, e.g., been included by Kong et al. when considering the LPDC of wheels as an actual application scenario [310]. In addition, this method may

be prone to the misassignment of properties to the detectable types of defects in cases where others exist but may have gone unnoticed. Candidates of the latter kind include, e.g., oxide bi-films, which are critical specifically in high-pressure die casting [311–313] but hard to uncover via conventional X-ray or CT techniques alone [314]. Extending the scope to quality control in general, an additional challenge is the automated detection and accurate classification of defects via non-destructive techniques, as it directly affects reject rates in production and, thus, both economic and ecological aspects. While a reliance on human evaluation remains widespread, automated defect recognition (ADR) is gaining ground, as it profits from combination with AI image analysis techniques [315]. In practice, however, supervised machine learning, as usually employed, requires large amounts of training data. To generate such data sets is a major effort and usually precludes running the ADR system from the very start of production. Providing synthetic training data may elegantly solve this problem by virtually generating component models—or submodels of specific regions of interest—containing varied defect distributions and simulating the X-ray scanning or CT process. A secondary advantage of this concept is that it may help solve the issue of missing ground truth data, as it eliminates the need for manually labeled training data and, thus, the possibility of errors running up in the labeling process, which is tedious enough as it stands [316,317]. Fuchs et al. discuss this issue in detail, highlighting and even showcasing the variations observed in labeling, even when entrusting domain experts with this task. In their study, they build their models from basic elements like cylinders or cubes, which are randomly distributed in space, leading to final models of 80 mm edge length with internal features (defects) ranging from 200 μm to 3 mm in size. Of these, virtual projections and CT scans are generated using ray tracing algorithms reflecting realistic scanning parameters. These provide ground truth training data on an individual voxel level [318]. Mery follows a similar approach, comparing several established feature detection methods applied to X-ray scans and providing training data by merging images of defect-free samples with simulations of the appearance of defects in various locations of the part. While the restriction to ellipsoidal defect shapes may be seen as a drawback, an additional benefit of their work is that they provide a broad overview of publications dealing with the topic. According to their research, initial work in the field stems from the 1980s. The use of ellipsoidal defects superimposed to physical X-ray images led to improved performance compared to GAN-based images [319,320]. An application to the outer defects of castings using synthetic images created via the latter method has been reported by Ghansiyal et al. [321].

2.6. Industry 4.0: Digitalization of an Ancient Industry

Industry 4.0 translates to Foundry 4.0 for the casting industry, but what is actually meant by this term in this specific area? Kovacevic et al. addressed this question in their recent study and developed a concise description of the change that the manufacturing industry in general has recently experienced: in their own words, it has evolved “from factories where lack of real-time production information caused daily struggles, to factories where engineers need to deal with information overload and transfer parts of the decision making to machine learning and artificial intelligence systems” [293]. In further evaluating this process, they formulate nine pillars, which in their opinion characterize the transition from Foundry 3.0 to 4.0 [293]:

- Industrial internet of things (IIoT)
- Big data and data analytics
- Autonomous robots and cyberphysical systems (CPS)
- Horizontal and vertical system integration
- Simulation
- Virtual and augmented reality (VR/AR)
- Rapid prototyping resp. additive manufacturing (AM)
- The cloud
- Cyber security

Most of these aspects are interconnected. For example, horizontal and vertical system integration will build on IIoT implementations using, among others, CPS—the aim will be to consistently gather large amounts of data and analyze them to improve part quality [322]. The prerequisites of the latter are simulation techniques that can keep pace with manufacturing—a challenge specifically for high-pressure die casting—and, thus, enable digital twin approaches. Cloud services, be they centered on a single enterprise or sourced externally, may support the storage and management of data. Virtual and augmented reality may ease information transfer between automated systems and the human workforce [323], or between locations in remote maintenance or process optimization support scenarios [324,325]. Furthermore, VR has been suggested as a tool to optimize mold design, linking it to process simulation. Mold design itself can gain new freedom through AM techniques, as is discussed in Section 2.3.3. Finally, maintaining cyber security despite increased connectivity is an obvious must. In a separate analysis, Ravi stresses simulation techniques, optimization approaches for processes and tools, ubiquitous access via cloud-based solutions and extended data capture and analytics as critical technologies for a next generation foundry capable of “closing the loop between design and manufacturing” [326]. The following text will concentrate on glimpses at data collection and analytics, as well as digital twins and the advanced simulation techniques facilitating them.

2.6.1. Gathering Data and Managing Its Flow, Storage and Accessibility

It is a well-known statement that 80% percent of the time and effort of a data science project are devoted to gathering and preparing the data before any analysis can actually begin. Casting processes generate excessive amounts of data, and some, like HPDC, do so within seconds, or even milliseconds [300,327]. Figure 11, which is most likely still incomplete, attempts to illustrate the sheer amount of information running up during a single shot, as well as the different types of data which need to be handled within a timeframe of some 10 s. The magnitude of this task is illustrated in an example cited by Kopper, according to whom a year of HPDC production data provided by a partner company amounted to 956,986 rows times 109 columns of HPDC process data alone, plus 980 rows times 17 columns of alloy analysis and 1634 rows times 14 columns of tensile test data. It may be assumed that this huge dataset did not necessarily include all the time series and image data that a closely monitored HPDC process might generate [328].

However, the gathering of data within a relatively short time is an issue for which several solutions have already been suggested and tested in smart manufacturing or other contexts, not the least in this present Special Issue [329]. Similarly critical is the need to achieve the following:

- Include several devices within a manufacturing cell in the data collection effort,
- Associate this data with individual parts,
- Store it in a way that ascertains access to all data for a single part,
- Provide meaning to data points that is transferable from part to part, manufacturing cell to manufacturing cell, plant to plant and maybe even company to company,
- Secure a compromise between timeliness and the accuracy of information derived from the data, and
- Ascertain real-time capabilities in terms of data analysis.

All the above issues are not limited to metal casting, but they need solutions that work for the casting industry, too. Essentially, it boils down to the data analysis and preparation problem, to ways of lightening this burden, and to means of storage and retrieval that meet the aforementioned demands. Naturally, several steps in this direction have already been taken by the industry. However, casting machines are long-lived. Thus, it will take time before the latest generation’s capabilities have fully penetrated the whole industry. For this reason, in a foundry industry context, the retrofitting of systems deserves special attention, and it opens up a field for newcomers beyond the original equipment manufacturers focusing on ensuring connectivity as well as data sourcing, management and analysis.

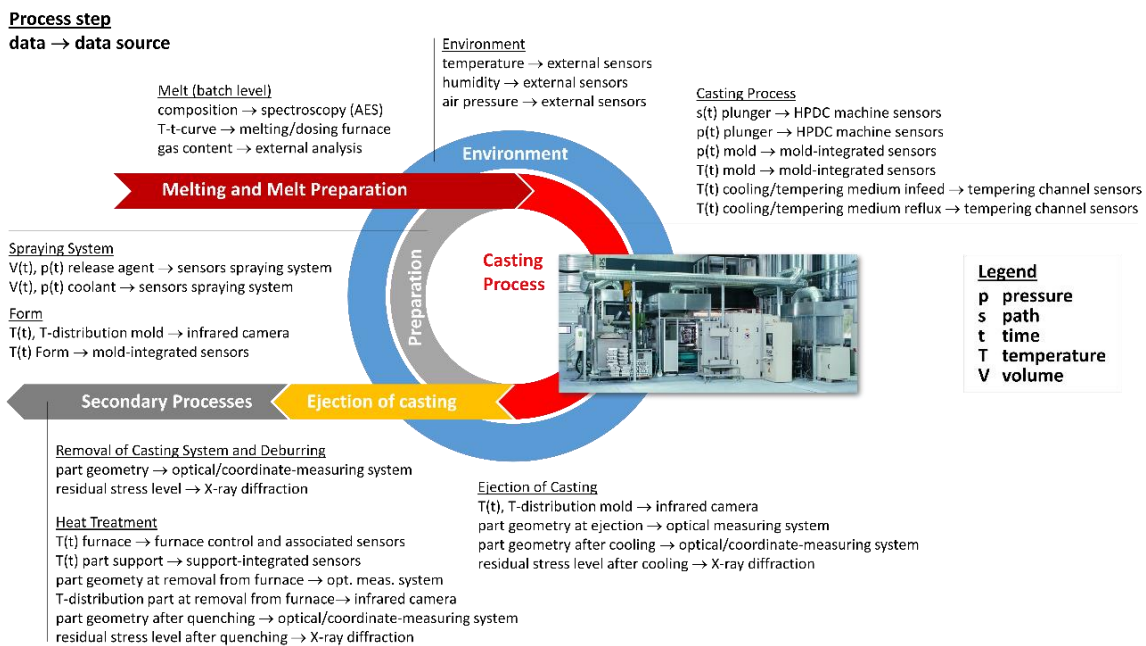


Figure 11. Digitalization meets the HPDC challenge. So much to measure, so much to correlate, and mere seconds left to do it in time to react on a part-by-part basis. Note that the list of parameters suggested here is indicative of the breadth of the issue only and certainly not complete.

Linking numerous sources of information is a specific need in high-pressure die casting, as several individual systems must interact to create the final product in an HPDC cell. Common interfaces and communication protocols are a must to handle the flow of data and guarantee the correct association to an individual product. One such standard is OPC UA—its aim and capability is encoded in its name, which translates to Open Platform Communication Unified Architecture. Originating in 2006 and now codified as the IEC62541 family of standards, it ensures cross-platform data exchange and has developed into a widely accepted basis of inter-system communication in smart manufacturing environments, including the foundry industry [330]. Alternatives to OPC UA as middleware ensuring communication in smart manufacturing systems include ROS, DDS and MQTT, all of which were compared by Profanter et al. in an Industry 4.0 context [331]. Among them, MQTT has also been suggested for metal casting applications [332]. On the semantic side, communication within an assumed manufacturing cell affords a clear terminology describing the manufacturing process itself, the tools involved in its execution and the information collected during each cycle. Ontologies can provide such definitions, and Yang et al. provide a detailed analysis of their capabilities and implementation in production engineering [333], while Sanfilippo et al. offer a general overview of ontology-related research in a manufacturing context, distinguishing between two different research strands, i.e., foundational and application-oriented ontologies [334]. Nilsson and Sandin discuss their role in guaranteeing “semantic interoperability” in this field [335]. Specific solutions have been proposed for covering aspects of casting technology; Kluska-Nawarecka et al. developed an ontology classifying casting defects [336], and they use the ontological approach in a further publication to create an extendable knowledge base on casting-related topics [337]. Ameri et al. describe an extension to the manufacturing service description language (MSDL) as formal ontology specifically dedicated to metal casting. However, their business case is management- rather than technology-oriented, addressing scenarios such as supplier selection [338].

Software architectures for data storage and information retrieval in a manufacturing context have been reviewed by Singh et al. [339]. Closer to the topic of metal casting is a work by Pennekamp et al., which includes HPDC as one of three case studies when discussing the broader framework of an envisaged overarching Internet of Production [340].

A fundamental approach in this respect is the so-called Lambda Architecture and its derivatives, such as Lambda XX and Kappa [339,341]. Figure 12 illustrates the fundamental concept of the former, highlighting the batch, speed and serving layer as main elements of this architecture. Information on open-source software tools which can be used for the construction of these elements plus an accessible explanation of the main aspects of the aforementioned big data architectures is offered by Singh et al. [339].

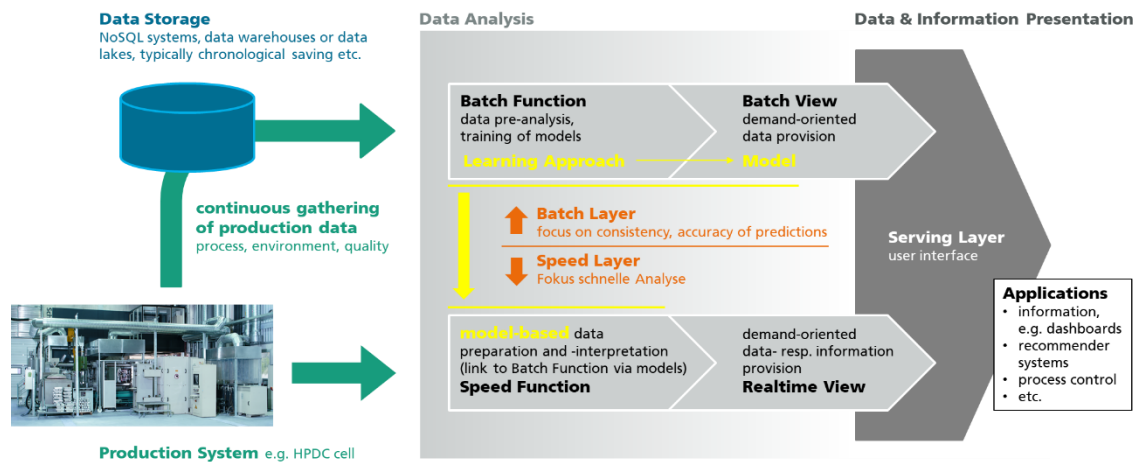


Figure 12. The Lambda Architecture, an example of a compromise between securing accuracy and speed in data analytics by providing two interconnected analysis paths differing in timeliness and accuracy of information provided.

Proponents of the Lambda Architecture claim that it attempts to circumvent an issue described by the CAP theorem, i.e., the fact that consistency, availability and partition tolerance cannot be optimized at the same time. Thus, the Lambda Architecture branches data processing, introducing a discontinuous and a parallel continuous analysis process, represented by the batch layer on one hand and the speed layer on the other hand. The former retrieves data from the continuously fed data storage in regular intervals to train predictive models, which are then used in the latter. Thus, real-time information as output of the speed layer does not account for the very latest data. This should be tolerable in large-scale production, as it can be assumed that the limited data inflow in between two updates of the speed layer will not affect the speed layer's models in any excessive way. Hence, it remains a necessary compromise, and, thus, object of criticism [342]; however, it has proven useful in many practical applications.

Data storage and extraction can be handled differently, too, irrespective of the overarching architecture. Common data storage and management solutions include conventional relational databases, NoSQL solutions, data warehouses and data lakes [343]. The main difference between the latter two is a partial reversal in data handling. Data warehouses follow an extract, transform, load (ETL) paradigm and, thus, employ generalized approaches for data storage, management and retrieval. In contrast, data lakes are built on an extract, load, transform (ELT) strategy. This implies that the adaptation of data to a common data storage and management concept is not foreseen, as the application-oriented transformation of data is left to the latter. In principle, this allows for greater flexibility in terms of extracting information, but it carries the risk of the lake turning into a data swamp, or even a graveyard, if one does not keep track and make use of incoming data. In general, despite some ambiguities in definitions, the main characteristic of data lakes is that they are assumed to be capable of ingesting all kinds of data without changing the original format. From this point of view, it appears that a data lake confined to a specific domain in which types of incoming data are known and subject only to limited change might in fact be an attractive solution if the data are heterogeneous. Considering the foundry industry, such heterogeneity is likely a primary characteristic of casting processes, as, e.g.,

as exemplified in Figure 11 above. The same is true for several other production processes. For this reason, it is not surprising that Rudack et al. chose this solution for capturing, storing and analyzing data in an HPDC context [329]. Beyond their study, there are several other examples of data collection and management solutions matched to foundry industry needs. Rix et al. built an information-processing framework dedicated specifically to high-pressure die casting on OPC UA-based communication and an adaptation of the Lambda Architecture [344]. Also, in conjunction with HPDC, Lipp et al. discuss the issue of load balancing in order to make optimum use of the available bandwidth when the data load exceeds recording capabilities, pointing toward domain expertise as a criterion for deciding which data to store and which to ignore [327,345]. Gramegna et al. also use OPC UA to gather information from HPDC manufacturing cell components and link the respective data to individual parts and associated simulation metamodels constituting a digital twin of the process, with the final aim of directly, during the casting process or immediately thereafter, identifying faulty parts [346]. Kim and Lee identify several tasks occurring in a die-casting fracture which can be supported via big data analytics using AI methods. These include, among others, algorithms for defect prediction, cause of defects diagnosis and casting parameter tuning, the latter effectively constituting a digital twin (see Section 2.6.3). In terms of the actual information extraction, they compare several AI methods like decision trees, random forests, neural networks and support vector machines (SVM). These various approaches are compared to each other in terms of accuracy achieved, both in a bare state and when using training data imbalance compensation [347]. The interested reader may find several more examples of this or similar cases.

2.6.2. Data Analytics: Finding Information in a Sea of Data

Data analytics can be categorized based on the aims it pursues, as visualized in Figure 13.

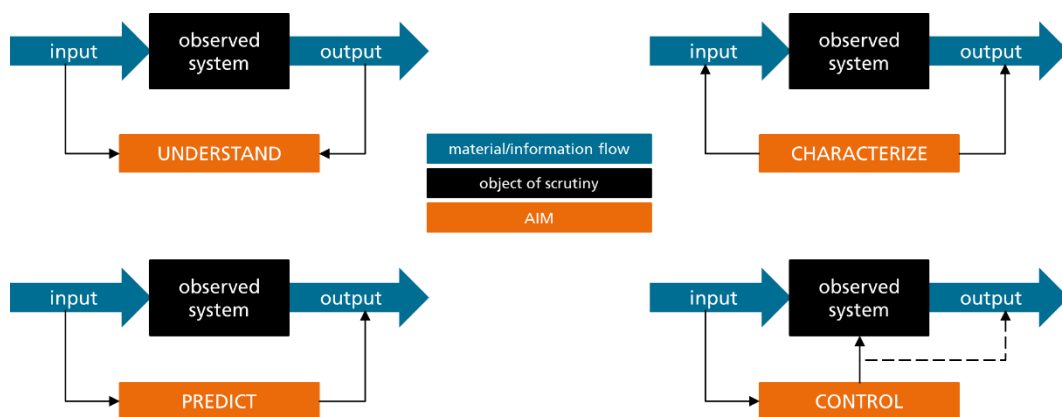


Figure 13. Ways of making use of data analytics—a general scheme in which almost anything, including casting processes, can take on the role of the object of observation represented by the black box.

Finding meaning in data in the sense of Figure 13 requires some kind of model that describes the link between input and output data. Different from physics-based approaches as described in Sections 2.5.1 and 2.5.2, purely data-driven solutions typically contain no inherent knowledge regarding the problem to which they are applied, like, e.g., the laws of physics. Instead, they rely on “experience”, or techniques for reliably detecting, e.g., commonalities in datasets (cluster analysis and feature detection) or correlations between input and output data (typically completed via supervised learning, thus requiring manual or automated labelling). The most common case for applications of such techniques in casting is to link process parameters to critical defects. What may sound simple actually requires a number of prerequisites to be achieved. First of all, suitable training data are needed—thus, the correct labelling of data becomes an issue, as does the availability of

data at the moment in time when one would like to have them, i.e., in a process control scenario, at the start of production. The latter may sound trivial, but as large data sets may be required for training, the practical benefit of some methods can only become apparent after a significant production volume has been reached. Furthermore, the available data should be balanced. Typically, for an established production process, this is not the case; in practice, there will be far more good quality parts than rejects [328], which means that compensation efforts are needed. On a theoretical basis, compensation can be achieved via techniques like SMOTE (synthetic minority oversampling technique)—also employed by Kim and Lee [347]—which increase numbers in the underrepresented group by numerically constructing additional input–output combinations [348]. Kim et al. used this technique in combination with random forest (RF) algorithms in order to improve training data for a defect prediction task in an HPDC setting [349].

Furthermore, while having stated at the beginning of this section that AI approaches in data analytics function without an analytical understanding of the underlying problem, this statement must be put into perspective in view of recent developmental trends; it is a common issue that data-driven techniques require a large amount of precisely that—data. Consequently, their value increases over time but is limited in early phases of use, or, in our present scenario, during production. To compensate for this, three fundamental approaches are possible:

- Execution of test casts covering optimized combinations of process parameters, i.e., **running a DoE** in order to improve predictive capabilities despite limited data availability.
- Use of **synthetic training data** derived from physics-based, numerical simulation to compensate for the lack of real-world data.
- Applying **physics-informed machine learning** methods to speed up the identification of causal relationships.

The first option addresses the problem that production data tends to be biased toward good quality, thus providing less information on critical parameter combinations. A test series which deliberately produces both good parts and scrap by covering an extended spectrum of processing conditions will, thus, provide additional input but at a cost that is acceptable only in medium- to large-scale series production. The extent of such a DoE can be subject to need-based adaptation, which can be realized by balancing the amount of information gathered from the dedicated training program and the actual production run.

The second option has already been discussed in the context of the effects of defect analysis and detection (see Section 2.5.2)—where physical data are not available, virtual data may be generated via simulation techniques matched to the problem in question. A possible drawback of this option is that the quality of synthetic training data is determined by the simulation’s ability to correctly cover correlations between processing conditions and part quality. This issue is recognized more often regarding simulation outcomes, but strictly speaking, it applies to test casts, too, as the capture of processing conditions and defect data may also be subject to ambiguity. However, the method can be applied separately to several individual issues within the broader field of relating process data and part quality. As implied above, casting simulation can be employed to directly generate virtual outcomes for various processing parameter sets. However, the results will not extend beyond the often still very generic information that casting simulation may provide today. On a more detailed level, aspects such as the correlation between features describing defect populations (size, volume fraction, spatial distribution, etc.) or stochastic distributions of such parameters may be linked to the resulting material properties by modelling and testing virtual samples via an FEM analysis (see Section 2.5.2).

Physics-informed machine learning, in contrast, attempts to further empower conventional machine learning techniques by endowing them with added information about the physics of the system under scrutiny. The basic principles of this approach were recently described by Karniadakis et al. [350]. By implementing such physics-based constraints, the

arbitrary training dataset that is necessary to achieve a given accuracy of the learned model may be significantly reduced.

In the end, what AI use comes down to is attaining speed—the prerequisite of a simulation that can predict the outcome of a process, or even allow the direct compensation of any adverse effects, while that process is still running. The casting process determines the degree to which this is possible. In HPDC, the time available to react is limited unless secondary processes can be adopted for compensation [351], while in large-scale gravity sand casting, where the solidification and cooling of parts may take days, access to a variation in the process may be difficult.

2.6.3. Digital Twins and Metamodels: A Matter of Speed

Though widely used, the term digital twin is subject to varying definitions [352]. The most common of these implies that a simulation model of a process or process chain—but not necessarily a production process—exists, as does a link to the physical process itself, by means of which model parameters can be adapted to reflect variations in the physical process under simulation [353]. Thus, the term implies a usage beyond the simulation model alone; in a production engineering context, the latter must foresee the possibility of feeding in real-world data on a part-by-part basis, and it must ideally allow the simulation to run in parallel to the process. This final aspect very much determines the digital twin's value beyond documentation and ex-post verification, as it allows for a reaction to the findings while the manufacturing process is still running. For a casting recognized as probably defective, subsequent manufacturing operations like machining can, thus, be spared, or, in the best of cases, processing conditions can be adapted to prevent any defects from occurring at all, or reduce their likelihood and extent.

The aforementioned review by Jones et al. analyzes 92 studies altogether that were published between 2009 and 2018, identifies specific themes related to the overall topics and associates the collected papers to them. Within the timeframe covered, an exponential growth in the number of publications is observed; meanwhile, judging from later data gathered by Moiceanu and Paraschiv, the number of publications has likely reached saturation [352,354]. Beyond the physical-to-virtual connection, in a subset of studies, Jones et al. also identified the opposite link, i.e., the manipulation of the physical entity, process or environment based on the findings facilitated by its virtual counterpart, as would be the case in a process control application [352]. Such concepts are collected by Kritzinger et al., whose literature review specifically focuses on digital twins in manufacturing environments. In their work, a stricter definition of the term digital twin is suggested, which Kritzinger et al. would only accept for systems of physical and virtual objects characterized by an automated two-way connection between both worlds; in contrast, systems realizing only the physical-to-virtual connection in this way, even if providing a manual link in the opposite direction, are classified as digital shadows (sometimes also called digital shades). A further distinction is introduced between the former two and what Kritzinger et al. call a digital model, which is manually connected to the real world [355]. Also focusing on manufacturing, He and Bai provide their own summary of the topic, listing several alternative definitions, though not insisting on the bidirectional automated link that Kritzinger et al. demand [356]. In the following, we will follow the definition of the latter, Kritzinger et al., to recognize our twins among the shades. The interested reader may find additional information about digital twin classification and disambiguation in the works of Shen et al., Kendrick et al. or Melesse et al. [357–359]. Among these, the survey by Kendrick et al. deserves special attention, as it includes considerations on the computational background of such systems encompassing hardware architecture, data exchange protocols and middleware platform candidates [358].

Due to its limited cycle time, which forbids the use of conventional casting simulation to establish the required bidirectionality, HPDC is among the most challenging scenarios when it comes to setting up a digital twin.: Since the time physics-based models require to solve complex multi-parameter, non-linear engineering problems is typically still measured

in hours, higherlevel models, i.e., metamodels, are needed to achieve the desired response times. Not surprisingly, data-driven methodologies have, thus, always been the focus of digital twin research. An overview of links between AI and digital twin concepts in manufacturing environments has been provided by Huang et al. [360]. Alternative paths toward the same aim—stepping up speed, or rather, reducing or eliminating latency—rely on model order reduction (MOR) or reduced order modelling (ROM) techniques [361,362]. On a broader scale, Simpson et al. summarize common types of metamodels for engineering tasks in their 2001 review [363], while Anglada et al. investigate their promise for high-pressure die casting [364]. Using surrogate models of this kind essentially translates to a simplification of complex descriptions of physical problems, such as casting processes, without losing (too much) meaning. In mastering this art, a fine balance must be maintained between the reduction in complexity and computational effort and the predictive capability of the model. Thus, evaluating and, ideally, quantifying the trustworthiness of the resulting models becomes an important side aspect of any research in the field. The motivation behind establishing metamodels is easy to comprehend. This prohibits the introduction of conventional simulation techniques as a tool for process control, while it also complicates optimization in the design phase of the part, tool and process.

The simplification of numerical models can be undertaken via several paths, many of which are linked to the replacement of physics-based models with data-driven ones, and, thus, to data analytics, AI and specifically machine learning. A major disadvantage of classical AI approaches for realizing a digital twin is the amount of training data required to achieve sufficient accuracy (see Section 2.6.2). In a digital twin context, there are two general solutions to this problem. The first would be to have the digital twin run in parallel to the process, which is initially supervised and controlled conventionally. During this phase, labeled data are generated that contain process parameters and boundary conditions as inputs and the resulting quality as the associated output data, based either on the usual or an extended quality control procedure. The respective datasets are used to train the AI model according to a supervised learning approach. In a following, transitional phase, the digital twin is validated against further real-world datasets. Predictions based on process parameters and boundary conditions are contrasted with the actual quality data obtained. The drawback of this method is the time lag between the start of production and the final deployment of the digital twin, following its successful validation, which means that its advantages can be used to the full extent only after an extended period of production.

The second approach involves limiting the amount of real-world training data. This option has already been described in Section 2.6.2 above. It can either mean relying fully or partially on synthetic, i.e., simulated, training data, or providing the training process with some amount of additional background information on the physics of the system to be modelled, e.g., via physics-informed machine learning [350]. The former approach affords the certainty that the conventional simulation model employed accurately captures the characteristics of the system under scrutiny. It must be assumed that in practice, deviations from optimum parameters will be limited, which means that the simulation must be capable of resolving such small changes, as well as correctly describing their consequences both in terms of tendency and magnitude. An alternative is a further scrutiny of simulation models using essentially non-AI techniques. Here, the MOR concept comes into effect. Strategies of this kind differ from classic machine learning methods, in that they take an existing system described by some complex transfer function relating an input or state vector (or state space, basically describing the system's degrees of freedom) to a certain output and attempt to limit the number of degrees of freedom to be accounted for to those that primarily control the response of the system. One such technique is proper orthogonal decomposition (POD), which is in turn closely related to principal component analysis (PCA), as known from statistics. Providing a detailed account of MOR techniques is not within the scope of the present text. For introductions and overviews, the reader is referred to works by Lucia et al. [365], Benner and Faßbender [361], Baur et al. [362] or Lu et al. [366].

Figure 14 provides a concept of a digital twin tasked with assessing and managing quality in a casting process, assuming that synthetic training data are generated via a physics-based model in order to establish and validate, on a virtual level, a metamodel which allows for the investigation of mold design variations on a much broader scope than is possible using the physical model alone. Following the design freeze and production of the mold, the concept envisages a test run reflecting a DoE covering the principal process parameters and allowing a final validation of the physical model as well as the metamodel. With this step successfully passed, the metamodel is available for use in process control. In this latter phase, a Lambda Architecture is assumed, which allows for continuous updates and improvements to the metamodel. Alternatively, the now validated physics-based model can be employed to supply additional virtual training data.

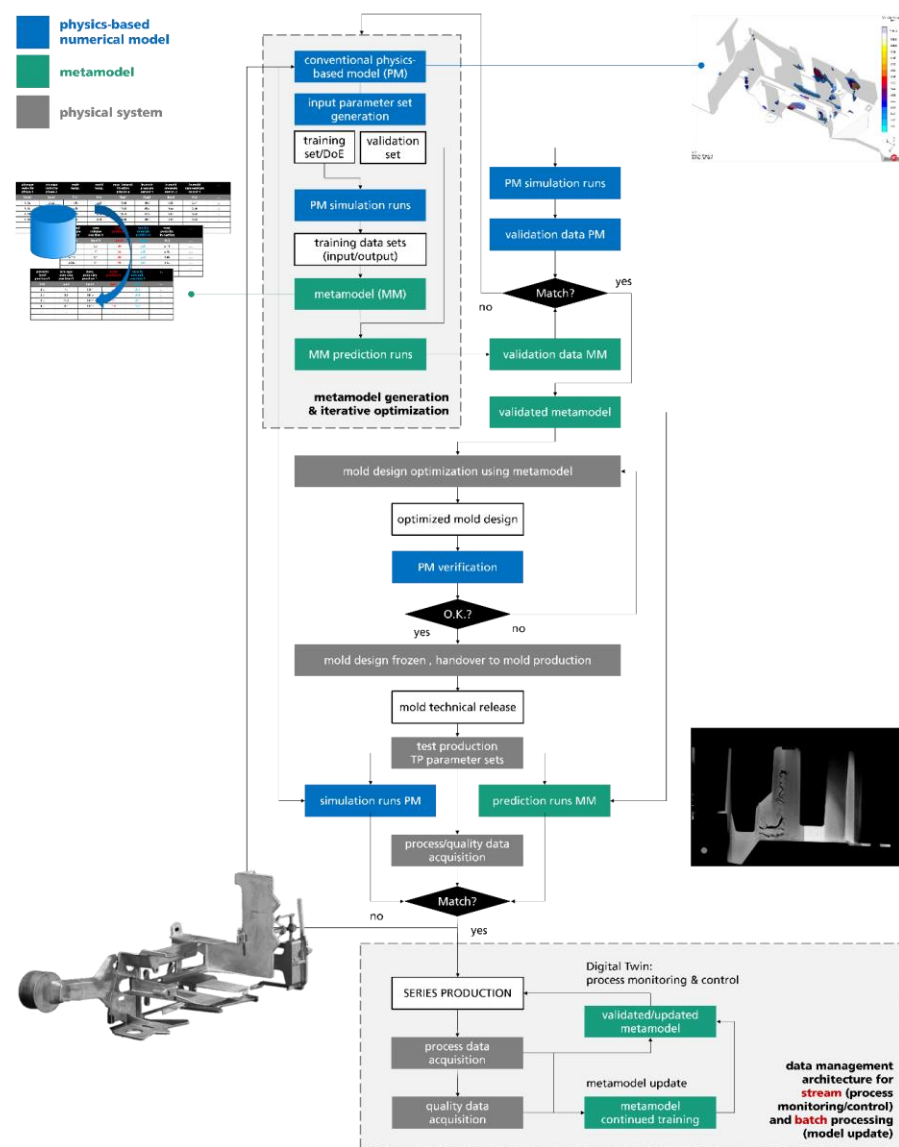


Figure 14. Combining advanced simulation and modelling and AI or MOR techniques to realize a digital twin in casting technology covering both the design and production phase.

Table 6 offers a glimpse at publications on digital twin and similar approaches associated with casting processes. It is noteworthy that many of these studies actually describe digital shadows or models in the strict sense proposed by Kritzinger et al. [355]. However, HPDC apparently receives increased attention from the research community, likely due to

the fact that it represents the greatest challenge and, thus, most urgently requires advanced low latency simulation techniques.

Table 6. Selected examples of publications on digital twins and similar concepts in metal casting.

Process	Material	Type → Method → Purpose/Results	Ref.
HPDC	Al alloys	Digital twin → Casting simulation ¹ , FEM, MOR and AI techniques based on ODYSSEE software package → Prediction of residual stress state, distortion to optimize spray quenching following solution heat treatment or casting, concept level. Bidirectional coupling envisaged on a process chain level (adaptation of spray cooling process).	[351]
HPDC	Undefined, typical alloys used in HPDC	Digital shadow → Real-world data collection and transformation, random forest classification → Detection of surface defects, real-time data processing facilitated by a complex event processing (CEP) engine. Physical to virtual, but no bidirectional coupling.	[367]
HPDC	Undefined, typical alloys used in HPDC	Digital shadow → FEM-based casting simulation ¹ , to which gradient-boosting regressor techniques are applied → Prediction of defects and microstructural characteristics like shrinkage, micro- and macro-porosity, secondary dendrite arm spacing (SDAS), etc., with response times of approx. 1 s suggested for use in inline process monitoring systems with unidirectional physical–virtual coupling, though not tested in this role yet.	[364]
HPDC	Undefined, typical alloys used in HPDC	Digital shadow → Real-world data collection and preparation, various AI techniques incl. decision trees, neural networks → Real-time monitoring for prediction of quality parameters related to various defects including misruns, shrinkage, blowholes and cold shuts. Unidirectional coupling realized.	[368]
SC	Al alloys	Digital model → Casting simulation ¹ , feed-forward back-propagation neural network → Optimization of gating system design, use of AI to facilitate broader search space. No direct virtual–physical coupling; hence, neither twin nor shade according to the definition by Kritzinger et al. [355].	[369]
IC/PC	Single-crystal superalloys	Digital model → Casting simulation ¹ , multiphase solidification modeling → Enhanced simulation technique for understanding formation of freckles. Coupling of two simulation approaches, but not of physical and virtual worlds; hence, essentially a digital model not relying on any metamodeling techniques. Potential for use as digital shadow or twin primarily based on the extended process duration, which does not require excessive speed.	[370]
LFC/EPC		Digital shadow → Casting simulation, thermodynamic simulation, inductive modelling → Concept of a base-level digital for lost foam/evaporative pattern casting production tasks. Potential for use in process control rather than prediction of outcomes and thus transition to digital twin status not elaborated in detail.	[371]

¹ Casting simulation typically refers to conventional, physics-based simulation approaches here.

3. Contributions to the Special Issue

This two-part Editorial introduces a Special Issue, in which the contributions gathered reflect several of the aspects discussed in the preceding chapters.

Fiedler et al. present results on complex, functionally graded composites produced by means of casting processes using porous filler materials. Metal matrix syntactic foams [187] of this type are based on A356 aluminum alloy and expanded pearlite particle beds, which are infiltrated by the aluminum melt, essentially forming a special kind of interpenetrating phase composite. This paper investigates the application of pre-compaction to the particle bed in order to achieve a density gradient that is also reflected in the final syntactic foam. Their investigation confirms that such density gradients can in fact be achieved and employed to tailor the mechanical behavior of the foam material. Pre-compaction leads to lower density in the respective area, with its level controlling the stiffness and

initial strength of the foam, while plateau stress and energy absorption depend primarily on overall density. Combining volume partitions containing non- and pre-compacted particles allows the direct adaption of stress–strain curves, e.g., by introducing multiple stress plateau levels in a single casting [372].

Gimmler et al. investigate the microstructure and properties of Zn–Al–Cu alloys of varied compositions used for bearing applications, combining phase field simulations of microstructure evolution during solidification with casting experiments for the validation of simulation results. The data show good correlation between predicted and experimentally obtained microstructures; furthermore, they indicate that mechanical properties, in this case, macroscopic hardness, may also reliably be predicted based on the applied modelling approaches [373]. From a global perspective, the study may support future approaches aimed at forecasting local material properties based on detailed knowledge of the local thermal history, stemming, e.g., from conventional macroscopic casting simulation and associated microscale modelling techniques, such as those employed in the present case.

Clearly related to the digitalization issue, Rudack et al. address first steps toward solving the problem of data collection and analysis in an HPDC context. The solution proposed is based on a data lake in which inputs are fed from several sources, mainly the components of a highly automated HPDC manufacturing cell. The connection between individual systems relies on the OPC UA standard as well as Node-RED and Apache Kafka implementations. The system is capable of handling several thousand measurements per minute, thus reflecting needs associated with the complexity of the HPDC process and matching the requirements as deduced from practical experiments, which pointed at a rate of 3000 messages transferred per minute during the operation of the system. While these messages may already contain scalar numerical data, vectors, arrays or annotated information, the transfer and storage of image data are not yet enabled and remain a future task, based on the importance of this kind of information in an HPDC context. Data storage as employed in the current setup, which is using the MinIO solution for the high-performance unstructured object storage of data lake type, is generally capable of handling such information. The study shifts the topic of analyzing the data to future investigations, focusing at this stage on the provision of a proven data management architecture that meets the needs of the HPDC process [329].

The studies by Wolff et al. [283] and Kouki et al. [282] are linked to virtual casting and simulation approaches, as they both consider the heat transfer coefficient (HTC), a crucial though difficult to determine parameter in casting. Kouki et al. propose and evaluate a tool for measuring time-dependent HTCs in permanent mold casting. In order to accurately capture both the heat transfer itself and the main factors influencing it, such as the possible formation of a gap between the casting and the mold during solidification, a multi-sensor setup has been selected, consisting of a multi-depth temperature sensor, a pyrometer and a displacement sensor, all of which are integrated in the experimental gravity die casting mold. Gravity die casting experiments aimed at validating the approach and gaining initial insights on actual HTCs were performed in open molds. Over time, as determined via an inverse calculation method previously verified in simulation, the resulting curves of HTCs show initial peak values of approximately $7500 \text{ W}/(\text{m}^2\text{K})$, followed by maxima of roughly $6000\text{--}7000 \text{ W}/(\text{m}^2\text{K})$, when casting an AlSi10Mg alloy at $700 \text{ }^\circ\text{C}$, with the level of the initial as well as the following main peak depending on the number of preceding casting cycles. With the general approach justified, future work will be oriented toward transferring the measurement principle first to closed models then to HPDC molds. The expectations are that results from the coming experiments will improve the predictability of cast part properties [282].

Wolff et al., on the other hand, study the way that HTCs in gravity die casting are influenced by process parameters. Using a dedicated test tool and analyzing the results using statistical methods such as variance analysis, they were able to not only identify but also quantify differences in the relevance of primary controlling parameters like mold material and coating depending on the change in contact conditions between casting and

mold. Specifically, the question of whether a gap was formed or, if this was not the case, contact pressure varied significantly in the course of solidification and cooling [283]. Thus, this work provides valuable new insights to be taken into account during mold and thermal control system design.

Sama et al. make use of 3D sand printing flexibility to integrate capacitive and magnetic sensors into printed molds [374]. By this means, they are able to measure melt flow velocity as well as velocity over time profile and can, thus, show good correlation—within a 5% margin—between simulated and experimental data. The study is related to earlier work by the authors on using the geometrical freedom of mold generation via an additive manufacturing process in order to reduce detrimental aspects like turbulent flow by means of adapting a casting system and specifically sprue design [210] and to derive generalized design rules facilitating this for arbitrary parts [209]. By confirming simulated results, the present study further validates the general approach chosen in the earlier works. Furthermore, the investigation is related to several other studies involving this group of authors on the realization of smart sand molds addressing different monitoring issues arising in sand casting, such as core shift [212] or ventilation [213].

A very different approach to improving the understanding of solidification sequences is presented by Niu et al., who perform model experiments on NH_4Cl –70% H_2O solution to facilitate the optical observation of solidification and crystallization processes. Their specific objective is to study the influence of a consumable cooler lowered into the fluid on the formation of crystallites and later grains. Their findings indicate that the melting of the cooler supports the formation of equiaxed crystallites and can, thus, lead to the formation of a favorable microstructure containing lower volume fractions of columnar dendrites. The transfer of these results to actual casting experiments is still pending [375].

The study by Avila-Salgado et al. is focused on the optimization of HPDC equipment, investigating two different Cu–Ni–Co–Cr–Si alloys modified with B and Nb as new materials for plungers. Samples of the materials were produced, subjected to solution and ageing heat treatments and extensively characterized in terms of phase composition, microstructural characteristics like secondary dendrite arm spacing (SDAS) and wear resistance. Based on these experiments, an alloy of composition Cu–9Ni–1Co–1.6Cr–2Si–0.1Fe–0.2Nb was identified which outclassed the wear resistance of the standard plunger material C17530 by a margin of almost 40% [376]. The study of this class of materials has, in the meantime, led to further improvements based on the variation in Ni and Co contents, as well as Zr addition [377].

The contributions by Wan et al. and Yan et al. do not center on shape casting but rather on the processing of semi-finished casting products, such as billets or ingots [378,379]. The paper by Wan et al. is concerned with the avoidance of carbon segregation typically occurring during the casting of high-carbon steel billets. Wan et al. concentrate on the use of final electromagnetic stirring (F-EMS) to mitigate this effect and employ different parameter combinations in terms of current intensity and frequency to identify the settings which would minimize the observed local variation in carbon content [378]. Yan et al. discuss the formation and characteristics of freckle segregation, as seen during the electroslag remelting (ESR) of bearing steel ingots of composition GCr15SiMn. Experimental investigations addressing location, compositions, structure and geometrical features of segregates in sample ingots were accompanied by theoretical considerations (e.g., CALPHAD approaches realized using the Thermo-Calc software package), finally leading to a model of freckle segregation formation which integrates, among others, geometric, thermodynamic, fluid dynamic and compositional aspects as well as composition-dependent viscosity levels. As a result, a threshold for freckle formation was suggested in terms of a relative Rayleigh number limit for the material in question [379].

4. Conclusions

The present text concludes a two-part Editorial introducing a Special Issue on Advances in Metal Casting Technology. Part I, published in 2022, provided a perspective on

the global output of the casting industry, linking certain developmental trends to changing markets and products. The latter includes automotive structural castings as well as new applications linked to e-mobility. E-mobility is also a main driver for the industry's transition, as BEV powertrains require far less cast weight than those of conventional ICEVs. Environmental concerns, which specifically affect the energy-intensive casting industry, introduce a further resetting of boundary conditions. At the same time, new manufacturing techniques, such as AM or 3D printing, establish potential challenges to which the industry must find answers [1].

Part II attempts to provide such answers in terms of technological developments which address both the competitiveness and environmental impact of the foundry industry. The techniques covered are partly new and partly revived by new boundary conditions improving their economic standing. Among the latter, **semi-solid casting** approaches have emerged from the valley which followed an initial hype in the early 2000s; now, it has become a technology to be reckoned with. This has become possible in part due to the refinement of processes, which has led to diversification, as well as to the crystallization of techniques, which are improved in both reproducibility and ease of implementation, showing considerable promise for industrial success.

Compound and hybrid casting may provide economic solutions for realizing larger components while eliminating some of the difficulties encountered in the notorious Gigacasting approach for the production of automotive structural components. In a direct comparison, such approaches could limit shot weights and locking force requirements, thus allowing production to rely on smaller HPDC equipment. Similarly, tool weight could be reduced, and, thus, logistics could be simplified, as less support is needed in the regions of the die which provide backing for the insert only and not for the casting. Further applications of hybrid casting are linked to e-mobility and associated with thermal or electric contact rather than structural strength. Examples of this kind include cooling channels for housings as well as hybrid rotor designs. Establishing satisfactory interface characteristics remains a challenge irrespective of the nature of the application. Linked to it is the need to develop simulation techniques based on which local properties of joints can reliably be predicted, irrespective of the nature of the interface—material joint, form or force fit, or combinations of these.

Complexity is a hallmark of castings in general, though the possibilities of achieving it may differ among the various casting processes. The use of cores is limited by the harsh conditions typical of the HPDC process; hence, many efforts are taken to develop solutions which can overcome these obstacles. Candidates include cast or reinforced salt cores, but by now, there are also solutions for qualifying sand cores for use in HPDC, even though the intricacy of geometries achievable is more limited in this case. An alternative is the integration of additively manufactured inserts in HPDC via a compound casting approach. Additive manufacturing as such, on the other hand, is fully commercialized in sand casting, where it enables the production of casting systems and component geometries that are difficult to fabricate using, e.g., model-based molding processes, which may prevail in large scale series production, even though binder jetting processes constantly evolve in terms of achievable part size and productivity.

Another type of complexity is introduced by **smart castings**, which add functionality in terms of communication, sensing, energy harvesting or actuation capabilities, or combinations of these. The field is still young, and the approaches are accordingly diverse and often hampered by economic consideration when it comes to real-world application. There is hope, though—looking at the automotive industry, it is the advent of autonomous driving which may raise interest in the self-sensing or SHM capabilities of safety-critical castings. The latter will gain importance via the trend toward Gigacasting, while the high cost of such castings may render the extra effort introduced by a sensor or RFID system almost negligible, and the potential benefit considerable.

Simulation techniques and their further development, especially in view of capturing the occurrence of defects, the prediction of their characteristics and the effect on material and

component properties, represent a focal area in their own right. Beyond their improvement along classic lines of development, the need for speed experienced by many applications supports studies on metamodel development following, e.g., AI approaches, or alternatives like MOR. The potential of these techniques is vast, and so is the scope of publications in the field. Future developments may lead to the identification of certain optimum solutions to attain specific objectives. In general, reducing latency in this field will support die and part design by allowing the evaluation of additional variants, and it will facilitate the step from process monitoring to control even for the fastest of processes, progressing from mere digital shades to actual digital twins.

Digital twins, as such, are the subject of many research efforts on the application of advanced big **data analytics and AI** techniques in metal casting. The trend toward Industry 4.0 has reached the foundry industry, too, and is slowly being adopted. In most cases, the focus is on the following: recognizing, as early as possible, potential casting defects; deciding on compensating measures, ideally while the process is still running; and adapting parameters accordingly. The challenge is in finding the relevant information in the incoming stream of data. Even though this is not a problem unique to the casting industry, solutions have to be found to securely handle the vast amount of data and to cope with its diversity. To do so, several different data handling and storing solutions are being evaluated, ranging from conventional databases to concepts like data warehouses and data lakes.

Not surprisingly, the individual contributions to this Special Issue touch upon many of the aforementioned points and can, thus, be seen as a good indication of the relevance of the respective topics, as well as the fact that both the industry and research communities are actually accepting the challenges previously outlined. This confirms the statement put forward already at the end of Part I of this editorial—that the casting industry may be in difficult waters, but its innovative power should not be underestimated, and neither should its capability to hold its ground in a highly competitive global manufacturing environment [1]. Metal casting may be among the oldest manufacturing technologies, but it is certainly not outdated, and there is absolutely no indication that it might ever be. The future holds exciting prospects for the metal casting industry.

Funding: This research received no external funding.

Acknowledgments: The author wishes to thank Staffan Zetterström of Comptech AB, as well as Martin Kaiser and Anica Melia of ExOne, for providing the images needed to illustrate the points made in this article, specifically regarding the RSF/RheoMetalTM rheocasting process and with respect to the capabilities of sand printing by means of the binder jetting process.

Conflicts of Interest: The author declares no conflicts of interest.

Abbreviations

3DSP	3D Sand Printing (AM process)
ABS	Acrylonitrile Butadiene Styrene
ADR	Automated Defect Recognition
AI	Artificial Intelligence
AM	Additive Manufacturing
AR	Augmented Reality
BEV	Battery Electric Vehicle
BJ	Binder Jetting (AM process)
CA	Cellular Automaton
CAD	Computer Aided Design
CALPHAD	CALculation of PHase Diagrams
CAP	Consistency Availability Partition (tolerance)
CFD	Computational Fluid Dynamics
CFRP	Carbon Fibre Reinforced Polymer
CIP	Cold Isostatic Pressing

CPS	Cyber-Physical System
CT	Computed Tomography
CTE	Coefficient of Thermal Expansion
DC	Direct Chill (casting)
DDS	Data Distribution Service
DED	Directed Energy Deposition (AM process)
DEM	Discrete Element Method
DFT	Density Functional Theory
DLC	Diamond-Like Carbon
DLP	Digital Light Processing (AM process)
DoE	Design of Experiments
EaF	Elongation at Failure
ELT	Extract, Load, Transform
EMS	Electro-Magnetic Stirring
EPC	Evaporative Pattern Casting
EPS	Expanded Polystyrene
ESR	ElectroSlag Remelting
ETL	Extract, Transform, Load
FBG	Fiber Bragg Grating (optical sensor/sensing principle)
FDM	Finite Difference Method (numerical simulation approach)
FDM	Fused Deposition Modeling (AM process)
FEM	Finite Element Method (numerical simulation approach)
FFF	Fused Filament Fabrication (AM process)
FVM	Finite Volume Method (numerical simulation approach)
GAN	Generative Adversarial Networks/Nets
GDC	Gravity Die Casting
GISS	Gas-Induced Semi-Solid casting (rheocasting technique)
GSC	Gravity Sand Casting
HPDC	High Pressure Die Casting
HTC	Heat Transfer Coefficient
IC	Investment Casting
IIoT	Industrial Internet of Things
ICEV	Internal Combustion Engine Vehicle
LBM	Laser Beam Melting (AM process)
LENS	Laser Engineered Net Shaping (AM process)
LFC	Lost Foam Casting
LPBF	Laser Powder Bed Fusion (AM process)
LPDC	Low Pressure Die Casting
LTCC	Low-Temperature Co-fired Ceramics
MSDL	Manufacturing Service Description Language
MJM	Multi-Jet Modeling (AM process)
MOR	Model Order Reduction
MPTO	Multi-Phase Topology Optimization
MQTT	Message Queuing Telemetry Transport
MRF	Markov Random Fields
NRC	New RheoCasting (rheocasting process)
OPC UA	Open Platform Communication Unified Architecture
PA	PolyAmide
PCA	Principal Component Analysis
PEEK	PolyEther Ether Ketone
PLA	polylactic acid
PMMA	PolyMethyl Methacrylate
POD	Proper Orthogonal Decomposition
PVA	PolyVinyl Acetate, PolyVinyl Alcohol
PVB	Polyvinyl Butyral
RFBG	Regenerated Fiber Bragg Grating (FBG-type optical sensor)

RFID	Radio Frequency IDentification
RIC	Rapid Investment Casting
ROM	Reduced Order Modelling
ROS	Robot Operating System
RSF	Rapid Slurry Formation (rheocasting process)
RVE	Representative Volume Element
SC	Sand Casting
SEED	Swirled Enthalpy Equilibration Device (rheocasting process)
SDAS	Secondary Dendrite Arm Spacing
SHM	Structural Health Monitoring
SLA	Stereolithography (AM process)
SLS	Selective Laser Sintering (AM process)
SMOTE	Synthetic Minority Oversampling TEchnique
SOM	Segmented Object Manufacturing (AM process)
SPH	Solid Particle Hydrodynamics
SSR TM	Semi-Solid Rheocasting (rheocasting process)
SVM	Support Vector Machine
UAV	Unmanned Aerial Vehicle
UTS	Ultimate Tensile Strength
VOF	Volume of Fluid (numerical simulation approach)
VR	Virtual Reality
WAAM	Wire Arc Additive Manufacturing (AM process)
WBAM	Wire-Based Additive Manufacturing (AM process)
YS	Yield Strength

References

- Lehmhus, D. Advances in Metal Casting Technology: A Review of State of the Art, Challenges and Trends—Part I: Changing Markets, Changing Products. *Metals* **2022**, *12*, 1959. [CrossRef]
- Steinert, M.; Leifer, L. Scrutinizing Gartner’s Hype Cycle Approach. In *PICMET 2010 Proceedings: Technology Management for Global Economic Growth*; Kocaoglu, D.F., Anderson, T.R., Daim, T.U., Eds.; IEEE: Phuket, Thailand, 2010; pp. 1–13.
- Campani, M.; Vaglio, A. A simple interpretation of scientific/technological research impact leading to hype-type evolution curves. *Scientometrics* **2015**, *103*, 75–83. [CrossRef]
- Gartner Hype Cycle. Available online: <https://www.gartner.com/en/research/methodologies/gartner-hype-cycle> (accessed on 4 January 2023).
- Kondratjew, N.D. Die langen Wellen der Konjunktur. *Arch. Für Sozialwissenschaft Und Sozialpolitik* **1926**, *56*, 573–609.
- Flemings, M.C.; Riek, R.C.; Young, K.P. Rheocasting. *Mater. Sci. Eng. A* **1976**, *25*, 103–117. [CrossRef]
- Young, R.M.K. The Processing of Metals as Semi-Solid Slurries. Ph.D. Thesis, University of Surrey, Guildford, UK, 1986.
- Jorstad, J.L. Semi-Solid Metal Processing from an Industrial Perspective: The Best is Yet to Come! *Solid State Phenom.* **2016**, *256*, 9–14. [CrossRef]
- Czerwinski, F. Semisolid Processing—Origin of Magnesium Molding. In *Magnesium Injection Molding*; Springer: New York, NY, USA, 2008; pp. 81–147.
- Decker, R.; LeBeau, S. Thixomolding. *Adv. Mater. Process.* **2008**, *166*, 28–29.
- Huang, J.; Arbel, T.; Ligeski, L.; McCaffrey, J.; Kulkarni, S.; Jones, J.; Pollock, T.; Decker, R.; LeBeau, S. On Mechanical Properties & Microstructure of TTMP Wrought Mg Alloys. In *Magnesium Technology 2010*; Agnew, S., Ed.; The Minerals, Metals and Materials Society (TMS): Warrendale, PA, USA, 2010; pp. 489–493.
- Zhu, Y.; Midson, S. The Status of Magnesium Injection Molding in China. *Solid State Phenom.* **2019**, *285*, 436–440. [CrossRef]
- Decker, R.; LeBeau, S.; Wilson, B.; Reagan, J.; Moskovich, N.; Bronfin, B. Thixomolding[®] at 25 years. *Solid State Phenom.* **2016**, *256*, 3–8. [CrossRef]
- Mohammed, N.N.; Omar, M.Z.; Salleh, M.S.; Alhawari, K.S.; Kapranos, P. Semisolid Metal Processing Techniques for Nondendritic Feedstock Production. *Sci. World J.* **2013**, *2013*, 752175. [CrossRef]
- Kapranos, P. Current State of Semi-Solid Net-Shape Die Casting. *Metals* **2019**, *9*, 1301. [CrossRef]
- Midson, S.P. Rheocasting processes for semi-solid casting of aluminum alloys. *Die Cast. Eng.* **2006**, *50*, 48–51.
- Midson, S.P.; Jackson, A. A Comparison of Thixocasting and Rheocasting. In Proceedings of the 67th World Foundry Congress, Harrogate, UK, 5–7 June 2006; Institute of Cast Metals Engineers (ICME): Tipton, UK, 2006; pp. 22/1–22/10, ISBN 9781604236767.
- Bakhtiyarov, S.; Siginer, D.A. Rheoprocessing of Semisolid Aluminum Alloys. In *Encyclopedia of Aluminum and Its Alloys*, 1st ed.; Totten, G.E., Tiryakioğlu, M., Kessler, O., Eds.; Taylor & Francis Group: London, UK, 2018. [CrossRef]
- Jarfors, A.E.W. A Comparison Between Semisolid Casting Methods for Aluminium Alloys. *Metals* **2020**, *10*, 1368. [CrossRef]

20. Li, G.; Qu, W.-Y.; Cheng, L.; Guo, C.; Li, X.-G.; Xu, Z.; Hu, X.-G.; Li, D.-Q.; Lu, H.-X.; Zhu, Q. Semi-solid processing of aluminum and magnesium alloys: Status, opportunity and challenge in China. *Trans. Nonferrous Met. Soc. China* **2021**, *31*, 3255–3280. [CrossRef]
21. Wannasin, J. Applications of Semi-solid Slurry Casting using the Gas Induced Semi-Solid Technique. *Solid State Phenom.* **2013**, *192–193*, 28–35. [CrossRef]
22. Kaufmann, H.; Uggowitzer, P.J. Fundamentals of the New Rheocasting Process for Magnesium Alloys. *Adv. Eng. Mater.* **2001**, *3*, 963–967. [CrossRef]
23. Wabusseg, H.; Kaufmann, H.; Wahlen, A.; Uggowitzer, P.J. Theoretische Grundlagen und praktische Umsetzung von New Rheocasting von Al-Legierungen. *Druckguss-Praxis* **2002**, *1*, 16–19.
24. Uggowitzer, P.J.; Kaufmann, H. Evolution of Globular Microstructure in New Rheocasting and Super Rheocasting Semi-Solid Slurries. *Steel Res. Int.* **2004**, *75*, 525–530. [CrossRef]
25. Wessén, M.; Cao, H. The RSF Technology: A Possible Breakthrough for Semi-Solid Casting Processes. In Proceedings of the International Conference of High Tech Die Casting, Vicenza, Italy, 21–22 September 2006.
26. Ratke, L.; Sharma, A.; Kohli, D. The RSF Technology for Semi-Solid Casting Processes. *Indian Foundry J.* **2011**, *57*, 33–36.
27. Doutre, D.; Hay, G.; Wales, P.; Gabathuler, J.-P. SEED: A new process for semi-solid forming. *Can. Metall. Q.* **2004**, *43*, 265–272. [CrossRef]
28. Yurko, J.A.; Martinez, R.A.; Flemings, M.C. The Use of Semi-Solid Rheocasting (SSR) for Aluminum Automotive Castings. *SAE Trans. J. Mater. Manuf.* **2003**, *112*, 119–123.
29. Serving the Platform of Tomorrow! Available online: <https://comptech.se/> (accessed on 11 March 2023).
30. Li, M.; Du, W.; Elwany, A.; Pei, Z.; Ma, C. Metal binder jetting additive manufacturing: A literature review. *J. Manuf. Sci. Eng.* **2020**, *142*, 090810. [CrossRef]
31. Zetterström, S.; Comptech AB, Skillingaryd, Sweden. Private communication, 2022.
32. Chauke, L.; Möller, H.; Curle, U.A.; Govender, G. Industrial heat treatment of R-HPDC A356 automotive brake callipers. *Solid State Phenom.* **2013**, *192–193*, 533–538. [CrossRef]
33. Dey, A.K.; Poddar, P.; Singh, K.K.; Sahoo, K.L. Mechanical and wear properties of rheocast and conventional gravity die cast A356 alloy. *Mater. Sci. Eng. A* **2006**, *435–436*, 521–529. [CrossRef]
34. Govender, G.; Ivanchev, L.; Jahajeeah, N.; Bëan, R. Application of CSIR Rheocasting Technology for the Production of an Automotive Component. *Solid State Phenom.* **2006**, *116–117*, 501–504. [CrossRef]
35. Guo, H.M.; Yang, X.J.; Wang, J.X. Microstructure and mechanical properties of Al alloys by semi-solid processing with LSPSF technology. *Mater. Sci. Forum* **2009**, *628–629*, 477–482. [CrossRef]
36. Gupta, R.; Sharma, A.; Pandel, U.; Ratke, L. Effect of heat treatment on microstructures and mechanical properties of A356 alloy cast through rapid slurry formation (RSF) process. *Int. J. Cast Met. Res.* **2017**, *30*, 283–292. [CrossRef]
37. Möller, H.; Govender, G.; Stumpf, W.E.; Knutsen, R.D. Influence of temper condition on microstructure and mechanical properties of semisolid metal processed Al-Si-Mg alloy 356. *Int. J. Cast Met. Res.* **2009**, *22*, 417–421. [CrossRef]
38. Möller, H.; Govender, G.; Stumpf, W.E. Comparison of the heat treatment response of SSM-HPDC 6082 and 6004 wrought alloys with A356 and F357 casting alloys. *Mater. Sci. Forum* **2011**, *690*, 53–56. [CrossRef]
39. Anticorodal@—Unendlich Anpassungs Fähig. Available online: <https://rheinfeldens-alloys.eu/legierungen/anticorodal/> (accessed on 21 February 2022).
40. Rosso, M.; Peter, I.; Villa, R. Effect of T5 and T6 Heat Treatments Applied to Rheocast A356 Parts for Automotive Applications. *Solid State Phenom.* **2008**, *141–143*, 237–242. [CrossRef]
41. Rosso, M. Thixocasting and rheocasting technologies, improvements going on. *J. Achiev. Mater. Manuf. Eng.* **2012**, *54*, 110–119.
42. Tahamtan, S.; Fadavi Boostani, A.; Nazemi, H. Mechanical properties and fracture behavior of thixofomed, rheocast and gravity-cast A356 alloy. *J. Alloys Compd.* **2009**, *468*, 107–114. [CrossRef]
43. Zhang, L. Technology Innovation & Green Development—Chinese Foundry Industry Status and Outlook. Chinese Foundry Association. 2015. Available online: https://www.foundry-planet.com/fileadmin/redakteur/pdf-dateien/18.09.2015BRICS_2015_China.pdf (accessed on 13 May 2020).
44. Atkinson, H.V. Alloys for Semi-Solid Processing. *Solid State Phenom.* **2012**, *192–193*, 16–27. [CrossRef]
45. Curle, U.A. Semi-solid near-net shape rheocasting of heat treatable wrought aluminum alloys. *Trans. Nonferrous Met. Soc. China* **2010**, *20*, 1719–1724. [CrossRef]
46. Li, G.; Lu, H.; Hu, X.; Lin, F.; Li, X.; Zhu, Q. Current Progress in Rheoforming of Wrought Aluminum Alloys: A Review. *Metals* **2020**, *10*, 238. [CrossRef]
47. Sauermann, R.; Friedrich, B.; Bünck, M.; Bührig-Polaczek, A.; Uggowitzer, P.J. Semi-Solid Processing of Tailored Aluminium-Lithium Alloys for Automotive Applications. *Adv. Eng. Mater.* **2007**, *9*, 253–258. [CrossRef]
48. Bünck, M.; Kütke, F.; Bührig-Polaczek, A.; Arnold, A.; Friedrich, B.; Sauermann, R. Semi-solid Casting of High-reactive Wrought Alloys by Means of the Alloy AlLi₂.1Mg5.5ScZr (AA1420*). *Solid State Phenom.* **2008**, *141–143*, 145–150. [CrossRef]
49. Langlais, J.; Lemieux, A. The SEED Technology for Semi-solid Processing of Aluminum Alloys: A Metallurgical and Process Overview. *Solid State Phenom.* **2006**, *116–117*, 472–477. [CrossRef]
50. Langlais, J.; Andrade, N.; Lemieux, A.; Chen, X.G.; Bucher, L. The Semi-Solid Forming of an Improved AA6061 Wrought Aluminum Alloy Composition. *Solid State Phenom.* **2008**, *141–143*, 511–516. [CrossRef]

51. Curle, U.A.; Govender, G. Semi-solid rheocasting of grain-refined aluminum alloy 7075. *Trans. Nonferrous Met. Soc. China* **2010**, *20*, s832–s836. [CrossRef]
52. Qi, M.F.; Kang, Y.L.; Zhou, B.; Liao, W.N.; Zhu, G.M.; Yan, D.L.; Li, W.R. A forced convection stirring process for Rheo-HPDC aluminum and magnesium alloys. *J. Mater. Process. Technol.* **2016**, *234*, 353–367. [CrossRef]
53. Kang, Y.; Li, J.; Li, G.; Wang, J.; Liu, A.; Chen, J.; Qi, M. Preparation and rheological die-casting of 7075 aluminum alloy semisolid slurry. *J. Netshape Form. Eng.* **2020**, *12*, 74–80.
54. Kongiang, S.; Plookphol, T.; Wannasin, J.; Wisutmethangoon, S. Effect of Two-Step Solution Heat Treatment on the Microstructure Of Semisolid Cast 075 Aluminum Alloy. *Adv. Mater. Res.* **2012**, *488–489*, 243–247. [CrossRef]
55. Payakkapol, S.; Chayopitak, N.; Kunsuwan, P.; Ohtake, N.; Srimanosawapak, S. Production of low impurity aluminum rotor for motor efficiency enhancement. *MATEC Web Conf.* **2018**, *192*, 01043. [CrossRef]
56. Aluman®—Widerstand Auch bei Höchsten Temperaturen. Available online: <https://rheinfeldens-alloys.eu/legierungen/aluman/> (accessed on 10 February 2022).
57. Palanivel, S.; Kuehmann, C.; Edwards, P.; Filip, E. Casting Aluminum Alloys for High-Performance Applications. U.S. Patent Application US2019/0127824A1, 2 May 2019.
58. Evans, J.M.; Hagan, R.J.; Routh, W.C.; Gibbs, R.N. Aluminum Alloys for Die Casting. Patent Application WO2020/028730A1, 6 February 2020.
59. Schweigert, D.; Mileti, M.; Morhard, B.; Fromberger, M.; Sedlmair, M.; Lohner, T.; Otto, M.; Stahl, K. Innovative transmission concepts for hyper-high-speed electromechanical powertrains. In Proceedings of the EDrive 2019 International Conference, Bonn, Germany, 10–11 July 2019.
60. Schweigert, D.; Gerlach, M.E.; Hoffmann, A.; Morhard, B.; Tripps, A.; Lohner, T.; Otto, M.; Ponick, B.; Stahl, K. On the Impact of Maximum Speed on the Power Density of Electromechanical Powertrains. *Vehicles* **2020**, *2*, 365–397. [CrossRef]
61. Ley, M.; Al-Zuhairi, A.; Teutsch, R. Classification approach for hybrid components in mechanical engineering with a focus on additive manufacturing. *Procedia CIRP* **2021**, *100*, 738–743. [CrossRef]
62. Schuh, G.; Bergweiler, G.; Dworog, L.; Fiedler, F. Die Karosserie aus dem Aluminium-Druckguss. *WT Werkstattstech.* **2022**, *112*, 580–585.
63. Volk, W. Giga-Casting Ist Geeignet, den Karosseriebau neu zu Denken. Available online: <https://www.automobil-produktion.de/produktion/gigacasting-ist-geeignet-den-karosseriebau-neu-zu-denken-501.html> (accessed on 7 March 2024).
64. Bork, H. Teslas Konstruktionsmethode Verbreitet Sich in China. Available online: <https://www.konstruktionspraxis.vogel.de/teslas-konstruktionsmethode-verbreitet-sich-in-china-a-1081294/> (accessed on 5 January 2023).
65. HiPhi and Tuopu Jointly Announces the Production of Ultra-large Die-Casting Integrated Rear Body Structure. Available online: https://www.human-horizons.com/main/en/news_detail?id=78 (accessed on 22 September 2022).
66. Yuan, L. In China, Tesla Is a Catfish and Turns Auto Companies into Sharks. Available online: <https://www.nytimes.com/2021/11/30/business/china-tesla-electric-cars.html> (accessed on 5 January 2023).
67. Zhang, P. HiPhi Becomes Latest Chinese EV Startup to Use Large Die-Casting Technology. Available online: <https://cnevpost.com/2022/03/01/hiphi-becomes-latest-chinese-ev-startup-to-use-large-die-casting-technology/> (accessed on 5 January 2023).
68. Loveday, S. VW’s Project Trinity to Use Giga-Casting & Automation to Compete with Tesla. Available online: <https://insideevs.com/news/577128/volkswagen-compete-tesla-gigapress-robots/> (accessed on 5 January 2023).
69. Waldersee, V.; Schwartz, J.; Schimroszik, N. Gigacasting and Robots: How Volkswagen’s Trinity Aims to Catch up with Tesla. Available online: <https://www.reuters.com/business/autos-transportation/giga-casting-robots-how-volkswagens-trinity-aims-catch-up-with-tesla-2022-03-31/> (accessed on 5 January 2023).
70. Ludwig, C.; Holt, N. The Die Is Cast for Volvo’s Future EV Production. Available online: https://automotivemanufacturingsolutions.h5mag.com/ams_january-march_2022/oem_volvo_mega-casting (accessed on 5 January 2023).
71. Die Casting Machine Carat. Available online: https://www.buhlergroup.com/content/buhlergroup/global/en/products/carat_die-castingmachine.html (accessed on 4 January 2022).
72. Bühler Adds Volvo Cars to Its Megacasting Customers. Available online: https://www.buhlergroup.com/content/buhlergroup/global/en/media/media-releases/buehler_adds_volvocarstoitsmegacastingcustomers.html (accessed on 5 January 2023).
73. Blala, H.; Pengzhi, C.; Gang, C.; Shenglun, Z.; Shangwen, R.; Zhang, M. Innovative Hybrid High-Pressure Die-Casting Process for Load-Bearing Body-in-White Structural Components. *Int. J. Met.* **2024**. [CrossRef]
74. Lehmus, D.; Pille, C.; Rahn, T.; Struss, A.; Gromzig, P.; Seibel, A.; Wischeropp, T.; Becker, H.; Diefenthal, F. Druckgießen und Additive Fertigung: Durch strategische Kombination das Beste aus zwei Welten nutzen. *Giesserei* **2021**, *108*, 36–43.
75. Jiang, W.; Fan, Z.; Li, C. Improved steel/aluminum bonding in bimetallic castings by a compound casting process. *J. Mater. Process. Technol.* **2015**, *226*, 25–31. [CrossRef]
76. Fang, X. Evaluation of Coating Systems for Steel Aluminum Hybrid Casting. *J. Mater. Sci. Eng. A* **2017**, *7*, 51–67.
77. Schittenhelm, D.; Burbli, A.; Busse, M. Stahlverstärkter Aluminiumguss—Bauraumreduzierung durch lastfallgerechte Auslegung eines Verbund-Längsträgers mittels Mehrphasen-Topologieoptimierung. *Forsch. Ingenieurwesen* **2018**, *82*, 131–147. [CrossRef]
78. Papis, K.J.M.; Hallstedt, B.; Löffler, J.F.; Uggowitzer, P.J. Interface formation in aluminum-aluminum compound casting. *Acta Mater.* **2008**, *56*, 3036–3043. [CrossRef]
79. Papis, K.J.M.; Löffler, J.F.; Uggowitzer, P.J. Light metal compound casting. *Sci. China Ser. E Technol. Sci.* **2009**, *52*, 46–51. [CrossRef]

80. Rübner, M.; Günzl, M.; Körner, C.; Singer, R.F. Aluminum-aluminum compound fabrication by high pressure die casting. *Mater. Sci. Eng. A* **2011**, *528*, 7024–7029. [[CrossRef](#)]
81. Schwankl, M.; Kellner, R.; Singer, R.F.; Körner, C. The influence of sandblasting on the morphology of electrolessdeposited zinclayers on aluminum sheets. *Appl. Surf. Sci.* **2013**, *283*, 202–208. [[CrossRef](#)]
82. Koerner, C.; Schwankl, M.; Himmler, D. Aluminum-aluminum compound castings by electroless deposited zinc layers. *J. Mater. Process. Technol.* **2014**, *214*, 1094–1101. [[CrossRef](#)]
83. Schwankl, N.; Wedler, J.; Körner, C. Wrought Al-Cast Al compound casting based in zincate treatment for aluminum alloy inserts. *J. Mater. Process. Technol.* **2016**, *238*, 160–168. [[CrossRef](#)]
84. Feng, J.; Ye, B.; Zuo, L.; Wang, Q.; Wang, Q.; Jiang, H.; Ding, W. Bonding of Aluminum Alloys in Compound Casting. *Metall. Mater. Trans. A* **2017**, *48A*, 4632–4644. [[CrossRef](#)]
85. Liu, G.; Wang, Q.; Liu, T.; Ye, B.; Jiang, H.; Ding, W. Effect of T6 heat treatment on microstructure and mechanical property of 6101/A356 bimetal fabricated by squeeze casting. *Mater. Sci. Eng. A* **2017**, *696*, 208–215. [[CrossRef](#)]
86. Liu, J.C.; Hu, J.; Nie, X.Y.; Li, H.X.; Du, Q.; Zhang, J.S.; Zhuang, L.Z. The interface bonding mechanism and related mechanical properties of Mg/Al compound materials fabricated by insert molding. *Mater. Sci. Eng. A* **2015**, *635*, 70–76. [[CrossRef](#)]
87. Vicario, I.; Crespo, I.; Plaza, L.M.; Caballero, P.; Idoaga, I.K. Aluminum foam and magnesium compound casting produced by high-pressure die casting. *Metals* **2016**, *6*, 24. [[CrossRef](#)]
88. Cheng, J.; Zhao, J.-H.; Zhang, J.-Y.; Guo, Y.; He, K.; Shang-guan, J.-J.; Wen, F.-L. Microstructure and Mechanical Properties of Galvanized-45 Steel/AZ91D Bimetallic Material by Liquid-Solid Compound Casting. *Materials* **2019**, *12*, 1651. [[CrossRef](#)] [[PubMed](#)]
89. Liu, T.; Wang, Q.; Sui, Y.; Wang, Q.; Ding, W. An investigation into interface formation and mechanical properties of aluminum-copper bi-metal by squeeze casting. *Mater. Des.* **2016**, *89*, 1137–1146. [[CrossRef](#)]
90. Hu, Y.; Chen, Y.; Li, L.; Hu, H.; Zhu, Z. Microstructure and properties of Al/Cu bi-metal in liquid–solid compound casting process. *Trans. Nonferrous Met. Soc. China* **2016**, *26*, 1555–1563. [[CrossRef](#)]
91. Liu, H.; Fu, D.; Dong, Z.; Huang, S.; Zhang, H. Bonding interfacial characterization of SiCp/8009Al composite and A356 aluminum alloy using compound casting. *J. Mater. Process. Technol.* **2019**, *263*, 42–49. [[CrossRef](#)]
92. Nie, X.Y.; Liu, J.C.; Li, H.X.; Du, Q.; Zhang, J.S.; Zhuang, L.Z. An investigation on bonding mechanisms and mechanical properties of Al/Ti compound materials prepared by insert moulding. *Mater. Des.* **2014**, *63*, 142–150. [[CrossRef](#)]
93. Pawlowski, A.E.; Splitter, D.A.; Muth, T.R.; Shyam, A.; Carver, J.K.; Dinwiddie, R.B.; Elliot, A.M.; Cordero, Z.C.; French, M.R. Producing hybrid metal composites by combining additive manufacturing and casting. *Adv. Mater. Process.* **2017**, *175*, 16–21.
94. Lao, B. Druckgegossene Metallhybridstrukturen für den Leichtbau-Prozess, Werkstoffe und Gefüge der Metallhybriden. Ph.D. Thesis, Gießerei-Institut, RWTH Aachen, Aachen, Germany, 2013.
95. Burbli, A.; Busse, M. Computer-based porosity design by multi-phase topology optimization. In Proceedings of the Multiscale & Functionally Graded Materials Conference (FGM), Honolulu, HI, USA, 15–18 October 2006.
96. Mounchili, A.P.; Bosse, S.; Lehms, D.; Struss, A. Putting stiffness where it's needed: Optimizing the mechanical response of multi-material structures. *MATEC Web Conf.* **2021**, *349*, 03001. [[CrossRef](#)]
97. Chen, B.; Moon, S.K.; Yao, X.; Bi, G.; Shen, J.; Umeda, J.; Kondoh, K. Comparison Study on Additive Manufacturing (AM) and Powder Metallurgy (PM) AlSi10Mg Alloys. *JOM* **2018**, *70*, 644–649. [[CrossRef](#)]
98. Potesser, M.; Schoeberl, T.; Antrekowitsch, H.; Bruckner, J. The characterization of the intermetallic Fe-Al layer of steel-aluminum weldings. In Proceedings of the EPD Congress 2006; The Minerals, Metals and Materials Society: Pittsburgh, PA, USA, 2006.
99. Borrisutthekul, R.; Yachi, T.; Miyashita, Y.; Mutoh, Y. Suppression of intermetallic reaction layer formation by controlling heat flow in dissimilar joining of steel and aluminum alloy. *Mater. Sci. Eng. A* **2007**, *467*, 108–113. [[CrossRef](#)]
100. Yin, F.-C.; Zhao, M.; Liu, Y.; Han, W.; Li, Z. Effect of Si on growth kinetics of intermetallic compounds during reaction between solid iron and molten aluminium. *Trans. Nonferrous Met. Soc. China* **2013**, *23*, 556–561. [[CrossRef](#)]
101. Bobzin, K.; Öte, M.; Wiesner, S.; Gerdt, L.; Senge, S.; Hirt, G.; Bührig-Polaczek, A.; Brachmann, J. Effect of Alloying Elements on Growth Behavior of Intermetallic Compounds at the Cold-Sprayed Coating/Steel-Interface during Immersion in Aluminum Melt. *Int. J. Met.* **2018**, *12*, 712–721.
102. Jiang, W.; Fan, Z.; Li, G.; Li, C. Effects of zinc coating on interfacial microstructures and mechanical properties of aluminum/steel bi-metallic composites. *J. Alloys Compd.* **2016**, *678*, 249–257. [[CrossRef](#)]
103. Bobzin, K.; Öte, M.; Wiesner, S.; Gerdt, L.; Senge, S.; Hirt, G. Investigation on the cold rolling and structuring of cold sprayed copper-coated steel sheets. *IOP Conf. Ser. Mater. Sci. Eng.* **2017**, *181*, 012028. [[CrossRef](#)]
104. Senge, S.; Brachmann, J.; Hirt, G.; Bührig-Polaczek, A. Evaluation of interlocking bond strength between structured 1.0338 steel sheets and high pressure die cast AlMg₅Si₂. *AIP Conf. Proc.* **2018**, *1960*, 040019.
105. Ukar, E.; Liébana, F.; Andrés, M.; Marcos, I.; Lamikiz, A. Laser texturing and dissimilar material joining. *Procedia Manuf.* **2017**, *13*, 671–678. [[CrossRef](#)]
106. Bizi-Bandoki, P.; Benayoun, S.; Valette, S.; Beaugiraud, B.; Audouard, E. Modifications of roughness and wettability properties of metals induced by femtosecond laser treatment. *Appl. Surf. Sci.* **2011**, *257*, 5213–5218. [[CrossRef](#)]
107. Cunha, A.P.; Serro, V.; Oliveira, A.; Almeida, A.; Vilar, R.; Durrieu, M. Wetting behaviour of femtosecond laser textured Ti–6Al–4V surfaces. *Appl. Surf. Sci.* **2013**, *265*, 688–696. [[CrossRef](#)]

108. Lao, B.; Bührig-Polaczek, A. Funktionsintegrierte Leichtbaustrukturen in gussintensiver Metall-Hybridbauweise. In Proceedings of the 18th Symposium Verbundwerkstoffe und Werkstoffverbunde, Chemnitz, Germany, 30 March–1 April 2011; pp. 413–421.
109. Nayak, B.K.; Gupta, M.C.; Kolasinski, K.W. Formation of nano-textured conical microstructures in titanium metal surface by femtosecond laser irradiation. *Appl. Phys. A* **2008**, *90*, 399–402. [[CrossRef](#)]
110. Bo, W.; Ming, Z.; Jian, L.; Xia, Y.; Gang, L.; Lan, C. Superhydrophobic surfaces fabricated by microstructuring of stainless steel using a femtosecond laser. *Appl. Surf. Sci.* **2009**, *256*, 61–66.
111. Nolte, N.; Specht, U.; Fischer, M.; Lukasczyk, T.; Lehmus, D.; Wilken, R. Laser Surface Pretreatment for Aluminium-Aluminium Compound Casting: Effect of Surface Topography and Wetting Behavior. In Proceedings of the Euromat 2019 Conference, Stockholm, Sweden, 1–5 September 2019.
112. Nolte, N. Untersuchungen Lasermikrostrukturierter Metalloberflächen zur Her-Stellung Formschlüssiger Aluminium-Aluminium Verbindungen im Druckgussverfahren. Master's Thesis, University of Bremen, Bremen, Germany, 2019.
113. Voss, F. Herstellung Eines Stoffschlüssigen Aluminium-Aluminium-Verbundes im Niederdruckgießverfahren—Ermittlung von Übergangsparametern Durch Gießsimulationen und Deren Validierung. Master's Thesis, University of Bremen, Bremen, Germany, 2020.
114. Technisches Datenblatt. Available online: <https://multimedia.3m.com/mws/media/1853182O/3m-impact-resistant-structural-adhesive-07333-german-tds.pdf> (accessed on 4 January 2023).
115. Lehmus, D.; Clausen, J.; Woestmann, F.-J.; Gärtner, F.; List, A.; Klassen, T. Verfahren zur Erzeugung Einer Stoffschlüssigen Verbindung im Verbundguss. German Patent Application DE 10 2020 206 009 A1, 18 November 2021.
116. Pintore, M.; Mittler, T.; Volk, W.; Sarykov, O.; Tonn, B. Experimental investigation on the influence of thermal conditions during composite casting on the microstructure of Cu-Al bilayer compounds. *Int. J. Met.* **2018**, *12*, 79–88. [[CrossRef](#)]
117. Pintore, M.; Wölck, J.; Mittler, T.; Greß, T.; Volk, W.; Tonn, B. Composite Casting and Characterization of Cu-Al Bilayer Compounds. *Int. J. Met.* **2020**, *14*, 155–166. [[CrossRef](#)]
118. Liu, G.; Wang, Q.; Zhang, L.; Ye, B.; Jiang, H.; Ding, W. Effect of Cooling Rate on the Microstructure and Mechanical Properties of Cu/Al Bimetal Fabricated by Compound Casting. *Metall. Mater. Trans. A* **2018**, *49A*, 661–672. [[CrossRef](#)]
119. Klose, C.; Freytag, P.; Otten, M.; Thüerer, S.E.; Naier, H.J. Thermal Properties of Intermetallic Phases at the Interface of Aluminum-Copper Compound Castings. *Adv. Eng. Mater.* **2018**, *20*, 1701027. [[CrossRef](#)]
120. Stein, S.; Wedler, J.; Rhein, S.; Schmidt, M.; Koerner, C.; Michaelis, A.; Gebhardt, S. A process chain for integrating piezoelectric transducers into aluminum die castings to generate smart lightweight structures. *Results Phys.* **2017**, *7*, 2534–2539. [[CrossRef](#)]
121. Schwankl, M.; Himmler, D.; Urban, M.; Körner, C. Optimization of Mechanical Properties of Al–Al-Compound Castings by Adapted Heat Treatment. *Adv. Eng. Mater.* **2018**, *20*, 1800400. [[CrossRef](#)]
122. Lehmus, D.; List, A.; Gärtner, F.; Klassen, T. Aluminum-Aluminum Compound Casting Approaches Supported by Cold Sprayed Interlayers. 2024; *unpublished work*.
123. Jiang, W.; Jiang, Z.; Li, G.; Wu, Y.; Fan, Z. Microstructure of Al/Al bimetallic composites by lost foam casting with Zn interlayer. *Mater. Sci. Technol.* **2018**, *34*, 487–492. [[CrossRef](#)]
124. Guler, K.A.; Kiasoz, A.; Karaaslan, A. Fabrication of Al/Mg Bimetal Compound Casting by Lost Foam Technique and Liquid-Solid Process. *Mater. Test.* **2014**, *56*, 700–702. [[CrossRef](#)]
125. Bakke, A.O.; Arnberg, L.; Løland, J.-O.; Jørgensen, S.; Kvinge, J.; Li, Y. Formation and evolution of the interfacial structure in al/steel compound castings during solidification and heat treatment. *J. Alloys Compd.* **2020**, *849*, 156685. [[CrossRef](#)]
126. Fadaeinia, M.; Raiszadeh, R. Bonding of compound casted Ti/Al bimetal by heat treatment. *Int. J. Miner. Metall. Mater.* **2021**, *28*, 1515–1524. [[CrossRef](#)]
127. Ho, J.-S.; Lin, C.B.; Liu, C.H. The Effect of Heat Treatment on Interface Properties of S45C Steel/Copper Compound Casting. *Tamkang J. Sci. Eng.* **2003**, *6*, 49–56.
128. Mola, R.; Bucki, T.; Dziadon, A. Microstructure of the Bonding Zone Between AZ91 and AlSi17 Formed by Compound Casting. *Arch. Foundry Eng.* **2017**, *17*, 202–206. [[CrossRef](#)]
129. Tayal, R.K.; Singh, V.; Gupta, A.; Kumar, S.; Ujjawal, D. Experimental investigation and evaluation of joint strength of A356/Mg bimetallic fabricated using compound casting. *Int. J. Met.* **2019**, *13*, 686–699. [[CrossRef](#)]
130. Zhao, K.N.; Li, H.X.; Luo, J.R.; Liu, Y.J.; Du, Q.; Zhang, J.S. Interfacial bonding mechanism and mechanical properties of novel AZ31/WE43 bimetal composites fabricated by insert molding method. *J. Alloys Compd.* **2017**, *729*, 344–353. [[CrossRef](#)]
131. Schmid, A.; Arnaut, K.; Clausen, J.; Koerdt, M.; Struss, A.; Woestmann, F.-J.; Busse, M. Process Concepts for the Manufacturing of Hybrid Composites from Aluminum and CFRP with a Polymer-based Decoupling Layer. In Proceedings of the Hybrid Materials and Structures Conference, Bremen, Germany, 18–19 April 2018.
132. Schmid, A.; Arnaut, K.; Clausen, J.; Koerdt, M.; Struss, A.; Wöstmann, F.-J.; Busse, M. Intrinsic Aluminum CFRP Hybrid Composites Produced in High Pressure Die Casting with Polymer Based Decoupling Layer. *Key Eng. Mater.* **2017**, *742*, 197–204. [[CrossRef](#)]
133. Clausen, J.; Kelch, M.; Wöstmann, F.-J.; Busse, M. Development of a high pressure die casting tool for partial integration of glass fiber structures. *Key Eng. Mater.* **2017**, *742*, 520–526. [[CrossRef](#)]
134. Clausen, J.; Kelch, M.; Wöstmann, F.-J.; Busse, M. Mechanical characterization of integral aluminum-FRP-structures produced by high pressure die-casting. *Prod. Eng.* **2018**, *12*, 269–278. [[CrossRef](#)]

135. Struss, A.; Schmid, A.; Ebrahimi, A.; Jablonski, F.; Busse, M. Description of the Boundary Layer Behavior of an Aluminum–Carbon-Fiber-Reinforced Polymer Hybrid Compound Using a Cohesive Zone Model. *J. Fail. Anal. Prev.* **2020**, *20*, 930–935. [[CrossRef](#)]
136. Schmid, A.; Haubold, T.; Koschek, K.; Marx, A.; Pursche, L.; Struss, A.; Thiel, K.; Wiesing, M.; Busse, M. Hybrid casting—An investigation into the interface of high pressure die-cast intrinsic aluminum-PEEK-CFRP hybrid composites. *IOP Conf. Ser. Mater. Sci. Eng.* **2021**, *1147*, 012022. [[CrossRef](#)]
137. Bitsche, R.D. Design and Computational Analysis of Compound Castings and other Multi-Material Structures. Ph.D. Thesis, Technical University of Vienna, Vienna, Austria, 2009.
138. Leinenbach, F.; Sukowski, F.; Clausen, J.; Straß, B.; Wolter, B. Detection of quality features in hybrid cast components using NDT. In Proceedings of the 1st Congress for intelligent Combining of Design, Casting, Computer Simulation, Checking and Cyclic Behaviour for efficient Cast Components (InEight Casting C⁸), Darmstadt, Germany, 2–3 March 2021; pp. 171–180.
139. Holub, W.; Haßler, U.; Schorr, C.; Maisl, M.; Janello, P.; Jahnke, P. XXL-Micro-CT—Comparative Evaluation of Microscopic Computed Tomography for Macroscopic Objects. In Proceedings of the Digital Industrial Radiology and Computed Tomography (DIR 2015), Ghent, Belgium, 22–25 June 2015.
140. Holub, W.; Brunner, F.; Schön, T. RoboCT—Application for in-situ inspection of join technologies of large scale objects. *Int. Symp. Digit. Ind. Radiol. Comput. Tomogr.* **2019**, *11*, 1–9.
141. Nagai, Y.; Holub, W. Overview of Robot guided Computed Tomography—Production Monitoring in Automotive Industry 4.0. *J. Jpn. Soc. Precis. Eng.* **2020**, *86*, 316–322. [[CrossRef](#)]
142. Glück Nardi, V.; Greß, T.; Tonn, B.; Volk, W. Modelling of intermetallic layers formation during solid-liquid joining of dissimilar metallic materials. *IOP Conf. Ser. Mater. Sci. Eng.* **2020**, *861*, 012058. [[CrossRef](#)]
143. Joshi, D.; Ravi, B. Quantifying the shape complexity of cast parts. *Comput.-Aided Des. Appl.* **2010**, *7*, 685–700. [[CrossRef](#)]
144. Johnson, M.D.; Valverde, L.M.; Thomison, W.D. An investigation and evaluation of computer-aided design model complexity metrics. *Comput.-Aided Des. Appl.* **2018**, *15*, 61–75. [[CrossRef](#)]
145. Camba, J.D.; Contero, M.; Company, P.; Perez-Lopez, D.; Otey, J. Identifying high-value CAD models: An exploratory study on dimensional variability as complexity indicator. In Proceedings of the ASME 2018 13th International Manufacturing Science and Engineering Conference (MSEC 2018), College Station, TX, USA, 18–22 June 2018.
146. Almaghariz, E.S. Determining when to Use 3D Sand Printing: Quantifying the Role of Complexity. Master’s Thesis, Youngstown State University, Youngstown, OH, USA, 2015.
147. Almaghariz, E.S.; Conner, B.P.; Lenner, L.; Gullapalli, R.; Manogharan, G.; Lamoncha, B.; Fang, M. Quantifying the role of part design complexity in using 3D sand printing for molds and cores. *Int. J. Met.* **2016**, *10*, 240–252. [[CrossRef](#)]
148. Martof, A.; Gullapalli, R.; Kelly, J.; Rea, A.; Lamoncha, B.; Walker, J.M.; Conner, B.; MacDonald, E. Economies of complexity of 3D printed sand molds for casting. In Proceedings of the Solid Freeform Fabrication 2018: Proceedings of the 29th Annual International Solid Freeform Fabrication Symposium, Austin, TX, USA, 13–15 August 2018; p. 117.
149. Wang, J.; Sama, S.R.; Manogharan, G. Re-thinking design methodology for castings: 3D sand-printing and topology optimization. *Int. J. Met.* **2019**, *13*, 2–17. [[CrossRef](#)]
150. Mukhtarkhanov, M.; Perveen, A.; Talamona, D. Application of Stereolithography Based 3D Printing Technology in Investment Casting. *Micromachines* **2020**, *11*, 946. [[CrossRef](#)]
151. Hafsa, M.N.; Kassim, N.; Ismail, S.; Kamaruddin, S.A.; Hafeez, T.M. Study on surface roughness quality of FDM and MJM additive manufacturing model for implementation as investment casting sacrificial pattern. *J. Mech. Eng.* **2018**, *5*, 25–34.
152. Kumar, R.; Kapil, S.; Negi, S.; Gehlot, N.; Gopalakrishna, S.H.; Karunakaran, K.P. Rapid Prototyping of EPS Pattern for Complicated Casting. In Proceedings of the Solid Freeform Fabrication 2017: Proceedings of the 28th Annual International Solid Freeform Fabrication Symposium—An Additive Manufacturing Conference, Austin, TX, USA, 7–9 August 2017.
153. Gote, G.; Kamble, P.; Kori, S.; Karunakaran, K.P. Process Optimization of Segmented Object Manufacturing for Expandable Polystyrene Foam. In *Advances in Lightweight Materials and Structures: Select Proceedings of ICALMS 2020*; Praveen Kumar, A., Dirgantara, T., Krishna, P.V., Eds.; Springer Proceedings in Materials Book Series; Springer: Berlin/Heidelberg, Germany, 2020; Volume 8, pp. 695–704.
154. Upadhyay, T.; Sivarupan, I.; El Mansori, M. 3D printing for rapid sand casting—A review. *J. Manuf. Process.* **2017**, *29*, 211–220. [[CrossRef](#)]
155. Sivarupan, T.; Balasubramanian, N.; Saxena, P.; Nagarajan, D.; El Mansori, M.; Salonitis, K.; Jolly, M.; Dargusch, M.S. A review on the progress and challenges of binder jet 3D printing of sand moulds for advanced casting. *Addit. Manuf.* **2021**, *40*, 101889. [[CrossRef](#)]
156. Tu, S.; Liu, F.; Li, G.; Jiang, W.; Liu, X.; Fan, Z. Fabrication and characterization of high-strength water-soluble composite salt core for zinc alloy die casting. *Int. J. Adv. Manuf. Technol.* **2018**, *95*, 505–512. [[CrossRef](#)]
157. Findeisen, S.; Van der Auwera, R.; Heuser, M.; Woestmann, F. Gießtechnische Fertigung von E-Motorenhäusen mit interner Kühlung. *Giesserei* **2019**, *106*, 72–78.
158. Gong, X.; Jiang, W.; Liu, F.; Yang, Z.; Guan, F.; Fan, Z. Effects of glass fiber size and content on microstructures and properties of KNO₃-based water-soluble salt core for high pressure die casting. *Int. J. Met.* **2021**, *15*, 520–529. [[CrossRef](#)]
159. Gong, X.; Liu, X.; Chen, Z.; Yang, Z.; Jiang, W.; Fan, Z. 3D printing of high-strength water-soluble salt cores via material extrusion. *Int. J. Adv. Manuf. Technol.* **2022**, *118*, 2993–3003. [[CrossRef](#)]

160. Cornacchia, G.; Dioni, D.; Fccoli, M.; Gislon, C.; Solazzi, L.; Panvini, A.; Cecchel, S. Experimental and Numerical Study of an Automotive Component Produced with Innovative Ceramic Core in High Pressure Die Casting (HPDC). *Metals* **2019**, *9*, 217. [CrossRef]
161. Koya, E.; Fukuda, Y.; Kitagawa, S. Manufacturing Technology for Hollow Structure Large Aluminum Parts Production by HPDC. *SAE Int. J. Passeng. Cars Mech. Syst.* **2015**, *8*, 65–72. [CrossRef]
162. The Platform for the Entire Casting Industry. Available online: <https://www.foundry-planet.com/d/innovative-sand-cores-with-watersoluble-binder-systems-for-the-non-ferrous-sector/> (accessed on 16 March 2023).
163. Ams. Available online: <https://www.automotivemanufacturingsolutions.com/bmw/bmw-landshut-is-now-using-new-multi-plate-die-casting-technology/42923.article> (accessed on 16 March 2023).
164. Winklhofer, J. Semi-Solid Casting of Aluminum from an Industrial Point of View. *Solid State Phenom.* **2019**, *285*, 24–30. [CrossRef]
165. Imran, M.K.; Masood, S.H.; Brandt, M. Bimetallic dies with direct metal-deposited steel on Moldmax for high-pressure die casting application. *Int. J. Adv. Manuf. Technol.* **2011**, *52*, 855–863. [CrossRef]
166. Armillotta, A.; Baraggi, R.; Fasoli, S. SLM tooling for die casting with conformal cooling channels. *Int. J. Adv. Manuf. Technol.* **2014**, *71*, 573–583. [CrossRef]
167. Anand, A.; Nagarajan, D.; El Mansori, M.; Sivarupan, T. Integration of Additive Fabrication with High-Pressure Die Casting for Quality Structural Castings of Aluminium Alloys; Optimising Energy Consumption. *Trans. Indian Inst. Met.* **2023**, *76*, 347–379. [CrossRef]
168. Lehmhus, D.; von Hehl, A.; Hausmann, J.; Kayvantash, K.; Alderliesten, R.; Hohe, J. New Materials and Processes for Transport Applications: Going Hybrid and Beyond. *Adv. Eng. Mater.* **2019**, *21*, 1900056. [CrossRef]
169. Weise, J.; Hilbers, J.; Handels, F.; Lehmhus, D.; Busse, M.; Heuser, M. New core technology for light metal casting. *Adv. Eng. Mater.* **2019**, *21*, 1800608. [CrossRef]
170. Kohlstädt, S. On Determining Lost Core Viability in High-Pressure Die Casting Using Computational Continuum Mechanics. Ph.D. Thesis, KTH Royal Institute of Technology, Stockholm, Sweden, 2019.
171. Kohlstädt, S.; Vynnycky, M.; Jäckel, J. Towards the modelling of fluid-structure interactive lost core deformation in high-pressure die casting. *Appl. Math. Model.* **2020**, *80*, 319–333. [CrossRef]
172. Kohlstädt, S.; Vynnycky, M.; Goeke, S. On the CFD Modelling of Slamming of the Metal Melt in High-Pressure Die Casting Involving Lost Cores. *Metals* **2021**, *11*, 78. [CrossRef]
173. Fuchs, B.; Eibisch, H.; Körner, C. Core Viability Simulation for Salt Core Technology in High-Pressure Die Casting. *Int. J. Met.* **2013**, *7*, 39–45. [CrossRef]
174. Jelínek, P.; Adámková, E. Lost Cores for High Pressure Die Casting. *Arch. Foundry Eng.* **2014**, *14*, 101–104. [CrossRef]
175. Kallien, L. Salzkerne im Druckguss. Available online: https://www.hs-aalen.de/uploads/publication/file/9730/2016-Salzkerne_im_Druckguss.pdf (accessed on 26 April 2023).
176. Pierri, D.; Roos, H.J.; Padovan, S. Verfahren zur Herstellung von Salzkerne. European Patent Application EP 2647451 A1, 4 April 2012.
177. Fabbroni, M. Lost Core—Industrieller Prozesspfad für Hochwertige Salzkerne: Das Salz in der Suppe. Available online: <https://automobilkonstruktion.industrie.de/allgemein/das-salz-in-der-suppe/> (accessed on 26 April 2023).
178. Becker, M. Hohle Aluminiumstrukturbauteile Durch Salzkerne im Druckguss. Ph.D. Thesis, TU Clausthal, Clausthal, Germany, 2021.
179. Gong, X.; Xiao, X.; Liu, X.; Fan, Z. Fabrication of high-strength salt cores for manufacturing hollow aluminum alloy die castings. *Mater. Manuf. Process.* **2023**, *38*, 188–196. [CrossRef]
180. Serghini, A. Konzept zum Einsatz von verlorenen Kernen im HPDC. In Proceedings of the 3. VDI-Fachkonferenz Gießtechnik und E-Mobilität, Bremen, Germany, 18–19 October 2022.
181. Reberger, E. Entwicklung von mehrschichtigen Sandkernen für den Druckguss. *Giesserei* **2023**, *110*, 68.
182. Michels, H.; Bünck, M.; Bührig-Polaczek, A. Suitability of lost cores in rheocasting process. *Trans. Nonferrous Met. Soc. China* **2010**, *20*, s948–s953. [CrossRef]
183. Lehmhus, D.; Weise, J.; Baumeister, J.; Peroni, L.; Scapin, M.; Fichera, C.; Avalle, M.; Busse, M. Quasi-static and Dynamic Mechanical Performance of Glass Microsphere- and Cenosphere-based 316L Syntactic Foams. *Procedia Mater. Sci.* **2014**, *4*, 383–387. [CrossRef]
184. Szlancsik, A.; Katona, B.; Kemény, A.; Károly, D. On the Filler Materials of Metal Matrix Syntactic Foams. *Materials* **2019**, *12*, 2023. [CrossRef] [PubMed]
185. Hobaica, E.C.; Cook, S.D. The Characteristics of Syntactic Foams Used for Buoyancy. *J. Cell. Plast.* **1968**, *4*, 143–148. [CrossRef]
186. Gupta, N.; Zeltmann, S.; Schunmugasamy, V.C.; Pinisetty, D. Applications of Polymer Matrix Syntactic Foams. *JOM* **2014**, *66*, 245–254. [CrossRef]
187. Gupta, N.; Rohatgi, P.K. (Eds.) *Metal Matrix Syntactic Foams*, 1st ed.; DEStech Publications, Inc.: Lancaster, PA, USA, 2015.
188. Pille, D.; Soltmann, C.; Lehmhus, D.; Heuser, M.; Horeis, R.; Peters, M. Kollabierbare Kerne: Ein neuer Ansatz für den Aluminium-Feinguss? *Giesserei* **2023**, *110*, 89–94.
189. Ziaee, M.; Crane, N.B. Binder jetting: A review of process, materials, and methods. *Addit. Manuf.* **2019**, *28*, 781–801. [CrossRef]

190. Chowdhury, S.; Yadaiah, N.; Prakash, C.; Ramakrishna, S.; Dixit, S.; Gupta, L.R.; Buddhi, D. Laser powder bed fusion: A state-of-the-art review of the technology, materials, properties & defects, and numerical modelling. *J. Mater. Res. Technol.* **2022**, *20*, 2109–2172.
191. Azar, A.S.; Diplas, S. Fundamental aspects of processing multi-metallic components using additive manufacturing technologies. *Eur. J. Mater.* **2022**, *2*, 234–364. [[CrossRef](#)]
192. Hasanov, S.; Alkunte, S.; Rajeshirke, M.; Gupta, A.; Hseyonov, O.; Fidan, I.; Alifui-Segbaya, F.; Rennie, A. Review on Additive Manufacturing of Multi-Material Parts: Progress and Challenges. *J. Manuf. Process. Mater. Process.* **2021**, *6*, 4. [[CrossRef](#)]
193. Mussatto, A. Research progress in multi-material laser-powder bed fusion additive manufacturing: A review of the state-of-the-art techniques for depositing multiple powders with spatial selectivity in a single layer. *Results Eng.* **2022**, *16*, 100769. [[CrossRef](#)]
194. Gibson, I.; Rosen, D.; Stucker, B. (Eds.) Directed Energy Deposition Processes. In *Additive Manufacturing Technologies*; Springer: New York, NY, USA, 2015. [[CrossRef](#)]
195. Mudge, R.P.; Wald, N.R. Laser engineered net shaping advances additive manufacturing and repair. *Weld. J.* **2007**, *86*, 44–48.
196. Deirmina, F.; Peghini, N.; AlMangour, B.; Grzesiak, D.; Pellizzari, M. Heat treatment and properties if a hot work tool steel fabricated by additive manufacturing. *Mater. Sci. Eng. A* **2019**, *753*, 109–121. [[CrossRef](#)]
197. Nandwana, P.; Kannan, R.; Siddel, D. Microstructural evolution during binder jet additive manufacturing of H13 tool steel. *Addit. Manuf.* **2020**, *36*, 101534.
198. Klocke, F.; Arntz, K.; Teli, M.; Winands, K.; Wegener, M.; Oliari, S. State-of-the-art Laser Additive Manufacturing for Hot-work Tool Steels. *Procedia CIRP* **2017**, *63*, 58–63. [[CrossRef](#)]
199. Bohlen, A.; Freiße, H.; Hunkel, M.; Vollertsen, F. Additive manufacturing of tool steel by laser metal deposition. *Procedia CIRP* **2018**, *74*, 192–195. [[CrossRef](#)]
200. Popovich, A.; Sufiiarov, V.; Polozov, I.; Borisov, E.; Masaylo, D.; Orlov, A. Microstructure and mechanical properties of additive manufactured copper alloy. *Mater. Lett.* **2016**, *179*, 38–41. [[CrossRef](#)]
201. Kumar, A.Y.; Wang, J.; Bai, Y.; Huxtable, S.T.; Williams, C.B. Impacts of process-induced porosity on material properties of copper made by binder jetting additive manufacturing. *Mater. Des.* **2019**, *182*, 108001. [[CrossRef](#)]
202. Jadhav, S.D.; Goossens, L.; Kinds, Y.; Van Hooreweder, B.; Vanmeensel, K. Laser-based powder bed fusion additive manufacturing of pure copper. *Addit. Manuf.* **2021**, *42*, 101990. [[CrossRef](#)]
203. Gobran, H. Herstellungsverfahren und Verwendung für ein Wolframlegierungsprodukt—Method of Preparation and Use for a Tungsten Alloy Product. European Patent EP 3 643 429 B1, 13 January 2021.
204. Adams, T.-E.; Mayr, P. The Path from Arc Welding to Additive Manufacturing of Multi-material Parts Using Directed Energy Deposition. *Berg. Huettenmann. Monatsh.* **2022**, *167*, 318–324. [[CrossRef](#)]
205. Treutler, K.; Wesling, V. The Current State of Research of Wire Arc Additive Manufacturing (WAAM): A Review. *Appl. Sci.* **2021**, *11*, 8619. [[CrossRef](#)]
206. Shah, M.; Patel, D.R.; Pande, S. Additive manufacturing integrated Casting—A review. *Mater. Proc.* **2022**, *62*, 7199–7203. [[CrossRef](#)]
207. Wen, S.; Shen, Q.; Wei, Q.; Yan, C.; Zhu, W.; Shi, Y.; Yang, J.; Shi, Y. Material optimization and post-processing of sand moulds manufactured by the selective laser sintering of binder-coated Al₂O₃ sands. *J. Mater. Process. Technol.* **2015**, *225*, 93–102. [[CrossRef](#)]
208. Yang, L.; Tang, S.-Y.; Fan, Z.-T.; Jiang, W.-M.; Liu, X.-W. Rapid Casting Technology based on Selective Laser Sintering. *China Foundry* **2021**, *18*, 296–306. [[CrossRef](#)]
209. Sama, S.R.; Wang, J.; Manogharan, G. Non-conventional mold design for metal casting using 3D sand-printing. *J. Manuf. Process.* **2018**, *34*, 765–775. [[CrossRef](#)]
210. Sama, S.R.; Badamo, T.; Lynch, P.; Manogharan, G. Novel sprue designs in metal casting via 3D sand-printing. *Addit. Manuf.* **2019**, *25*, 563–578. [[CrossRef](#)]
211. Walker, J.; Harris, E.; Lynagh, C.; Beck, A.; Vuksanovich, B.; Conner, B.; MacDonald, E.; Lonardo, R.; Thiel, J.; Rogers, K. 3D printed smart molds for sand casting. *Int. J. Met.* **2018**, *12*, 785–796. [[CrossRef](#)]
212. Walker, J.; Prokop, A.; Lynagh, C.; Vuksanovich, B.; Conner, B.; Rogers, K.; Thiel, J.; MacDonald, E. Real-time process monitoring of core shifts during metal casting with wireless sensing and 3D sand printing. *Addit. Manuf.* **2019**, *27*, 54–60. [[CrossRef](#)]
213. Vuksanovich, B.; Herberger, C.; Daugherty, T.; Waker, J.; Cortes, P.; MacDonald, E.; Jaric, D.; Gaffney, S.; Lonardo, R.; Clancy, M.; et al. Wireless ventilation measurement in 3D printed sand molds. *Int. J. Met.* **2022**, *16*, 80–92. [[CrossRef](#)]
214. Thiel, J.; Ravi, S.; Bryant, N. Advancements in materials for three-dimensional printing of molds and cores. *Int. J. Met.* **2017**, *11*, 3–13. [[CrossRef](#)]
215. Kaiser, M. Binder jetting additive manufacturing of sand moulds/cores and its newest developments—Machine and material. In Proceedings of the 1st Congress for intelligent Combining of Design, Casting, Computer Simulation, Checking and Cyclic Behaviour for efficient Cast Components (InCeight Casting C⁸), Darmstadt, Germany, 2–3 March 2021; pp. 89–97.
216. Zaretskiy, L. Modified silicate binders new developments and applications. *Int. J. Met.* **2016**, *10*, 88–99. [[CrossRef](#)]
217. Vykoukal, M.; Burian, A.; Prerovska, M. GEOPOL. The Innovated Environment Friendly Inorganic Binder System. *Arch. Foundry Eng.* **2019**, *19*, 109–116. [[CrossRef](#)]
218. Danko, R.; Kmita, A.; Holtzer, M.; Danko, J.; Lehms, D.; Tapola, S. Development of inorganic binder systems to minimise emissions in ferrous foundries. *Sustain. Mater. Technol.* **2023**, *37*, e00666.

219. Ramakrishnan, R.; Griebel, B.; Volk, W.; Günther, D.; Günther, J. 3D Printing of Inorganic Sand Moulds for Casting Applications. *Adv. Mater. Res.* **2014**, *1018*, 441–449. [CrossRef]
220. Pacurar, R.; Berce, P.; Nemes, O.; Baila, D.-I.; Stan, D.S.; Oarcea, A.; Popister, F.; Borzan, C.M.; Maricic, S.; Legutko, S.; et al. Cast Iron Parts Obtained in Ceramic Molds Produced by Binder Jetting 3D Printing—Morphological and Mechanical Characterization. *Materials* **2021**, *14*, 4502. [CrossRef] [PubMed]
221. Lynch, P.; Hasbrouck, C.R.; Wilck, J.; Kay, M.; Manogharan, G. Challenges and Opportunities to integrate the oldest and newest manufacturing processes; metal casting and additive manufacturing. *Rapid Prototyp. J.* **2020**, *26*, 1145–1154. [CrossRef]
222. Lee, C.W.; Chua, C.K.; Cheah, C.M.; Tan, L.H.; Feng, C. Rapid investment casting: Direct and indirect approaches via fused deposition modelling. *Int. J. Adv. Manuf. Technol.* **2004**, *23*, 93–101.
223. Cheah, C.M.; Chua, C.K.; Lee, C.W.; Feng, C.; Totong, K. Rapid prototyping and tooling techniques: A review of applications for rapid investment casting. *Int. J. Adv. Manuf. Technol.* **2005**, *25*, 308–320. [CrossRef]
224. Zocca, A.; Colombo, P.; Gomes, C.M.; Günster, J. Additive Manufacturing of Ceramics: Issues, Potentialities, and Opportunities. *J. Am. Cer. Soc.* **2015**, *98*, 1983–2001. [CrossRef]
225. Lakhdar, Y.; Tuck, C.; Binner, J.; Terry, A.; Goodridge, R. Additive manufacturing of advanced ceramic materials. *Prog. Mater. Sci.* **2021**, *116*, 100736. [CrossRef]
226. Kumar, P.; Ahuja, I.P.S.; Singh, R. Application of fusion deposition modelling for rapid investment casting—A review. *Int. J. Mater. Eng. Innov.* **2012**, *3*, 204–227. [CrossRef]
227. Hafsa, M.N.; Ibrahim, M.; Wahab, M.S.; Zahid, M.S. Evaluation of FDM pattern with ABS and PLA material. *Appl. Mech. Mater.* **2014**, *465–466*, 55–59. [CrossRef]
228. Andrew, K.; Weaver, J.M. Using Wax Filament Additive Manufacturing for Low-Volume Investment Casting. In Proceedings of the Solid Freeform Fabrication 2019: Proceedings of the 30th Annual International Solid Freeform Fabrication Symposium—An Additive Manufacturing Conference, Austin, TX, USA, 12–14 August 2019.
229. Votava, F.; Bricin, D. Options for Implementing Additive Manufacturing Technologies into a Foundry for Small Castings. *IOP Conf. Ser. Mater. Sci. Eng.* **2022**, *1243*, 012007. [CrossRef]
230. Badanova, N.; Perveen, A.; Talamona, D. Study of SLA Printing Parameters Affecting the Dimensional Accuracy of the Pattern and Casting in Rapid Investment Casting. *J. Manuf. Mater. Process.* **2022**, *6*, 109. [CrossRef]
231. Nguyen, T.T.; Tran, V.T.; Pham, T.H.N.; Nguyen, V.-T.; Thanh, N.C.; Thi, H.M.N.; Duy, N.V.A.; Thanh, D.N.; Nguyen, V.T.T. Influences of Material Selection, Infill Ratio, and Layer Height in the 3D Printing Cavity Process on the Surface Roughness of Printed Patterns and Casted Products in Investment Casting. *Micromachines* **2023**, *14*, 395. [CrossRef] [PubMed]
232. Frost, M.; Hong, I. Utilization of Resin-Based Additive Manufacturing for Investment Casting. Available online: <https://digitalcommons.calpoly.edu/mesp/637/> (accessed on 6 May 2023).
233. Nkhasi, N.P.; Preez, W.B.D.; van der Walt, J.G. Investment casting of Aluminium alloy A356 using Primecast® and PMMA additive manufacturing materials for sacrificial patterns. In Proceedings of the 19th Annual International RAPDASA Conference, Johannesburg, South Africa, 7–9 November 2018; pp. 22–31.
234. Bae, C.-J.; Kim, D.; Halloran, J.W. Mechanical and kinetic studies on the refractory fused silica of integrally cored ceramic mold fabricated by additive manufacturing. *J. Eur. Ceram. Soc.* **2019**, *39*, 618–623. [CrossRef]
235. Klocke, F.; Ader, C. Direct Laser Sintering of Ceramics. In Proceedings of the Solid Freeform Fabrication 2003: Proceedings of the 30th Annual International Solid Freeform Fabrication Symposium—An Additive Manufacturing Conference, Austin, TX, USA, 4–6 August 2003.
236. Liu, H.; Su, G.; Li, Y. Effect of wall structure on the dimensional accuracy of shell mould prepared by slurry extrusion-based additive manufacturing process. *Int. J. Cast Met. Res.* **2022**, *35*, 102–110. [CrossRef]
237. Bosse, S.; Lehnhus, D. On Concepts and Challenges of Realizing Material-Integrated Intelligent Systems. In *Material-Integrated Intelligent Systems—Technology and Applications*; Bosse, S., Lehnhus, D., Lang, W., Busse, M., Eds.; Wiley-VCH Verlag: Weinheim, Germany, 2018; pp. 1–28.
238. Hribernik, K.A.; Pille, C.; Jeken, O.; Thoben, K.-D.; Windt, K.; Busse, M. Autonomous control of intelligent products in beginning of life processes. In Proceedings of the 7th International Conference on Product Lifecycle Management, Bremen, Germany, 12–14 July 2010.
239. Lehnhus, D.; Busse, M. Structural Health Monitoring. In *Material-Integrated Intelligent Systems—Technology and Applications*; Bosse, S., Lehnhus, D., Lang, W., Busse, M., Eds.; Wiley-VCH Verlag: Weinheim, Germany, 2018; pp. 531–594.
240. Wuest, T.; Hribernik, K.; Thoben, K.-D. New Marktes/Opportunities through Availability of Product Life Cycle Data. In *Material-Integrated Intelligent Systems—Technology and Applications*; Bosse, S., Lehnhus, D., Lang, W., Busse, M., Eds.; Wiley-VCH Verlag: Weinheim, Germany, 2018; pp. 613–628.
241. Lehnhus, D.; Wuest, T.; Wellsandt, S.; Bosse, S.; Kaihara, T.; Thoben, K.-D.; Busse, M. Cloud-based automated design and additive manufacturing: A usage data-enabled paradigm shift. *Sensors* **2015**, *15*, 32079–32122. [CrossRef]
242. Carvalho, T.P.; Soares, F.A.A.M.N.; Vita, R.; Francisco, R.d.P.; Basto, J.P.; Alcalá, S.G.S. A systematic literature review of machine learning methods applied to predictive maintenance. *Comput. Ind. Eng.* **2019**, *137*, 106024. [CrossRef]
243. Zonta, T.; da Costa, C.A.; da Rosa Righi, R.; de Lima, M.J.; da Trindade, E.S.; Li, G.P. Predictive maintenance in the Industry 4.0: A systematic literature review. *Comput. Ind. Eng.* **2020**, *150*, 106889. [CrossRef]

244. Amafabia, D.M.; Montalvao, D.; David-West, O.; Haritos, G. A Review of Structural Health Monitoring Techniques as Applied to Composite Structures. *Struct. Damage Health Monit.* **2017**, *11*, 91–147.
245. Moghaddam, M.K.; Salas, M.; Koerdt, M.; Brauner, C.; Hübner, M.; Lehmus, D.; Lang, W. Sensor Integration in Fiber-Reinforced Polymers. In *Material-Integrated Intelligent Systems—Technology and Applications*; Bosse, S., Lehmus, D., Lang, W., Busse, M., Eds.; Wiley-VCH Verlag: Weinheim, Germany, 2018; pp. 161–200.
246. Güemes, A.; Fernandez-Lopez, A.; Pozo, A.R.; Sierra-Perez, J. Structural Health Monitoring for Advanced Composite Structures: A Review. *J. Compos. Sci.* **2020**, *4*, 13. [[CrossRef](#)]
247. Lehmus, D.; Rahn, T.; Pille, C.; Busse, M. Integrating Electronic Components, Sensors and Actuators in Cast Metal Components: An Overview of the State of the Art. *Springer Lect. Notes Netw. Syst.* **2023**, *556*, 350–361.
248. Busse, M.; Woestmann, F.-J.; Müller, T.; Melz, T.; Spies, P. Intelligente Gussteile—Einsatz adaptiver Komponenten in Kombination mit Gussteilen. *Giesserei* **2006**, *93*, 48–53.
249. Lang, W.; Jakobs, F.; Tolstosheeva, E.; Sturm, H.; Ibragimov, A.; Kesel, A.; Lehmus, D.; Dicke, U. From embedded sensors to sensorial materials—The road to function scale integration. *Sens. Actuators A Phys.* **2011**, *171*, 3–11. [[CrossRef](#)]
250. Bonollo, F.; Gramegna, N. *The MUSIC Guide to the Key-Parameters in High Pressure Die Casting*; Enginsoft, SpA; Assomet Servizi srl: Milano, Italy, 2014; ISBN 978-8887786-10-1.
251. Carlsson, R.; Elmquist, L.; Johansson, C. Cast metal with intelligence—From passive to intelligent cast components. In Proceedings of the 8th ECCOMAS Thematic Conference on Smart Structures and Materials (SMART 2017), Madrid, Spain, 5–8 June 2017.
252. Carlsson, R.; Elmquist, L.; Thore, A.; Ahrentorp, F.; Johansson, C.; Israelsson, B. Connecting sensors inside smart castings. In Proceedings of the 7th International Symposium on Aircraft Materials (ACMA2018), Compiègne, France, 24–26 April 2018.
253. Elmquist, L.; Carlsson, R.; Johansson, C. Cast Iron Components with Intelligence. *Mater. Sci. Forum* **2018**, *925*, 512–519. [[CrossRef](#)]
254. Carlsson, R.; Elmquist, L.; Thore, A.; Johansson, C.; Ahrentorp, F.; Schaller, V.; Johannisson, P.; Israelsson, B.; Törnvall, M.; Zander, P. Sensors integrated inside metal castings verified to respond to force. In Proceedings of the 9th ECCOMAS Thematic Conference on Smart Structures and Materials (SMART 2019), Paris, France, 8–11 July 2019.
255. Weraneck, K.; Heilmeier, F.; Lindner, M.; Graf, M.; Jakobi, M.; Volk, W.; Roths, J.; Koch, A.W. Strain Measurement in Aluminium Alloy during the Solidification Process using Embedded Fibre Bragg Gratings. *Sensors* **2016**, *16*, 1853. [[CrossRef](#)] [[PubMed](#)]
256. Lindner, M.; Tunc, E.; Weraneck, K.; Heilmeier, F.; Volk, W.; Jakobi, M.; Koch, A.W.; Roths, J. Regenerated Bragg Grating Sensor Array for Temperature Measurements During an Aluminum Casting Process. *IEEE Sens. J.* **2018**, *18*, 5352–5360. [[CrossRef](#)]
257. Heilmeier, F.; Koos, R.; Weraneck, K.; Lindner, M.; Jakobi, M.; Roths, J.; Koch, A.W.; Volk, W. In-situ strain measurements in the plastic deformation regime inside casted parts using fibre-optical strain sensors. *Prod. Eng.* **2019**, *13*, 351–360. [[CrossRef](#)]
258. Lindner, M.; Stadler, A.; Hamann, G.; Fischer, B.; Jakobi, M.; Heilmeier, F.; Bauer, C.; Volk, W.; Koch, A.W.; Roths, J. Fiber Bragg Sensors Embedded in Cast Aluminum Parts: Axial Strain and Temperature Response. *Sensors* **2021**, *21*, 1680. [[CrossRef](#)]
259. Bian, Q.; Bauer, C.; Stadler, A.; Jakobi, A.; Koch, A.W.; Roths, J. Multipoint Temperature Monitoring Based on a Regenerated Fiber Bragg Grating Temperature Sensor Array in Copper Casting. In Proceedings of the SPIE 11591, Sensors and Smart Structures Technologies for Civil, Mechanical, and Aerospace Systems 2021, Online, 22–26 March 2021; Volume 11591. [[CrossRef](#)]
260. Lehmus, D.; Klatt, A.; Struss, A.; Cen, M.; Pille, C.; Hepp, E.; Middelman, O.; Lang, W.; Busse, M. Metal casting meets smart systems—Integrating sensors and electronics as contribution to the digitalization of the foundry industry. In Proceedings of the 2nd Congress for Intelligent Combining of Design, Casting, Computer Simulation, Checking and Cyclic Behaviour for Efficient Cast Components (InCeight Casting C⁸), Darmstadt, Germany, 6–8 March 2023.
261. Lehmus, D.; Cen, M.; Struss, A.; de Rijk, T.; Pille, C.; Lang, W. Thick Film Sensor Manufacturing Techniques for Realization of Smart Components via Low Pressure Die Casting. *J. Phys. Conf. Ser.* **2024**, *2692*, 012007. [[CrossRef](#)]
262. Pille, C.; Biehl, S.; Busse, M. Encapsulating piezoresistive thin film sensors based on amorphous diamond-like carbon in aluminum castings. In Proceedings of the 1st Intern. Symposium on System-Integrated Intelligence (SysInt 2012), Hanover, Germany, 27–29 June 2012.
263. Dumstorff, G.; Pille, C.; Tiedemann, R.; Busse, M.; Lang, W. Smart aluminum components: Printed sensors for integration into aluminum during high-pressure casting. *J. Manuf. Process.* **2017**, *26*, 166–172. [[CrossRef](#)]
264. Ibragimov, A.; Pleteit, H.; Pille, C.; Lang, W. Micromachined Thermogenerator Directly Integrated into Metal Parts: Technological Aspects of the Embedding Process. In Proceedings of the 1st Joint International Symposium on System-Integrated Intelligence, Hanover, Germany, 27–29 June 2012; pp. 192–194.
265. Ibragimov, A.; Pleteit, H.; Pille, C.; Lang, W. A Thermoelectric Energy Harvester Directly Embedded into Casted Aluminum. *Electron Device Lett. IEEE* **2012**, *33*, 233–235. [[CrossRef](#)]
266. Schwankl, M.; Rübner, M.; Singer, R.F.; Körner, C. Integration of PZT-ceramic modules using hybrid structures in high pressure die casting. *Procedia Mater. Sci.* **2013**, *2*, 166–172. [[CrossRef](#)]
267. Schwankl, M.; Rübner, M.; Flössel, M.; Gebhardt, S.; Michaelis, A.; Singer, R.F.; Koerner, C. Active functionality of piezoceramic modules integrated in aluminum high pressure die castings. *Sens. Actuators A Phys.* **2014**, *207*, 84–90. [[CrossRef](#)]
268. Schwankl, M.; Kimme, S.; Pohle, C.; Drossel, W.-G.; Körner, C. Active vibration damping in structural aluminum die castings via piezoelectricity—Technology and characterization. *Adv. Eng. Mater.* **2015**, *17*, 969–975. [[CrossRef](#)]
269. Altimus, J.C.; Johnson, V.D. Remote Identification of Metal Castings. *Trans. Am. Foundrymens Soc.* **1998**, *106*, 605–608.
270. Pille, C. In-process embedding of piezo sensors and RFID transponders into cast parts for autonomous manufacturing logistics. In Proceedings of the Smart Systems Integration (SSI) 2010, Como, Italy, 23–24 March 2010.

271. Campbell, J. Review of computer simulation versus casting reality. In *Proceedings of Modeling of Casting, Welding and Advanced Solidification Processes VII*; Cross, M., Campbell, S., Eds.; The Minerals, Metals and Materials Society: London, UK, 1995; pp. 907–913.
272. Flender, E.; Sturm, J. Thirty years of casting process simulation. *Int. J. Met.* **2010**, *4*, 7–23. [[CrossRef](#)]
273. Jolly, M.; Katgerman, L. Modelling of defects in aluminium cast products. *Prog. Mater. Sci.* **2022**, *123*, 100824. [[CrossRef](#)]
274. Cleary, P.W.; Ha, J.; Alguine, V.; Nguyen, T. Flow modelling in casting processes. *Appl. Math. Model.* **2002**, *26*, 171–190. [[CrossRef](#)]
275. Cleary, P.W.; Ha, J. Three-dimensional smoothed particle hydrodynamics simulation of high pressure die casting of light metal components. *J. Light Met.* **2002**, *2*, 169–183. [[CrossRef](#)]
276. Cleary, P.W.; Ha, J.; Prakash, M.; Nguyen, T. 3D SPH flow predictions and validation for high pressure die casting of automotive components. *Appl. Math. Model.* **2006**, *30*, 1406–1427. [[CrossRef](#)]
277. Khan, M.A.A.; Sheikh, A.K. Simulation tools enhancing metal casting productivity and quality: A review. *J. Eng. Manuf.* **2016**, *230*, 1799–1817. [[CrossRef](#)]
278. Khan, M.A.A.; Sheikh, A.K. A comparative study of simulation software for modelling metal casting processes. *Int. J. Simul. Model* **2018**, *17*, 197–209. [[CrossRef](#)] [[PubMed](#)]
279. Khan, M.A.A.; Sheikh, A.K. Virtual Casting: State of the Art in Metal Casting Simulation Tools. *J. Eng. Res.* **2018**, *15*, 142–154.
280. Danylchenko, L. Comparative Analysis of Computer Systems for Casting Processes Simulation. In *Proceedings of the International Conference on Advanced Applied Energy and Information Technologies*, Ternopil, Ukraine, 15–17 December 2021; pp. 105–113.
281. Dhodare, A.S.; Ramanan, P.M.; Dodiya, N. A Review on Interfacial Heat Transfer Coefficient during Solidification in Casting. *Int. J. Eng. Res. Technol.* **2017**, *6*, 464–467.
282. Kouki, Y.; Müller, S.; Schuchardt, T.; Dilger, K. Development of an instrumented test tool for the determination of heat transfer coefficients for die casting applications. *Metals* **2020**, *10*, 1206. [[CrossRef](#)]
283. Wollf, N.; Zimmermann, G.; Vroomen, U.; Bührig-Polaczek, A. A statistical evaluation of the influence of different material and process parameters on the heat transfer coefficient in gravity die casting. *Metals* **2020**, *10*, 1367. [[CrossRef](#)]
284. Cao, L.; Liaon, D.; Sun, F.; Chen, T.; Teng, Z.; Tang, Y. Prediction of gas entrapment defects during zinc alloy high-pressure die casting based on a gas-liquid multiphase flow model. *Int. J. Adv. Manuf. Technol.* **2018**, *94*, 807–815. [[CrossRef](#)]
285. Jolly, M. Casting simulation: How well do reality and virtual casting match? State of the art review. *Int. J. Cast Met. Res.* **2002**, *14*, 303–313. [[CrossRef](#)]
286. Liu, Z.-K. Computational thermodynamics and its applications. *Acta Mater.* **2020**, *200*, 745–792. [[CrossRef](#)]
287. Liu, Z.K. Thermodynamics and its prediction and CALPHAD modeling: Review, state of the art, and perspectives. *Calphad* **2023**, *82*, 102580. [[CrossRef](#)]
288. The Microstructure Evolution Simulation Software. Available online: <https://micress.rwth-aachen.de/> (accessed on 16 February 2024).
289. Chen, R.; Xu, Q.; Liu, B. Cellular automaton simulation of three-dimensional dendrite growth in Al-7Si-Mg ternary aluminum alloys. *Comput. Mater. Sci.* **2015**, *105*, 90–100. [[CrossRef](#)]
290. Gu, C.; Lu, Y.; Cinkilic, E.; Miao, J.; Klarner, A.; Yan, X.; Luo, A.A. Predicting grain structure in high pressure die casting of aluminum alloys: A coupled cellular automaton and process model. *Comput. Mater. Sci.* **2019**, *161*, 64–75. [[CrossRef](#)]
291. Jakumeit, J.; Behnken, H.; Laqua, R.; Eiken, J.; Brachmann, J. Multi-scale simulation of hybrid light metal structures produced by high pressure die casting. *IOP Conf. Ser. Mater. Sci. Eng.* **2020**, *861*, 012035. [[CrossRef](#)]
292. Wang, Y.; Zhang, Y.; Liu, X.; Wang, J.; Xie, X.; Jiang, J.; Liu, J.; Liu, H.; Wu, Y.; Dong, S.; et al. Simulation of Microstructure Evolution in Mg Alloys by Phase-Field Methods: A Review. *Crystals* **2022**, *12*, 1305. [[CrossRef](#)]
293. Kovacevic, L.; Oliveira, R.; Terek, P.; Terek, V.; Pristavec, J.; Skoric, B. The Direction of Foundry Industry: Toward the Foundry 4.0. *J. Mechatron. Autom. Identif. Technol.* **2020**, *5*, 23–28.
294. Sikorski, S.; Dieckhues, G.W.; Sturm, J.C. Systematic Optimization of Aluminum Sand Casting Gating Systems. Am Foundry Society. 2012. Available online: https://www.magmaflow.de/export/shared/MAGMA/common/_galleries/_downloads/2012_Systematic-optimization-aluminum-gating-system.pdf (accessed on 13 February 2022).
295. Dojka, R.; Jezierski, J.; Campbell, J. Optimized Gating System for Steel Castings. *J. Mater. Eng. Perform.* **2018**, *27*, 5152–5163. [[CrossRef](#)]
296. Dojka, R.; Jezierski, J.; Tiedje, N.S. Geometric Form of Gating System Elements and Its Influence on the Initial Filling Phase. *J. Mater. Eng. Perform.* **2019**, *28*, 3922–3928. [[CrossRef](#)]
297. Yun, J.; Lee, S.B. Influence of Aluminum Die-Cast Rotor Porosity on the Efficiency of Induction Machines. *IEEE Trans. Magn.* **2018**, *54*, 8104905. [[CrossRef](#)]
298. Pille, C.; Mäurer, G. A Look into the hidden—The First Complete CT of Cast Rotors in Electric Asynchronous Motors. *Insp. Int.* **2020**, *2*, 12–13.
299. Blair, M.; Monroe, R.; Beckermann, C.; Hardin, R.; Carlson, K.; Monroe, C. Predicting the Occurrence and Effects of Defects in Castings. *JOM* **2005**, *57*, 29–34. [[CrossRef](#)]
300. Blondheim, D., Jr. Systems Understanding of High Pressure Die Casting Process and Data with Machine Learning Applications. Ph.D. Thesis, Colorado State University, Fort Collins, CO, USA, 2021.
301. Blondheim, D., Jr.; Monroe, A. Macro porosity formation: A study in high pressure die casting. *Int. J. Met.* **2022**, *16*, 330–341. [[CrossRef](#)]

302. Lauterbach, B.; Nigge, K.-M. Beurteilung von Volumendefekten—Struktursimulation auf Basis der Computertomografie. *Giesserei* **2021**, *108*, 48–53.
303. Zhang, Y.; Lordan, E.; Dou, K.; Wang, S.; Fan, Z. Influence of porosity characteristics on the variability in mechanical properties of high pressure die casting (HPDC) AlSi7MgMn alloys. *J. Manuf. Process.* **2019**, *56*, 500–509. [[CrossRef](#)]
304. Nourian-Avval, A.; Fatemi, A. Characterization and Analysis of Porosities in High Pressure Die Cast Aluminum by Using Metallography, X-Ray Radiography, and Micro-Computed Tomography. *Materials* **2020**, *13*, 3068. [[CrossRef](#)]
305. Andrieux, F.; Sun, D.; Burbliès, A. Multiscale Approach for the Damage Modeling of an Aluminum Casting Alloy with Stochastic Character. *Mater. Sci. Forum* **2017**, *877*, 680–685. [[CrossRef](#)]
306. Goodfellow, I.J.; Pouget-Abadiey, J.; Mirza, M.; Xu, B.; Warde-Farley, D.; Ozairz, S.; Courville, A.; Bengio, Y. Generative Adversarial Nets. In Proceedings of the 27th International Conference on Neural Information Processing Systems (ACM), Montreal, QC, Canada, 8–13 December 2014; pp. 2672–2680.
307. Gui, J.; Sun, Z.; Wen, Y.; Tao, D.; Ye, J. A Review on Generative Adversarial Networks: Algorithms, Theory and Applications. *IEEE Trans. Knowl. Data Eng.* **2023**, *35*, 3313–3332. [[CrossRef](#)]
308. Raghavendra, A.K.M.; Lacourt, L.; Marcin, L.; Maurel, V.; Proudhon, V. Generation of synthetic microstructures containing casting defects: A machine learning approach. *Nat. Sci. Rep.* **2023**, *13*, 11852. [[CrossRef](#)]
309. Andrieux, F.; Fehrenbach, C.; Oeser, S.; Sun, D.-Z.; Ebrahimi, A.; Heuser, M.; Lehmus, D.; Struss, A. *Modellierung der Einflüsse von Mikrodefekten auf das Versagensverhalten von Al-Druckgusskomponenten mit Stochastischem Aspekt für die Crashsimulation*; FAT-Schriftenreihe Band 338; Forschungsvereinigung Automobiltechnik e. V. (FAT): Berlin, Germany, 2020.
310. Kong, D.; Sun, D.-Z.; Yang, B.; Qiao, H.; Wie, C.; Lang, Y.; Song, H.; Gao, J. Characterization and modeling of damage behavior of a casting aluminum wheel considering inhomogeneity of microstructure and microdefects. *Eng. Fail. Anal.* **2023**, *145*, 107018. [[CrossRef](#)]
311. Campbell, J. An Overview of the Effects of Bifilms on the Structure and Properties of Cast Alloys. *Metall. Mater. Trans. B* **2006**, *37B*, 857–863. [[CrossRef](#)]
312. Gopalan, R.; Prabhu, N.K. Oxide bifilms in aluminium alloy castings—A review. *Mater. Sci. Technol.* **2011**, *27*, 1757–1769. [[CrossRef](#)]
313. El-Sayed, M.A.; Griffiths, W.D. Hydrogen, biofilms and mechanical properties of Al castings. *Int. J. Cast Met. Res.* **2014**, *27*, 282–287. [[CrossRef](#)]
314. Gyarmati, G.; Fegyverneki, G.; Mende, T.; Tokar, M. Characterization of the double oxide film content of liquid aluminum alloys by computed tomography. *Mater. Charact.* **2019**, *157*, 109925. [[CrossRef](#)]
315. Garcia-Perez, A.; Gomez Silva, M.J.; de la Escalera Huesco, A. Automated Defect Recognition of Casting Defects Using Neural Networks. *J. Nondestruct. Eval.* **2022**, *41*, 11. [[CrossRef](#)]
316. Bosse, S.; Lehmus, D. Automated Detection of Hidden Damages and Impurities in Aluminum Die Casting Materials and Fibre-Metal Laminates Using Low-Quality X-ray Radiography, Synthetic X-ray Data Augmentation by Simulation, and Machine Learning. *arXiv* **2023**, arXiv:2311.12041.
317. Hen, B.; Wei, Z.; Perron, L.; Ibarra Castanedo, C.; Maldague, X. Towards Enhancing Automated Defect Recognition (ADR) in Digital X-ray Radiography Applications: Synthesizing Training Data through X-ray Intensity Distribution Modeling for Deep Learning Algorithms. *Information* **2024**, *15*, 16. [[CrossRef](#)]
318. Fuchs, P.; Kröger, T.; Garbe, S. Defect detection in CT scans of cast aluminum parts: A machine vision perspective. *Neurocomputing* **2021**, *453*, 85–96. [[CrossRef](#)]
319. Mery, D. Aluminum Casting Inspection Using Deep Learning: A Method Based on Convolutional Neural Networks. *J. Nondestruct. Eval.* **2020**, *39*, 12. [[CrossRef](#)]
320. Mery, D. Aluminum Casting Inspection using Deep Object Detection Methods and Simulated Ellipsoidal Defects. *Mach. Vis. Appl.* **2021**, *32*, 72. [[CrossRef](#)]
321. Ghansiyal, S.; Yi, L.; Simon, P.M.; Klar, M.; Müller, M.M.; Glatt, M.; Aurich, J.C. Anomaly detection towards zero defect manufacturing using generative adversarial networks. *Procedia CIRP* **2023**, *120*, 1457–1462. [[CrossRef](#)]
322. Lee, J.H.; Noh, S.D.; Kim, H.-J.; Kang, Y.-S. Implementation of Cyber-Physical Production Systems for Quality Prediction and Operation Control in Metal Casting. *Sensors* **2018**, *18*, 1428. [[CrossRef](#)]
323. Wang, X.; Yew, A.W.W.; Ong, S.K.; Nee, A.Y.C. Enhancing smart shop floor management with ubiquitous augmented reality. *Int. J. Prod. Res.* **2020**, *58*, 2352–2367. [[CrossRef](#)]
324. Mourtzis, D.; Siatras, V.; Angelopoulos, J. Real-time remote maintenance support based on augmented reality (AR). *Appl. Sci.* **2020**, *10*, 1855. [[CrossRef](#)]
325. Mourtzis, D.; Angelopoulos, J.; Panopoulos, N. Challenges and Opportunities for Integrating Augmented Reality and Computational Fluid Dynamics Modeling under the Framework of Industry 4.0. *Procedia CIRP* **2022**, *106*, 215–220. [[CrossRef](#)]
326. Ravi, B. Metal Casting 4.0: Closing the loop between design and manufacturing. *Trans. Indian Inst. Met.* **2021**, *74*, 1017–1028. [[CrossRef](#)]
327. Lipp, J.; Rudack, M.; Vroomen, U.; Bührig-Polaczek, A. When to Collect What? Optimizing Data Load via Process-driven Data Collection. In Proceedings of the 22nd International Conference on Enterprise Information Systems (ICEIS 2020), Prague, Czech Republic, 5–7 May 2020; Volume 1, pp. 220–225. [[CrossRef](#)]

328. Kopper, A.E. Knowledge Creation via Data Analytics in a High Pressure Die Casting Operation. Ph.D. Thesis, Worcester Polytechnic Institute, Worcester, MA, USA, 2020.
329. Rudack, M.; Rath, M.; Vroomen, U.; Bührig-Polaczek, A. Towards a Data Lake for High Pressure Die Casting. *Metals* **2022**, *12*, 349. [CrossRef]
330. OPC. Unified Architecture—Part 1: Overview and Concepts. IEC TR 62541-1:2022. 2022. Available online: <https://reference.opcfoundation.org/Core/Part1/v105/docs/> (accessed on 7 March 2024).
331. Profanter, S.; Tekat, A.; Dorofeev, K.; Rickert, M.; Knoll, A. OPC UA versus ROS, DDS, and MQTT: Performance Evaluation of Industry 4.0 Protocols. In Proceedings of the 2019 IEEE International Conference on Industrial Technology (ICIT), Melbourne, VIC, Australia, 13–15 February 2019; pp. 955–962. [CrossRef]
332. Riedel, E. MQTT protocol for SME foundries: Potential as an entry point into industry 4.0, process transparency and sustainability. *Procedia CIRP* **2022**, *105*, 601–606. [CrossRef]
333. Yang, C.; Zheng, Y.; Tu, X.; Ala-Laurinaho, R.; Autiosalo, J.; Seppänen, O.; Tammi, K. Ontology-based knowledge representation of industrial production workflow. *Adv. Eng. Inform.* **2023**, *58*, 102185. [CrossRef]
334. Sanfilippo, E.M.; Kitamura, Y.; Young, R.I.M. Formal Ontologies in Manufacturing. *Appl. Ontol.* **2019**, *14*, 1. [CrossRef]
335. Nilsson, J.; Sandin, F. Semantic Interoperability in Industry 4.0: Survey of Recent Developments and Outlook. In Proceedings of the 2018 IEEE 16th International Conference on Industrial Informatics (INDIN), Porto, Portugal, 18–20 July 2018; pp. 127–132. [CrossRef]
336. Kluska-Nawarecka, S.; Smolarek-Grzyb, A.; Wilk-Kołodziejczyk, D.; Adrian, A. Knowledge Representation of Casting Metal Defects by Means of Ontology. *Arch. Foundry Eng.* **2007**, *7*, 75–78.
337. Kluska-Nawarecka, S.; Nawarecki, E.; Dobrowolski, G.; Haratym, A.; Regulski, K. The Platform for Semantic Integration and Sharing Technological Knowledge on Metal Processing. *Comput. Methods Mater. Sci.* **2013**, *13*, 304–312.
338. Ameri, F.; Urbanovsky, C.; McArthur, C. A systematic approach to developing ontologies for manufacturing service modeling. In Proceedings of the 2nd International Workshop on Ontology and Semantic web for Manufacturing (OSEMA 2012), Graz, Austria, 24–25 July 2012.
339. Singh, K.N.; Behera, R.K.; Mantri, J.K. Big Data Ecosystem: Review on Architectural Evolution. In *Emerging Technologies in Data Mining and Information Security*; Abraham, A., Dutta, P., Mandal, J., Bhattacharya, A., Dutta, S., Eds.; Book Series Advances in Intelligent Systems and Computing; Springer: Singapore, 2019; Volume 813. [CrossRef]
340. Pennekamp, J.; Glebke, R.; Henze, M.; Meisen, T.; Quix, C.; Hai, R.; Gleim, L.; Niemietyky, P.; Rudack, M.; Knape, S.; et al. Towards an infrastructure enabling the internet of production. In Proceedings of the 2019 IEEE International Conference on Industrial Cyber Physical Systems (ICPS), Taipei, Taiwan, 6–9 May 2019; pp. 31–37.
341. Lin, J. The Lambda and the Kappa. *IEEE Internet Comput.* **2017**, *17*, 60–66. [CrossRef]
342. Cerezo, F.; Cuesta, C.E.; Moreno-Herranz, J.C.; Vela, B. Deconstructing the Lambda Architecture: An Experience Report. In Proceedings of the 2019 IEEE International Conference on Software Architecture Companion (ICSA-C), Hamburg, Germany, 25–26 March 2019; pp. 196–201. [CrossRef]
343. Mathis, C. Data Lakes. *Datenbank Spektrum* **2017**, *17*, 289–293. [CrossRef]
344. Rix, M.; Kujat, B.; Meisen, T.; Jeschke, S. An agile information processing framework for high pressure die casting applications in modern manufacturing systems. *Procedia CIRP* **2016**, *41*, 1084–1089. [CrossRef]
345. Lipp, J.; Rath, M.; Rudack, M.; Vroomen, U.; Bührig-Polaczek, A. Flexible OPC UA Data Load Optimizations on the Edge of Production. In *Enterprise Information Systems, Proceedings of the 22nd International Conference (ICEIS 2020), Virtual Event, 5–7 May 2020*; Revised Selected Papers; Springer: Cham, Switzerland, 2020; pp. 43–61.
346. Gramegna, N.; Greggio, F.; Bonollo, F. Smart Factory Competitiveness Based on Real Time Monitoring and Quality Predictive Model Applied to Multi-stages Production Lines. In Proceedings of the IFIP International Conference on Advances in Production Management Systems (APMS), Novi Sad, Serbia, 30 August 2020; pp. 185–196.
347. Kim, J.; Lee, J.Y. Data-analytics-based factory operation strategies for die-casting quality enhancement. *Int. J. Adv. Manuf. Technol.* **2022**, *119*, 3865–3890. [CrossRef]
348. Fernandez, A.; Garcia, S.; Herrera, F.; Chawla, N.V. SMOTE for Learning from Imbalanced Data: Progress and Challenges, Marking the 15-year Anniversary. *J. Artif. Intell. Res.* **2018**, *61*, 863–905. [CrossRef]
349. Kim, J.S.; Kim, J.; Lee, J.Y. Die-Casting Defect Prediction and Diagnosis System using Process Condition Data. *Procedia Manuf.* **2020**, *51*, 359–364. [CrossRef]
350. Karniadakis, G.E.; Kevrekidis, I.G.; Lu, L.; Perdikaris, P.; Wang, S.; Yang, L. Physics-informed machine learning. *Nat. Rev. Phys.* **2021**, *3*, 422–440. [CrossRef]
351. Ebrahimi, A.; Fritsching, U.; Heuser, M.; Lehmhus, D.; Struß, A.; Toenjes, A.; von Hehl, A. A digital twin approach to predict and compensate distortion in a High Pressure Die Casting (HPDC) process chain. *Procedia Manuf.* **2020**, *52*, 144–149. [CrossRef]
352. Jones, D.; Snider, C.; Nassehi, A.; Yon, J.; Hicks, B. Characterising the Digital Twin: A systematic literature review. *CIRP J. Manuf. Sci. Technol.* **2020**, *29*, 36–52. [CrossRef]
353. Al-Sehrawy, R.; Kumar, B.; Watson, R. A mulit-dimensional digital twin use cases classification framework. In Proceedings of the 2021 European Conference on Computing in Construction, Online, 26–28 July 2021. [CrossRef]
354. Moiceanu, G.; Paraschiv, G. Digital Twin and Smart Manufacturing in Industries: A Bibliometric Analysis with a Focus on Industry 4.0. *Sensors* **2022**, *22*, 1388. [CrossRef]

355. Kritzinger, W.; Karner, M.; Traar, G.; Henjes, J.; Sihn, W. Digital Twin in manufacturing: A categorical literature review and classification. *IFAC PapersOnLine* **2018**, *51*, 1016–1022. [CrossRef]
356. He, B.; Bai, K.-J. Digital twin-based sustainable intelligent manufacturing: A review. *Adv. Manuf.* **2021**, *9*, 1–21. [CrossRef]
357. Shen, Z.J.M.; Wang, L.; Deng, T. Digital Twin: What It Is, Why Do It, Related Challenges, and Research Opportunities for Operations Research. 2021. Available online: https://papers.ssrn.com/sol3/papers.cfm?abstract_id=3777695 (accessed on 19 February 2024).
358. Kendrik, L.Y.H.; Zheng, P.; Chen, C.-H. A state-of-the-art survey of Digital Twin: Techniques, engineering product lifecycle management and business innovation perspectives. *J. Intell. Manuf.* **2020**, *31*, 1313–1337. [CrossRef]
359. Melesse, T.Y.; Di Pasquale, V.; Riemma, S. Digital Twin Models in Industrial Operations: A Systematic Literature Review. *Procedia Manuf.* **2020**, *42*, 267–272. [CrossRef]
360. Huang, Z.; Shen, Y.; Li, J.; Fey, M.; Brecher, C. A survey on AI-driven Digital Twins in Industry 4.0: Smart manufacturing and advanced robotics. *Sensors* **2021**, *21*, 6340. [CrossRef] [PubMed]
361. Benner, P.; Faßbender, H. Model order reduction: Techniques and tools. In *Encyclopedia of Systems and Control*; Springer: London, UK, 2013; pp. 1–10.
362. Baur, U.; Benner, P.; Feng, L. Model Order Reduction for Linear and Nonlinear Systems: A System-Theoretic Perspective. *Arch. Comput. Methods Eng.* **2014**, *21*, 331–358. [CrossRef]
363. Simpson, T.W.; Peplinski, J.D.; Koch, P.N.; Allen, J.K. Metamodels for computer-based engineering design: Survey and recommendations. *Eng. Comput.* **2001**, *17*, 129–150. [CrossRef]
364. Anglada, E.; Boto, F.; Garcia de Cortazar, M.; Garmendia, I. Metamodels Development for High Pressure Die Casting of Aluminum Alloy. *Metals* **2021**, *11*, 1747. [CrossRef]
365. Lucia, D.J.; Beran, P.S.; Silva, W.A. Reduced-order modeling: New approaches for computational physics. *Prog. Aerosp. Sci.* **2004**, *40*, 51–117. [CrossRef]
366. Lu, K.; Jin, Y.; Chen, Y.; Yang, Y.; Hu, L.; Zhang, Z.; Li, Z.; Fu, C. Review for order reduction based on proper orthogonal decomposition and outlooks of applications in mechanical systems. *Mech. Syst. Signal Process.* **2019**, *123*, 264–297. [CrossRef]
367. Chakrabarti, A.; Sukumar, R.P.; Jarke, M.; Rudack, M.; Buske, P.; Holly, C. Efficient Modeling of Digital Shadows for Production Processes: A Case Study for Quality Prediction in High Pressure Die Casting. In Proceedings of the 8th International Conference on Data Science and Analytics (DSAA), Porto, Portugal, 6–9 October 2021. [CrossRef]
368. Liu, D.; Du, Y.; Chai, W.; Lu, C.Q.; Cong, M. Digital Twin and Data-Driven Quality Prediction of Complex Die-Casting Manufacturing. *IEEE Trans. Ind. Inform.* **2022**, *18*, 8119–8128. [CrossRef]
369. Ktari, A.; El Mansori, M. Digital twin of functional gating system in 3D printed molds for sand casting using a neural network. *J. Intell. Manuf.* **2020**, *33*, 897–909. [CrossRef]
370. Zhang, H.; Liu, X.; Ma, D.; Song, M.; Ludwig, A.; Kharicha, A.; Wu, M. Digital twin for directional solidification of a single-crystal turbine blade. *Acta Mater.* **2023**, *244*, 118579. [CrossRef]
371. Doroshenko, V.S.; Kravchenko, V.P.; Tokova, O.V. Development of a digital twin of the technological process of consumable pattern casting using production data. *Control Syst. Comput.* **2020**, *3*, 41–49. [CrossRef]
372. Fiedler, T.; Movahedi, N.; York, L.; Broxtermann, S. Functionally-graded metallic syntactic foams produced via particle pre-compaction. *Metals* **2020**, *10*, 314. [CrossRef]
373. Gimpler, S.; Apel, M.; Bührig-Polaczek, A. Selection of dedicated as-cast microstructures in Zn-Al-Cu alloys for bearing applications supported by phase-field simulations. *Metals* **2020**, *10*, 1659. [CrossRef]
374. Sama, S.R.; MacDonald, E.; Voigt, R.; Manogharan, G. Measurement of Metal Velocity in Sand Casting during Mold Filling. *Metals* **2019**, *9*, 1079. [CrossRef]
375. Niu, R.; Li, B.; Liu, Z.; Bu, L.; Li, X.; Yang, X.; Tsukihashi, F. Experimental investigation of solidification in the cast mold with a consumable cooler introduced inside. *Metals* **2019**, *9*, 55. [CrossRef]
376. Avila-Salgado, D.A.; Juarez-Hernandez, A.; Medina-Ortiz, F.; Banda, M.L.; Hernandez-Rodriguez, M.A.L. Influence of B and Nb additions and heat treatments on the mechanical properties of Cu-Ni-Co-Cr-Si alloy for high pressure die casting application. *Metals* **2020**, *10*, 602. [CrossRef]
377. Avila-Salgado, D.A.; Juarez-Hernandez, A.; Cabral-Miramontes, J.; Camacho-Martinez, J.L. Strengthening Properties and Wear Resistance of the Cu-xNi-yCo-Cr-Si Alloy by Varying Ni/Co and Zr Addition. *Lubricants* **2021**, *9*, 96. [CrossRef]
378. Wan, Y.; Li, M.; Chen, L.; Wu, Y.; Li, J.; Pan, H.; Zhong, W. Effect of final electromagnetic stirring parameters on central cross-sectional carbon concentration distribution of high-carbon square billet. *Metals* **2019**, *9*, 665. [CrossRef]
379. Yan, W.; Zhang, Y.; Chen, W.; Li, J. Characteristics and formation tendency of freckle segregation in electroslag remelting of bearing steel. *Metals* **2020**, *10*, 246. [CrossRef]

Disclaimer/Publisher’s Note: The statements, opinions and data contained in all publications are solely those of the individual author(s) and contributor(s) and not of MDPI and/or the editor(s). MDPI and/or the editor(s) disclaim responsibility for any injury to people or property resulting from any ideas, methods, instructions or products referred to in the content.